Involvement of FlhG, FlhB and their interaction partners in the regulation of flagellation in the monotrichous bacterium Shewanella putrefaciens

Dissertation

Zur Erlangung des Grades eines

Doktor der Naturwissenschaften

(Dr. rer. nat)

des Fachbereichs Chemie der Philipps-Universität Marburg

Vorgelegt von

Vitan Blagotinsek, Master of Biochemistry

Aus Slovenj Gradec, Slowenien

Marburg, 2021

Die vorliegende Dissertation wurde von Februar 2018 bis Januar 2021 am LOEWE Zentrum für Synthetische Mikrobiologie (SYNMIKRO) der Fachbereich Chemie und Philipps Universität Marburg unter der Leitung von Prof. Dr. Gert Bange angefertigt.

Vom Fachbereich Chemie der Philipps-Universität Marburg
(Hochschulkennziffer 1180) als Dissertation angenommen am 1.3.2021

Erstgutachter: Prof. Dr. Gert Bange
(Fachbereich Chemie, Philipps Universität Marburg)

Zweitgutachter: Prof. Dr. Peter Graumann
(Fachbereich Chemie, Philipps Universität Marburg)

Weitere Mitglieder der Prüfungskommission:
Prof. Dr. Martin Thanbichler
(Fachbereich Biologie, Philipps Universität Marburg)

Prof. Dr. Olalla Vázquez
(Fachbereich Chemie, Philipps Universität Marburg)

Tag der Disputation: 25.3.2021

Erklärung

Ich erkläre, dass eine Promotion noch an keiner anderen Hochschule als der Philipps-Universität Marburg, Fachbereich Chemie, versucht wurde.

Hiermit versichere ich, dass ich die vorliegende Dissertation

Involvement of FlhG, FlhB and their interaction partners in the regulation of flagellation in the monotrichous bacterium Shewanella putrefaciens

selbstständig, ohne unerlaubte Hilfe Dritter angefertigt und andere als die in der Dissertation angegebenen Hilfsmittel nicht benutzt habe. Alle Stellen, die wörtlich oder sinngemäß aus veröffentlichten oder unveröffentlichten Schriften entnommen sind, habe ich als solche kenntlich gemacht. Dritte waren an der inhaltlich-materiellen Erstellung der Dissertation nicht beteiligt; insbesondere habe ich hierfür nicht die Hilfe eines Promotionsberaters in Anspruch genommen. Kein Teil dieser Arbeit ist in einem anderen Promotions- oder Habilitationsverfahren verwendet worden. Mit dem Einsatz von Software zur Erkennung von Plagiaten bin ich einverstanden.

Vitan Blagotinsek, Marburg, 31.1.2021

i. Acknowledgments

First of all, I would like to thank my supervisor and mentor, Prof. Dr. Gert Bange, for his scientific guidance, support and understanding during my PhD work. Thank you for giving me a variety of interesting projects to work on, for always being available when I needed help, with professional or personal topics, and for believing in me. Thank you for the many interesting and productive discussions on the Bange Balcony. I would also like to thank Prof. Dr. Bange for his help with the solving and analysis of the FlhB-C structure.

I would like to thank the AG Thormann in Gießen for productive collaborations, in particular Meike Schwan and John Hook for working together with me on the FlhG and FlhB projects and manuscripts (and other additional collaborations). Furthermore, I would like to thank Prof. Dr. Kai Thormann for numerous discussions and useful input during manuscript preparation, as well as being a member of my Thesis advisory committee within the IMPRS graduate school.

Many thanks go to Dr. Wieland Steinchen for performing the HDX experiments, the Mant-ADP experiments with FlhG, and for assistance with the ATP hydrolysis experiments, regarding the HPLC systems and data analysis. Also thank you for your continued support through the different stages of preparing the FlhG paper.

Thank you to Dr. Morgan Beeby and his colleagues for their contributions to the FlhG paper (cryo-tomography data, not shown in this thesis), as well as to Dr. Dieter Kressler for the Yeast-2-Hybrid experiments, also those included in the FlhG paper. Thank you to former members of the Bange lab, Sabrina Henche and Dr. Jan Schuhmacher for their early work on FlhG and FlrA.

I am very grateful for the phylogenetic research expertise and support of Dr. Jan Pane-Farre, and his contributions to the FlhB paper, as well as plenty of interesting scientific discussions.

Thank you also to my initial supervisor, Dr. Devid Mrusek, who laid strong foundations for the projects I include in my thesis, and whose work I continued. He provided my initial training in the lab, and provided support even after his departure from the lab.

You were also there for many interesting conversations, from ancient history to management consulting. I would also like to thank Devid for leaving behind and extensive collection of plasmids of flagellar proteins, as well as his contributions to the PNAS FlhG paper – the MST measurements and several pulldowns.

Thank you also to other members of AG Bange who were particularly helpful and supportive during my stay in the lab – especially Dr. Patricia Bedrunka, Dr. Alexander Lepak, Dr. Florian Altegoer, Anita Dornes, Pietro Giammarinaro, Nils Mais, Dr. Laura Czech, and others. You all helped make the lab a friendly and collaborative place to work in. Thank you also to the friendly masters students and lab assistants, Marvin, Paul, Galina and Lukas. Thank you in particular to Laura, Alex and Anita for assistance with cloning and providing plasmids. Thank you to Florian for his help with harvesting and freezing FlhB-C crystals and structure determination.

Thank you to Dr. Barbara Waidner and Dr. Philipp Reiß, for your guidance and support as I took my first steps as the supervisor of different practical courses – in German. Thank you to the teaching assistants and other co-supervisors, and a number of very talented and motivated students, too many to name here. At this point, I would also like to thank my Chemistry Vertiefer student, Nam Nguyen.

Thank you to my colleagues in the IMPRS graduate school, as well as to both coordinators I had during my participation in the school, Dr. Zrinka Gattin and Dr. Dusica Rados. You have all provided an invaluable international environment for the exchange of ideas, peer support and helpful feedback during my seminars and presentations, as well as career guidance in the context of the IMPRS.

I would like to thank my family for continuous emotional, personal and financial support during my previous and current studies. Most of all, thank you to my girlfriend Lisa, also a fellow researcher at the SYNMIKRO institute, who I met during my PhD studies in Marburg. I could never have made it through without you.

Thank you to the Slovenian Human Resources Development and Scholarship fund, for providing a generous scholarship for living costs during the previous stage of my education in the United Kingdom.

ii. Abstract

Bacteria rely on different motility mechanisms to explore their surroundings and interact with them. Key forms of motility, swimming and swarming, are dependent on a complex macromolecular system called the flagellum, which functions as a rotating molecular motor. This structure is highly relevant for a variety of processes that involve bacterial cells, such as biofilm formation, pathogenesis and chemotaxis. The primary focus of this thesis is the flagellar system of the model organism *Shewanella putrefaciens* CN-32, which possesses a single primary polar flagellum. To further delineate how the flagellum is assembled and positioned, the interactions of two highly conserved proteins were investigated. These proteins are the MinD-like ATPase FlhG, and the flagellar secretion system component FlhB.

This work has demonstrated that FlhG functions as a switch in the assembly of the flagellar C-ring. It is capable of binding, through an overlapping binding site, both the C-ring component FliM, as well as the transcriptional regulator FlrA. The switching of interaction partners depends on the dimerization state of FlhG, and the presence of the nucleotide ATP. FlrA interacts strictly with dimeric, ATP-bound FlhG. Upon binding of FlhG, FlrA can no longer act as a transcriptional activator, and the production of flagellar building blocks is halted. Furthermore, it has been demonstrated that a lack of interaction between FlhG and FlrA *in vivo* results in hyperflagellation.

Additionally, this work shows the structural characterization of the polar FlhB with the help of X-ray crystallography, and identifies a new C-terminal motif, termed the Proline-Rich Region (PRR). A removal of this region results in a decrease in flagellar filament and hook formation *in vivo.* With the help of further *in vitro* experiments involving FlhB, FliM was for the first time identified as a binding partner.

iii. Zusammenfassung

Für Bakterien ist es wichtig sich flexibel in ihrer Umgebung zu bewegen und auch mit dieser Umgebung zu interagieren. Swimming und Swarming sind die zentralen Bewegungsformen bei Bakterien und beruhen auf der Rotation eines Makromolekülkomplexes Namens Flagellum. Das Flagellum wird für einige wichtige Prozesse benötigt wie unteranderem Biofilmbildung, Pathogenität and Chemotaxis.

Im Fokus dieser Arbeit steht das Flagellum von dem Modelorganismus *Shewanella putrefaciens* CN-32, welches nur ein einziges Flagellum am Pol besitzt. Um zu verstehen wie das Flagellum gebildet und positioniert wird, wurde die Interaktion von zwei konservierten Proteinen, die MinD-ähnliche ATPase FlhG und dem Bestandteil des flagellaren Sekretionsystem FlhB, untersucht.

Es konnte gezeigt werden, dass FlhG eine regulierende Funktion beim Aufbau des flagellaren C-Ring spielt. Es kann durch eine überlappende Bindestelle, sowohl FliM (Bestandteil des C-Ringes) als auch den Transkriptionsfaktor FlrA binden. Der Wechsel des Interaktionspartners hängt davon ab, ob FlhG als Dimer oder Monomer vorliegt und ob ATP vorhanden ist. FlrA kann nur mit FlhG interagieren, wenn dieses als Dimer vorliegt und ATP gebunden hat. Woraufhin FlrA nicht mehr als Transkriptionsfaktor agieren kann und die Bildung von Flagellumbausteinen zum Erliegen kommt. Des weiteren konnte gezeigt werden, dass eine *in vivo* Deregulierung der Interaktion von FlhG und FlrA zu einer Hyperflagellierung führen kann.

Außerdem konnte die 3D Struktur von dem polarliegenden Protein FlhB mittels Röntgenstrahl Kristallographie charakterisiert und ein neues C-terminales Motiv mit der Bezeichnung Prolin-Reiche Region (PRR) identifiziert werden. Das entfernen dieser Region führt zu einer verringerten Bildung von Flagellen *in vivo.* Durch weiterführende *in vitro* Experimente würde FliM als neuer Interaktionspartner von FlhB entdeckt.

iv. Contents

i. Acknowledgments 4
ii. Abstract 6
iii. Zusammenfassung 7
iv. Contents 8
v. Publications and manuscripts 11
vi. List of figures 12
vii. Abbreviations 13
1. Introduction 14
1.1. Bacterial locomotion and surface interaction mechanisms 14
1.1.1. Swimming and swarming 15
1.1.2. Twitching 16
1.1.3. Sliding and gliding 18
1.2. The bacterial flagellum 20
1.2.1. Overview of assembly and structure 20
1.2.2. Membrane-bound secretion system and the ATPase complex 21
1.2.3. MS-ring and motor proteins 27
1.2.4. C-ring 27
1.2.5. Hook and hook length control 28
1.2.6. Accessory and regulatory proteins 30
1.3. Chemotaxis 35
1.4. Bacterial flagellation patterns and the importance of the FlhF/FlhG pair 38
1.4.1. Peritrichous, gram-negative (species lacking FlhF and FlhG) 39
1.4.2. Monopolar flagellation (dependent on FlhF and FlhG) 40
1.4.3. Peritrichous, gram-positive (dependent on FlhF and FlhG) 41
1.4.4. Other 42
1.5. Shewanella putrefaciens, the organism 44
1.5.1. Living environments and pathogenicity of *S. putrefaciens* and *Shewanellaceae* 44
1.5.2. Dual flagellation and its control 45
2. Aim of this work 50
3. Results 51
3.1 FlhG and its interaction partners, FliM and FlrA 51
3.1.1 Delineating the FlhG binding site on FlrA 51
3.1.2. ATPase assays with FlhG and FlrA 53
3.1.3. Purifications and purification optimizations for FlhG and FlrA 56

3.1.4. Is FliM a factor promoting ADP release from FlhG? 57
3.1.5. Hydrogen-deuterium exchange mass spectrometry experiments investigating the binding interfaces of FliM and FlrA on FlhG 58
3.1.6. Consurf, sequence analysis and structural models of FlhG, FliM and FlrA....63
3.1.7. Physiological and *in vitro* effects of mutations in the FlhG binding site on FlrA on *S. putrefaciens* 65
3.2. FlhB 69
3.2.1. FlhB-C WT and FlhB-C N269A 69
3.2.2. Crystallization and structure of FlhB-C 72
3.2.3. Consurf analysis of FlhB-C....74
3.2.4. Further FlhB structure analysis in context of Evans et. al 2013 and Inoue et. al 2019 77
3.2.5. LigPlot analysis of FlhB-C 79
3.2.5. Deleting the last 20 C-terminal residues of FlhB leads to a decrease in flagellation 81
3.2.6. Phylogenetic analysis of FlhB....83
3.2.7. Additional interaction partners of FlhB in *S. putrefaciens* 86
4. Discussion 88
4.1. FlhG and its interaction partners....88
4.1.2. Considering the *S. putrefaciens* FlhG/FlrA pair in the context of previous studies done on *P. aeruginosa* FleN/FleQ....96
4.1.3. Future perspectives/outlook 98
4.2.1. FlhB 100
4.2.2.Future perspectives and outlook....105
5. Methods and materials....109
5.1. Materials and consumables....109
5.2.Solutions and buffers....110
5.3. Methods....110
5.3.1. Transformation, protein expression and harvesting 110
5.3.2. Protein purification....111
5.3.3. Sequence alignments and analysis 111
5.3.4. Structural homology modelling and conservation analysis with Consurf 111
5.3.5. GST-pulldown assays 112
5.3.6. Protein crystallization and structure determination 112
5.3.7. Protein-protein interaction studies 113
5.3.8. ATPase assays and HPLC analysis 113
5.3.9. HDX-MS (hydrogen/deuterium exchange mass spectrometry) 114

5.3.10. Mant-ADP fluorescence experiments....115
5.3.11. SDS-PAGE....115
6. References....116
7. Appendix/supplementary data....128
7.1. Genome identification IDs of genes/proteins used....128
7.2. List of constructs used....128
7.3. FlhG and FlrA purification optimization gels....129
7.4. Refinement statistics for FlhB-C....130
7.5. Sequence alignments (EMBOSS Needle) and related analysis....131
7.5.1. SpFlhB (polar) and SalTyFlhB alignment and conservation of critical residues..131
7.5.2. SpFliK(1/2) and SalTyFliK alignment data....132
7.5.3: Identification of the Pfam Bac_export_2 domain....137
7.5.4 Alignment of *Sp*FlhG/*Pa*FleN and *Sp*FlrA /*Pa*FleQ....138
7.6. Supplementary fluorescence microscopy data....140
8. Academic curriculum....141

v. Publications and manuscripts

The majority of the work presented in this thesis has been included in the following articles:

A proline-rich element in the type III secretion protein FlhB contributes to flagellar biogenesis in the beta- and gamma-proteobacteria

Frontiers in Microbiology, https://doi.org/10.3389/fmicb.2020.564161

John Hook[1], **Vitan Blagotinsek[1]** , Jan Pane-Farre, Devid Mrusek, Florian Altegoer, Anita Dornes, Meike Schwan, Lukas Schier, Kai Thormann and Gert Bange

[1]The authors contributed equally to this work

An ATP-dependent partner switch links flagellar C-ring assembly with gene expression

PNAS, https://doi.org/10.1073/pnas.2006470117

Vitan Blagotinsek[1], Meike Schwan[1], Wieland Steinchen, Devid Mrusek, John Hook, Florian Rossmann, Sven A. Freibert, Hanna Kratzat, Guillaume Murat, Dieter Kressler, Roland Beckmann, Morgan Beeby, Kai Thormann and Gert Bange

[1]The authors contributed equally to this work

vi. List of figures

Figure 1: **Graphical summary of the five bacterial locomotion types**. 14
Figure 2: **Overview of pilus structure and twitching motility proteins**. 18
Figure 3: Overview of an assembled bacterial flagellum 21
Figure 4: **FlhB/FliK interaction and important FlhB residues**. 26
Figure 5: Structure and interplay of FlhF and FlhG 32
Figure 6: **Model of the FleQ/DNA binding interaction**. 33
Figure 7: **Overview of domains and known interaction partners for key proteins of interest – FlhG, FlrA, FliM and FlhB**. 35
Figure 8: Overview of chemotaxis-involved proteins. 38
Figure 9: Overview of different primary bacterial flagellation patterns. 39
Figure 10: **Primary and secondary (polar and lateral) flagellar gene clusters in S. putrefaciens** 46
Figure 11: overview of control of the flagellation pattern in S. putrefaciens 48
Figure 12: FlrA constructs and interaction partners identified in Y2H experiments. 51
Figure 13: **FlhG-involving in vitro GST pulldowns and FlhG kinetics**. 53
Figure 14: Endpoint measurements of FlrA and FlhG construct ATP hydrolysis.. 55
Figure 15:**Fluorescence Mant-ADP experiment**. 58
Figure 16: **HDX data on the interactions of FlhG with FlrA and FliM** 60
Figure 17: **HDX data of FlhG with and without FliM/N in the context of ADP binding.**. 62
Figure 18: **Consurf analysis of FlhG, FlrA and FliM with residues colour-coded for conservation scores.** 64
Figure 19.: Fluorescence microscopy data on the FlhG/FlrA interaction. 66
Figure 20: Transcriptional role of the interplay between FlhG and FlrA 68
Figure 21: **Pulldown experiments investigating the FlhG binding site on FlrA**.. 69
Figure 22 FlhB behaviour and crystallization. 71
Figure 23 Western blots and analysis of FlhB mutants. 72
Figure 24 : **Structure analysis of FlhB-C** 76
Figure 25 Consurf analysis of FlhB-C 74
Figure 26: **Visualisation of different residues in S. putrefaciens FlhB-C**. 78
Figure 27: LigPlot DIMPLOT data output. 80
Figure 28 Microscopy and quantification analysis of SpFlhB ΔPRR effects in comparison to wildtype and a ΔflhB mutant. 83
Figure 29 Occurrence of PRR within the g- and b-proteobacteria.. 85
Figure 30 Additional interaction partners of FlhB-C in S. putrefaciens. 87
Figure 31 Summary of different flagellar gene classes and their control. 89
Figure 32: **Summary of the roles of FlhG, FlrA and FliM in the context of transcriptional control and C-ring assembly**. 92
Figure 33: **Summary of key results and model information linking the FlrA/FlhG interaction to different flagellation phenotypes.** 96
Figure 34: FlhB and the PRR motif. 103
Figure 35: Model of the interaction between FlhA, FlhB and FliM/N, as well as potentially FlhG. 105

vii. Abbreviations

A – angstrom

AU – absorption unit

ADP – adenosine diphosphate

Amp - Ampicillin

ATP – adenosine triphosphate

BLAST – Basic Local Alignment Search Tool

CV – column volume

CW – clockwise

CCW - counterclockwise

GTP – guanosine triphosphate

JCSG – Joint Center for Structural Genomics

LB – Luria broth

GST – glutathione-s-transferase

HEPES - 4-(2-hydroxyethyl)-1-piperazineethanesulfonic acid

HDX/MS – hydrogen/deuterium exchange mass spectrometry

HPLC – high-performance liquid chromatography

Kan - Kanamycin

MR – molecular replacement

MTS – membrane targeting sequence

Ni-NTA – Nickel-nitrilotriacetic acid

qPCR – quantitative polymerase chain reaction

PDB – protein data bank

rpm – revolutions per minute

SDS-PAGE – sodium dodecyl sulphate polyacrylamide gel electrophoresis

SEC – size exclusion chromatography

T3SS – type III secretion system

T4P – type IV pili

UV - ultraviolet

WB – Western blot

1. Introduction

1.1. Bacterial locomotion and surface interaction mechanisms

Overall, a variety of movement techniques exist for different bacterial species, some employing flagella for this endeavour, and some not. The two forms of locomotion that involve bacterial flagella are swimming and swarming; the former refers to movement in solution (planktonic form). Twitching, gliding, sliding and spreading occur without flagellar involvement; twitching is caused by another macromolecular structure, called the (type IV) pilus [1,2]. These four movement types, together with swarming, are important for interaction with surfaces, and will be further discussed in this chapter. A graphical summary of the movement types is shown in **Figure 1.**

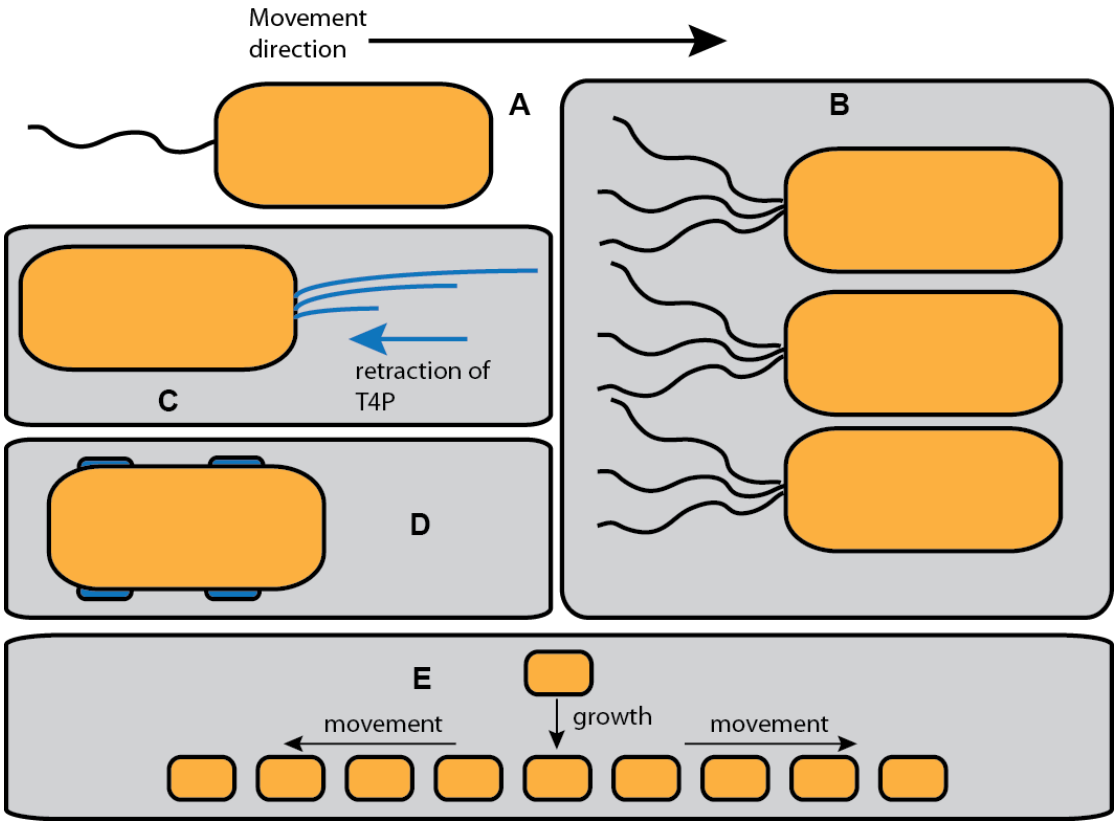

Figure 1: **graphical summary of the five bacterial locomotion types**. Inspired by reference [2]**.** A – swimming B – swarming C – twitching D – gliding E – sliding. Grey zones represent surfaces.

1.1.1. Swimming and swarming

When cultivated in a lab, swarming is more likely to occur in high-nutrient and high-agar concentration media, but different species will switch to swarming mode in response to different degrees of environmental/nutrition triggers. It has also been observed that cells transferred from a liquid culture medium to a solid surface fall into a period where they are non-motile, before they can switch from swimming to swarming motility [2]. In the context of surface colonization, both biofilm formation and swarming feature a closer proximity of bacterial cells and higher cell density, but are differently regulated (where biofilm formation leads to a repression of motility-related genes) [3].

Swimming, on the other hand, refers to the movement of a single bacterium in free (liquid) space, powered by its flagellum (or multiple flagella), whereas swarming refers to the movement of several closely associated bacteria over a solid surface, powered by their flagella [2]. To summarize: swarming, in contrast to swimming motility, is therefore a more complex and synchronous mode of movement, which requires coordination between adjacent cells, and occurs when local cell density is high, on surfaces and when nutrients are abundant. The switch from swimming to swarming is often conditioned by the formation of an increased number of flagella, particularly when the organism otherwise only has a primary polar flagellum.

Swarming has been linked both to a higher expression rate of virulence factors – such as extracellular proteases and type III secretion system components - as well as greater resistance of bacteria to the effects of antibiotics, compared to free-swimming cells (in *P. aeruginosa,* for example). Additionally, in *P. aeruginosa*, swarming-defective mutants were also found to have disruptions in biofilm formation ability, which indicates that a degree of common control over both is present [4,5].

Swarming bacteria are known to move side-by-side to each other in large structures called rafts, which are changing dynamically; new cells regularly associate with a raft, becoming motile themselves, while other cells are lost, temporarily becoming non-motile. Studies in *Proteus mirabilis* have shown that swarming bacteria can also form

repeating layers, associating with each other by forming bundles of flagella that are interwoven between swarming cells that are located next to each other [6]. *Proteus mirabilis*, which is also a human pathogen responsible for urinary tract infections through colonizing the surface of inserted catheters, was found to depend on swarming for pathogenicity. Upon detection of different dissolved compounds in human urine, especially in presence of the amino acid Glutamine, the organism initiates swarming, and more effectively associates with surfaces [7].

Overall, the presence of lateral flagella (or the ability of a bacterium to form lateral flagella) seems to be linked to better swarming ability, and a large proportion of bacteria that can swarm are peritrichous. There are also species that possess a primary polar and secondary/inducible lateral flagellar system, which are also capable of swarming; these include *Vibrio, Aeromonas* and *Pseudomonas* species [2,8].

An alternative to both swimming and swarming, which occurs under extreme nutrient depletion, is a complete lack of active motility. It has been discovered that after flagella have already been formed, and a bacterial cell was previously motile, it can (in the case of gammaproteobacteria) simply remove or eject their flagellum to conserve energy. This occurs at the bottom of the flagellar hook, leaving the rest of the flagellum intact and still embedded within the membrane. This has been observed in polar flagellates such as *P. aeruginosa, V. cholerae* and *S. putrefaciens* [9].

1.1.2. Twitching

Twitching depends on extension and retraction of type IV pili, which are located at cell poles. It is primarily observed in Gram-negative bacteria, and was most extensively studied in *M. xanthus* and *P. aeruginosa,* but also *N. gonorrhoeae.* Another term for twitching in the former two organisms is also “social gliding motility”[10]. In addition to motility roles, type IV pili are also important for adhesion to host cells for pathogenic organisms and for biofilm formation, for mediating signalling, among others [11]. Type IV can be divided into two subtypes, T4A and T4B, where type A pili come from organisms such as the previously mentioned *Pseudomonas* and *Neisseria* species, and type B pili are found in *Salmonella, E. coli and Vibrio* species, for example. The secretion system for type IV pili is itself related

in many components to the bacterial type II secretion system, and the flagellar system found in archaea [11,12].

The type IV pili are made up of polymers of major and minor pilin proteins, and are highly dynamic; the extension and retraction of the pili depend on polymerization and depolymerization of the macromolecular structures, and the process is dependent on the presence of ATP [13,14]. The pilus itself is held in place and directed by the so-called alignment and platform protein complexes. With the help of cryo-EM, detailed structural information could be gathered on assembled *P. aeruginosa* and *N. gonorrhoeae* type IV pili, highlighting that the macromolecular structures have a hydrophobic filament core. The assembly of the pili depends crucially on a Proline residue, which allows for a greater degree of flexibility between subunits within the filament, as well as correct packing of subunits [15].

The twitching of the pili themselves is governed by the assembly and retraction ATPases, which form active hexamers; the retraction ATPase is universally termed PilT in the studied organisms, whereas the assembly ATPase is termed PilB/F, depending on the organism in question [16]. The overall structure of a single pilus measures between 6 and 9 nm in width and can go up to the length of several micrometres, which has been investigated with electron microscopy. A single pilus can generate forces of greater than 100 pN, and can extend or retract itself at a rate of approximately 0.5 micrometres per second [17,18]. The protrusion of the growing pilus from the outer membrane is facilitated by secretins (also termed PilQ proteins), and the platform proteins (PilC/G) allow anchoring of the assembly/retraction ATPase complexes close to the inner membrane. A graphical summary of the structure of the pilus and retraction machinery is shown in **Figure 2.**

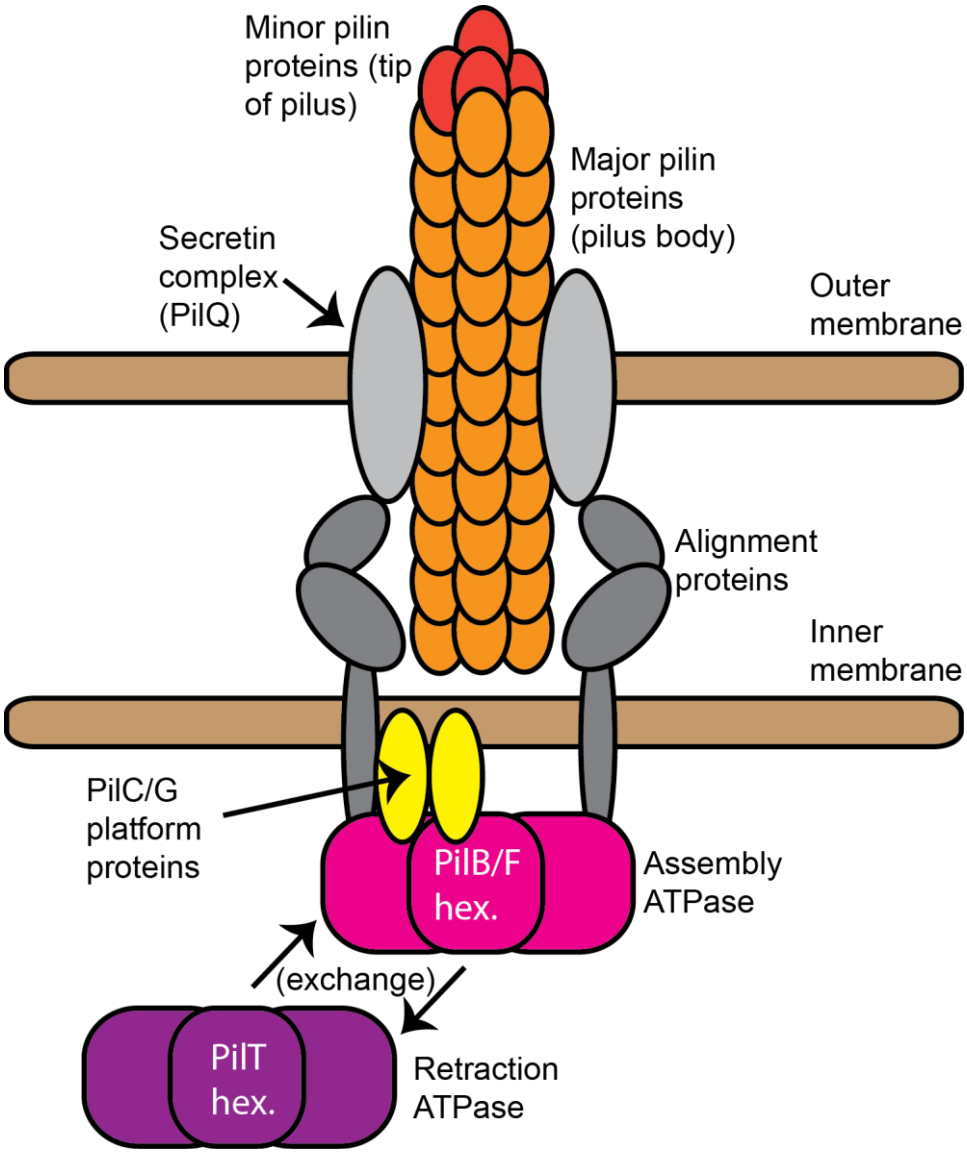

Figure 2*:* **Overview of pilus structure and twitching motility proteins**. Inspired by reference [16]

1.1.3. Sliding and gliding

As opposed to being caused by a molecular motor, sliding depends simply on the expansion of growing bacterial colonies, coupled with a decrease in surface tension, normally in the absence of pili or flagella. Just like molecular motors themselves, sliding/gliding motility has been observed in a variety of bacterial species, which will be discussed later in this section. Sliding/gliding motility is usually (but not exclusively) related to an increased production of bacterial surfactants, including lipopeptides and glyco(pepto)lipids [1,19]. In *P. aeruginosa* growing on agar plates, a loss of flagella or type IV pili leads to motility occurring through sliding, which requires

the secretion of rhamnolipid surfactants [20]. One of the earliest studies on the relevance of surfactants for sliding motility was performed in *Serratia marcescens*, where a surface tension-decreasing lipid serrawettin was detected [21].

In *E. coli* and *V. cholerae,* sliding motility was also observed in the absence of flagella [22]. It was additionally discovered that heat, protease and antibiotic treatments (with chloramphenicol, which inhibits protein synthesis) decrease sliding motility, leading the researchers to conclude that a protein component, and not a secreted surfactant, was the cause of the sliding motility. Electron microscopy also did not show the formation of pili [22].

In *Bacillus subtilis*, it has been determined that surface motility is enhanced in the presence of potassium and when the biotenside (extracellular lipopeptide) surfactin is secreted; this motility type was also identified as being independent of flagellar motility. This behaviour may assist with the movement of *B. subtilis* over plant roots, where it has also been isolated from in the past. This holds true despite *B. subtilis* being a soil-dwelling bacterium, not a plant symbiont [23].

More recently in *Salmonella typhimurium*, an article investigated the motility behaviour on semi-solid media in the presence of low magnesium concentrations. They discovered that a protein called PagM is essential for a form of motility that is not dependent either on flagella or pili-like structures (called “fimbriae”). Additionally, treatment of cells with Proteinase K showed that PagM, and potentially another surface protein, were located in the outer leaflet of the outer membrane of the cells, since proteinase treatment inhibited motility. Inactivating certain production pathways of different surface wetting agents did not decrease motility, however. The authors claim that PagM itself may “promote sliding motility”, especially since replication, as well as degree of motility, was higher in high magnesium environments. They do not exclude that an undiscovered wetting agent also plays a role [24].

1.2. The bacterial flagellum

1.2.1. Overview of assembly and structure

The bacterial flagellum is a large macromolecular structure that is found ubiquitously in a variety of bacterial species. Despite a significant degree of conservation/homology, particularly on the structural level, there are still differences between the flagellar systems and components of different species. Variation is particularly notable, for example, in the type of ion that powers the motor, how fast the motor rotates, and in the rotor and stator components [25]. The flagellum contains roughly 25 different proteins [26] that are organized into substructures serving specific roles in the flagellum. The process of assembly and the roles of different substructures that are of particular interest for the topic of this thesis will be discussed in the next subchapters. Not all components will be covered in detail.

Overall, the flagellum consists of the following components (substructures): 1) the flagellar filament, 2) the flagellar hook, 3) the flagellar rod, 4) the membrane-embedded type III secretion system, interacting on the cytoplasmic side with the FliIHJ ATPase complex, 5) the membrane-embedded MS-ring, consisting of FliF, 6) the membrane-embedded motor proteins, MotA and MotB, 7) the cytoplasmic C-ring, 8) additional accessory proteins that are either transiently associated with flagellar building blocks, or regulate the flagellar assembly and localization [27–29]. The actual secretion system (marked earlier as component number 4) involved in flagellar assembly is strongly related to the injectisome, a structure that injects bacterial virulence proteins into their target host cells [30,31]. The basal body and secretion

system components of the flagellum are depicted in detail in **Figure 3.**

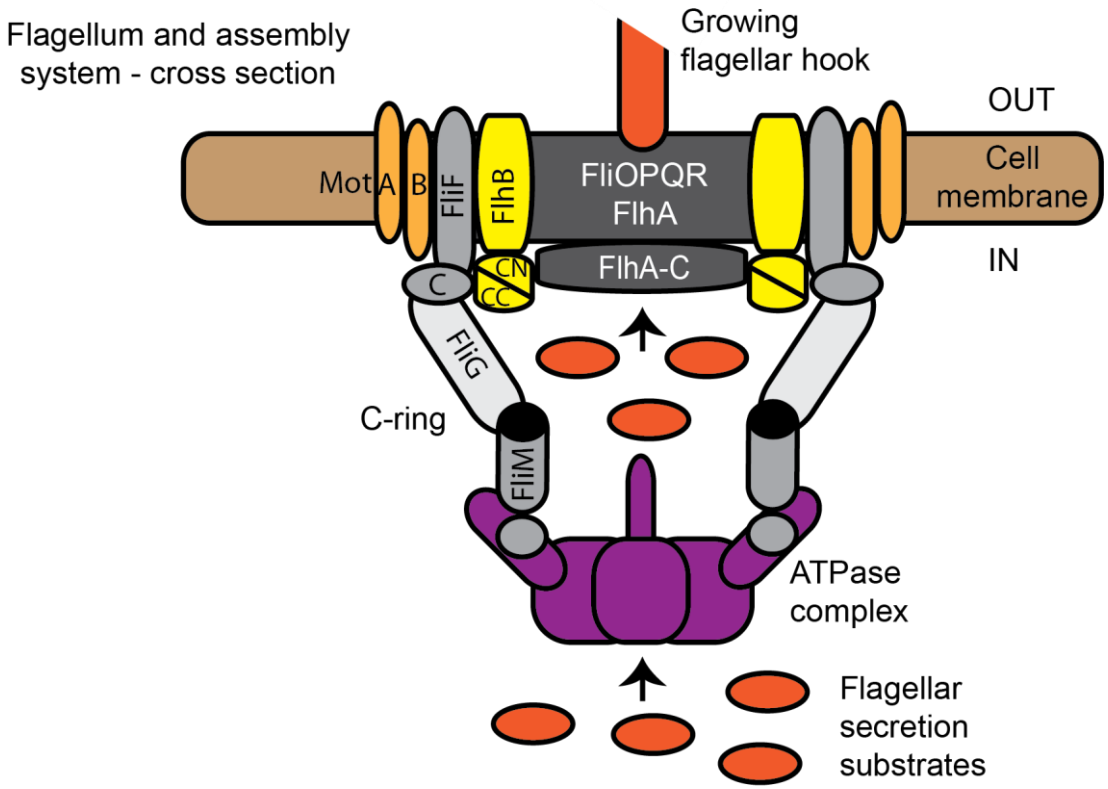

Figure 3: overview of an assembled bacterial flagellum. Inspired by references [26,29].

1.2.2. Membrane-bound secretion system and the ATPase complex

The membrane-bound type III secretion system consists of the proteins FliPQR, FlhA and FlhB. Of these, FlhA and FlhB are located in the centre of the secretion system, extending their cytoplasmic domains into the cell and away from the membrane-bound rest of the secretion system. Until recently, there was no high-resolution structural information available on the membrane-bound regions of the secretion system, until it was investigated in several cryo-EM studies in the last two years; see the next paragraphs [32,33]. The cytoplasmic regions of FlhA and FlhB were better investigated structurally, starting with FlhA-C in *Bacillus* [34], and several FlhB-C structures that were solved in the past. These include FlhB injectisome homologs YscU from *Y. pestis* [35] and Spa40 from *S. flexneri* [36], as well as flagellar FlhB from *Salmonella* and *A. aeolicus* [37].

The membrane domain of FlhA consists of 8 TM (transmembrane) helices. The cytoplasmic domain of FlhA is additionally known to interact with FliD and flagellin (both late-class flagellar substrates), after they are associated with their respective chaperones (FliT and FliS) [34]. It has been determined that FlhA can additionally interact with the MS-ring protein FliF [38], as well as FlhB itself, through FlhB-C [39]. Another study investigated interactions between a non-cleaver (N269A) FlhB-C and FlhA-C. The FlhB-C (since the mutant was lacking the ability to cleave) could not interact with FlhA-C, but the authors speculated that it may require functional cleavage to do so [40].

Beforehand, it was unknown how many copies of the core secretion complex components (FliPQR) would assemble together, until it was determined in *S. typhimurium* that the complex has a $FliP_5FliQ_4FliR_1$ stoichiometry. The study showed that the core resembles a hexameric shape and contains 5 FliP and 1 FliR subunit, with which the outer layer of FliQ subunits is associated [32]. Additionally, it has been determined using cryo-EM that a strong structural similarity exists between the *S. typhimurium* core secretion complex, and the T3SS export gate complex from *Shigella flexneri* [41]. This again confirms that the flagellum-specific and the injectisome-specific T3SS likely evolved from a common ancestor and are highly similar.

Regarding the role of FlhB in this complex; it has been determined using cryo-EM data from the *Vibrio* type III secretion system that the membrane domain of FlhB wraps around the FliPQR complex with its four transmembrane helices. An FlhB loop is involved in controlling the gating of the secretion system, where interactions between FlhB and FliPQR that trigger conformational changes are responsible for opening the secretion gate [33].

FlhA-C and FlhB-C together form an interface for the FliK interaction, which is suggested by the fact that an FlhB-C non-cleaver mutation (P270A) is relieved by an FlhA-C mutation (A489E), which allows FlgK and FliC secretion amounts to be restored to near wildtype levels [42]. Regarding FliK, it is proposed that the conformational change that happens within FlhB-C after interacting with FliK is the trigger that then causes the shift from hook export to filament export; this happens together with a

structural remodelling of the FlhA-C ring (which Minamino et. al [42] claim is responsible for the initiation of filament export).

The ATPase complex, which can interact with the cytoplasmic side of the secretion system, consists of the proteins FliI, FliJ and FliH. It has been determined that the rate of ATP hydrolysis by FliI is not coupled to the rate of export of flagellar substrates, and that even a strongly decreased rate of FliI activity is still sufficient to obtain functional flagella; evidenced by mutations to E211 and a deletion of the 401-410 region in *Salmonella* [43].

A brief overview of the role of FliH/I/J in regard to the interaction with FlhB/FlhA was previously presented as a model by [44]. Initially, a FliH/FliI/FliJ complex is formed in the cytoplasm, which then diffuses closer to the membrane and interacts with cytoplasmic domains of FlhA and FlhB. This temporary complex is positioned directly under the middle of the pore of the secretion system. ATP hydrolysis by FliI then causes substrate translocation, which is then followed by a dissociation of the FliH/I/J complex from FlhA and FlhB [44,45].

FliI itself is brought closer to its final position below the secretion system through an initial interaction of FliH with the C-ring protein FliN, as FliI forms a transitional complex with two FliH molecules. In the next step, FliH interacts with FlhA, which in turn leads to the formation of a hexamer of FliI, located close to the gate of the secretion system. A study from 2014 observes that $FliH_2$-FliI functions as a "dynamic substrate carrier", whereas the FliI hexamer is a "static substrate loader" for the secretion system [45]. Additionally, FlhB-C has also been found to interact with FliH and FliI [46].

1.2.2.1.FlhB

This protein consists of two domains, the membrane-embedded TM domain and the cytoplasmic C-domain (see **Figure 7**, also for a summary of known FlhB interaction partners). The cytoplasmic domain itself is further separated into two fragments, the N-terminal CN and C-terminal CC, after a pH-dependent autocleavage event, which can be prevented *in vitro* by a highly alkaline pH [47]. This occurs between an asparagine and proline residue, which are part of the highly conserved NP(T/E)H cleavage sequence. After the cleavage, the CN and CC fragments retain affinity for each other,

which allows them to be co-purified [48], also see **Figure 4,** top left panel. It has been determined (in *Salmonella*), that while mutating N269 completely inhibits cleavage, mutating P270 only reduces cleavage, without completely preventing it. As a result, both of these mutations cause different phenotypes in *Salmonella.* The N269A mutation led to no export of flagellin at all, while the P270A mutation caused reduced export of flagellin and decreased motility. Both mutants showed polyhooks getting formed [49].

The cleavage itself has important implications for the organism, because it prevents the switch from early to late class flagellar substrates, resulting in a polyhook mutant (in *Salmonella*), also observed in FliK deletion strains [50–52] (see **Figure 4**, top right panel). Despite these discoveries, it is not understood exactly how FlhB and FliK interact, even though different models/explanations for the regulation have been proposed. A study investigating the differences between WT (wildtype) and non-cleaver FlhBs did not find any significant changes in binding behaviour between FlhB and FliK, when a N269A mutation was introduced. The same study also suggests that additional proteins (on top of FliK) are likely involved in the regulation of the substrate switching event [53]

In *Salmonella*, it was additionally determined that several residues from the LARA(I/L)Y (318-323) motif are involved in hydrophobic interactions. Based on the information from the 3B0Z [37] *S. typhimurium* structure and additional experiments later on [54], the L318, A319, R320 and L322 are involved in hydrophobic interactions – partly with closely adjacent residues among themselves, partly with a hydrophobic patch containing A286, P286, A341 and L344. Also from the same paper, a R320A mutation (among others) has an effect both on hook length (longer but also more strongly varied length than wildtype) as well as secretion of FlgD and FlgE (flagellin components, higher secretion than in wildtype). Overall, these effects lead to a decrease in motility. While the authors also tested L318 and L322, results as described above were not observed for these residues [54]. For a visualisation of the discussed residues, see **Figure 4**, right panel.

Additionally, interactions of FlhB-C with rod- and hook-type substrates (FliE, FlgB, FlgE, and FlgD), and filament-type substrates (FlgK, FlgL, and FliC) have been

experimentally confirmed to occur. It was determined that FlhB-C binds more strongly to early substrates (rod/hook) than late (filament) substrates. These interactions are FliK-controlled [42].

Additionally, on the topic of the FlhB/FliK interaction, it was determined that 15 different extragenic suppressor mutations (relative to FliK) exist in FlhB in *Salmonella*, which are all located in the C-terminal part of the cytoplasmic domain of FlhB. These mutations suppress polyhook phenotypes caused by original FliK mutations. The FlhB mutants also showed poor swarming ability compared to WT cells; Williams et. al postulate that this is because the mutants affect not only hook length control but also ineffectively transition to filament assembly. Such phenotypes were termed as "leaky", which means that FlhB is no longer fully relying on a signal from FliK to initiate substrate switching, but there is still a degree of likelihood that it will switch on its own [51].

As discussed by references [55] and [51], another potential explanation for the roles of FliK and FlhB lies with the anti-sigma factor protein FlgM (which is flagellar specific, as well as an export substrate) [56]. A model by Kutsukake et. al [55] postulates that the C-terminal domain of FlhB inhibits the export of FlgM; and since FliK would only interact with FliK when the flagellum is ready for export of late-class flagellar substrates, FlgM could then be exported, which relieves the inhibition of expression of late-class flagellar genes. Williams et. al [51], on the other hand, suggest that FlhB positively regulates both early and late-class flagellar substrates, with FliK being the more important regulatory protein. Kutsukake et. al [55], mark the C-terminal region of FlhB as an inhibitory domain for protein export. Otherwise, in Bacillus, it was determined that mutations to FlhA, FlhB and FliK (also FliOPQR) abolish FlgM secretion [57], highlighting their importance for the successful production of export of late-class flagellar substrates.

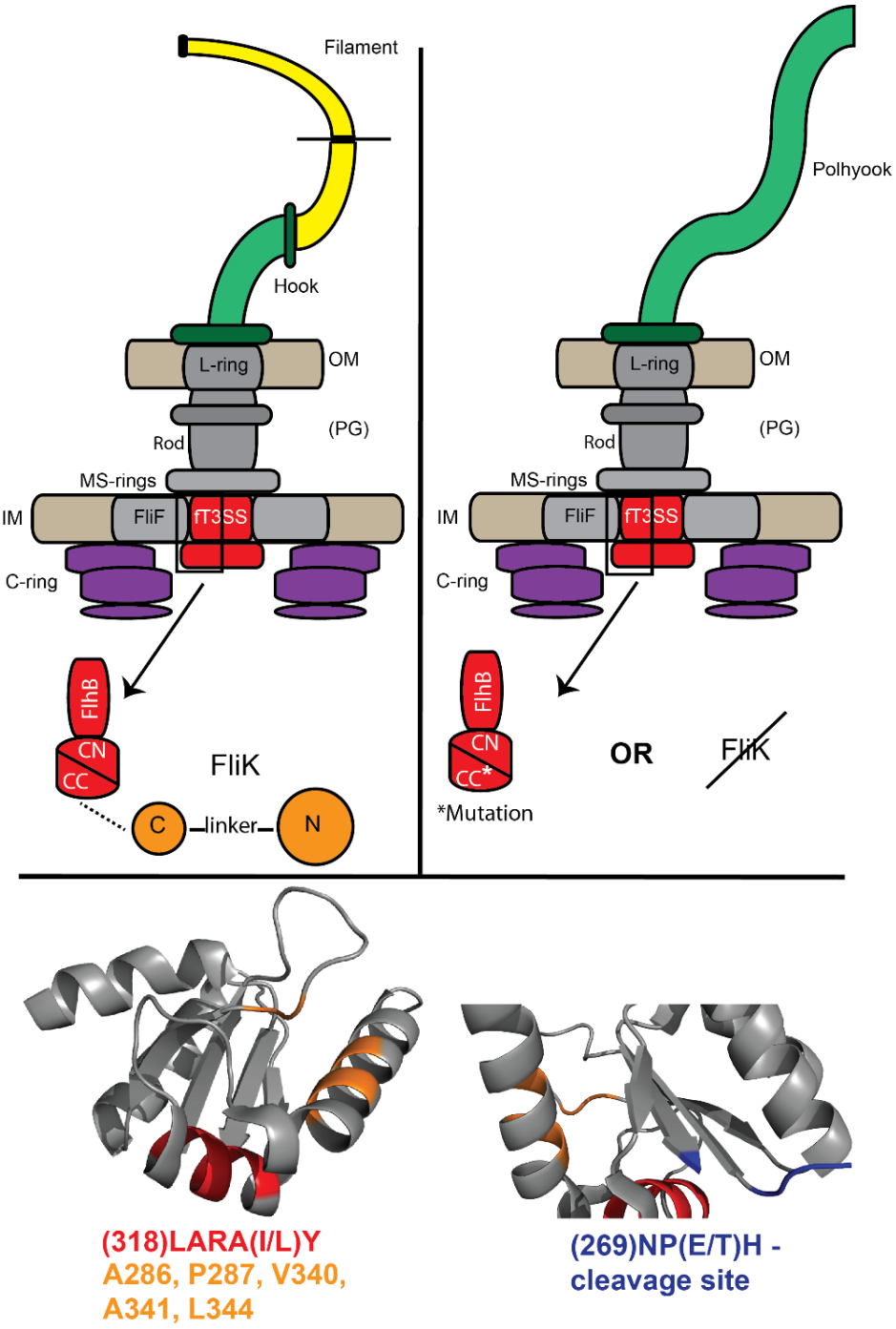

Figure 4*:* **FlhB/FliK interaction and important FlhB residues** (visualised on structure PDB ID 3B0Z with *Salmonella typhimurium* numbering used). Top left panel: WT phenotype, normal FlhB/FliK interaction possible. Top right panel: polyhook phenotype, with a mutation to the FlhB-C cleavage site or a FliK deletion. Bottom panel: colour-coded visualisation of identified key residues in FlhB-C; red: residues involved in stabilizing intra-FlhB-C hydrophobic interactions; orange: residues identified as participating in the hydrophobic patch interacting with hook/rod secretion substrates; blue: cleavage site.

1.2.3. MS-ring and motor proteins

The MS-ring consists of FliF, a membrane protein with a cytosolic domain. The membrane region envelops the membrane-embedded secretion system, and consists of 26 FliF monomers [58]. The C-ring discussed in the previous chapter is associated with the MS-ring through a direct interaction of FliG and FliF, which involves the cytoplasmic domain (=C-terminus) of FliF, and the N-terminal domain of FliG [59,60]. A very recent study performed in *Vibrio* organisms [61] has shown that FlhF somehow seems to promote the assembly of FliF into the MS-ring, and that FlhF increased the amount of FliF present at the pole. Overexpression of *Vibrio* FlhF and FliF together in *E. coli* cells led to a spontaneous assembly/formation of the MS-ring (this did not occur as effectively if FliF was expressed alone). FliG itself was also determined to facilitate the formation of the MS-ring [61].

The MS-ring ring is surrounded by another ring, formed by the MotA and MotB pair, which are the stators of the flagellar system. MotA and MotB contribute to the formation of ion channels, where the number of units depends on the species in question [62]. In the case of MotA/B, the function of the stator depends on the flow of protons, whereas in other cases, where the Mot homologues PomA/B are used, sodium ions are employed instead. In *E. coli,* where extensive research has been done into the roles of MotA/B, they form ion channels with a 4:2 stoichiometry [63]. In *E. coli*, it has been determined that MotA contains four transmembrane helices, whereas MotB only has one transmembrane segment, and a large periplasmic domain which has a conserved peptidoglycan-binding motif; this effectively links the MotA/B complex to the cell wall. There are conserved clusters of negatively charged residues on the (cytosolic) C-terminus of MotA, and positively charged residues on the cytosolic N-terminus of MotB; mutations to either of these regions lead to motility defects [64].

1.2.4. C-ring

The C-ring is a structure formed through oligomerization of three proteins: FliG, FliM and FliN/Y.

Regarding FliG, there is plenty of structural data available, particularly from *H. pylori*, *T. maritima* and *A. aeolicus.* Overall, structures of different individual domains as well as full-length FliG, together with partial complexes of FliG-FliM and FliG-FliF have

been structurally determined [65] [66,67] .FliG is a very flexible protein consisting of three domains, called the N, M and C domains. The domains are connected with linker regions of approximately 20 residues. The domains themselves contain only alpha helices and undergo conformational changes which cause the direction switch of flagellar rotation (CCW/CW). For this event, the M and C domains of FliG are crucial. Judging from structural data, helix C5 of FliG contains conserved triplets of charged residues, which are involved in a reorganization event that brings residues E192 and A193 close together, after they had previously been located 34A apart [68].

There are believed to be 24-26 copies of FliG per flagellum (=per assembled C-ring)[69]. The actual torque-generation is mediated by both FliG and MotA – this occurs through electrostatic interactions of the C-terminal domain of FliG with a cytoplasmic loop of MotA [70].

FliM is located one level below FliG in the C-ring, and then followed by FliN(Y). FliY in *B. subtilis* is significantly larger than FliN in *S. putrefaciens* and contains a domain homologous to FliN as well as an additional CheC-like phosphatase domain, which is involved in dephosphorylation of CheY [71,72]. FliM is, similar to FliG, also divided into three domains, the N, M and C domain. The C-terminal domain has a high degree of homology with FliN; the M domain is involved in FliG interactions [67]. The highly conserved EIDAL motif which allows an interaction with FlhG is found at the end N-terminal end of the N-domain of FliM in *S. putrefaciens*, and in FliY in *B. subtilis/G. thermodenitrificans* [73,74]. For a graphical representation of FliM domains and known interaction partners, see **Figure 7.**

1.2.5. Hook and hook length control

The control of production and secretion of flagellar components is tightly controlled. Flagellin production, due to the thickness and length of the filament, is an important and energy-demanding task for the cell, and the production of flagellin is linked to a successful assembly of the hook [56]. The promotor for transcription of flagellin genes is controlled by an alternative sigma factor, called FliA (also sigma-28). FliA itself is inhibited by FlgM, an anti-sigma factor. When hook length reaches a pre-defined length (controlled/measured by FliK, see next paragraph), FlgM itself functions as a flagellar secretion substrate, and is ejected from the cell, so it can no longer inhibit

FliA´s transcriptional activity. FlgM is also believed to interact with FlhB during this process [49,51,57]. This triggers the expression of flagellin.

A key protein identified in the control of hook length regulation that has already been mentioned in the previous chapter is FliK. Its role was primarily explored in *S. typhimurium,* where it was also determined that a deletion of FliK results in a polyhook phenotype. This phenotype shows that no switch from early to late class flagellar substrates occurs, and an extended hook is created. Such a hook is longer than the usual 55-70 nm hooks in *Salmonella.* [75]. FliK itself is also secreted during hook assembly.

The only structural information available on FliK was obtained in a solution NMR study [76], which was later also used to model a FlhB/FliK interaction, based on a solved crystal structure of FlhB-C from *S. typhimurium.* The study postulates that preventing the FlhB cleavage prevents FliK from interacting with the FlhB cleavage site, due to sterical hindrances resulting from different amino acid positions compared to a cleaved WT FlhB [76].

FliK itself consists of two domains, the N- and C-terminal domain, which are connected by a flexible linker. The N-terminal domain, which is putatively natively unstructured, is the region involved in measuring the length of the flagellar hook. The C-terminal domain, on the other hand, binds to FlhB-C; in addition to the modelling evidence [76], this has also been experimentally confirmed in recent years in *Salmonella* [77,78] . Using photo-crosslinking experiments, Val302 and Ile304, found in a compactly folded part of the C-terminal domain, called FliK-T3S4, were shown to bind to FlhB-C [78]. Additionally, the FliK linker region was shown to be important for a successful interaction between FlhB-C and FliK-C, where a deletion of residues 206-265 of FliK reduced the binding affinity of FliK-C for FlhB. The linker region itself contains a large number of proline residues (10) which causes it to be intrinsically disordered as well [77].

The overall fold of FliK as a whole was investigated by atomic force microscopy, revealing that it resembles a smaller and a larger sphere, connected by a string-like region. The larger sphere corresponds to the N-terminal domain, and the smaller sphere is the C-terminal region [79]. The Kinoshita et. al paper [77] postulates that as

soon as the previously mentioned residues Val302 and Ile304 of FliK are able to interact with FlhB-C, the switching event occurs. This, as they propose, is only possible when the linker region of FliK is fully extended [77] .

1.2.6. Accessory and regulatory proteins

Three different proteins with important roles for the context of this thesis are covered in this section (FlrA, FlhG and FlhF). FlhG and FlhF are discussed in **1.2.6.** only in the context of domain organization, interaction partners and structural studies that have been carried out with them. For their specific roles in organisms with different flagellation patterns and the physiological effects of FlhG and FlhF mutations, please see chapter **1.4.**

1.2.6.1. FlhG

FlhG is an ATPase protein present in many (but not all) flagellated bacteria. It is alternatively known under two additional names, which are FleN and YlxH. The protein is labelled as FlhG in *C. jejuni, S. putrefaciens* and *Vibrio* species [74,80,81] ,YlxH for example in *Bacillus subtilis/Geobacillus thermodenitrificans* and *Helicobacter pylori* [74,82,83]. As FleN it is known primarily in *Pseudomonas* species [84,85].

It is also a known interaction partner (and activator) of the SRP-like GTPase FlhF, which it stimulates through its N-terminal helix, more specifically through a conserved DQAxxLR motif [82,86,87]. Together, FlhF and FlhG control the number and positioning of flagella in different ways depending on the species they´re located in, and other accessory proteins. In certain monotrichous species, FlhG has an important interaction partner called FlrA/FleQ, which is involved in transcriptional control [85,88,89]. For more detail on FlrA/FleQ see chapter **1.2.6.3**.

FlhG itself is closely related to MinD, sharing with it the conserved regions involved in the binding of ATP and magnesium, as well as other regions involved in ATP hydrolysis[74,90]. Like MinD itself[91,92], FlhG can undergo ATP-dependent homodimerization, when it also interacts with the inner cell membrane through a C-terminal membrane-targeting sequence, which consists of an amphipathic helix (MTS) [74,93]. The only structural information available to date on FlhG itself comes from *G. thermodenitrificans*, available in both the monomeric and dimeric form (PDB structure 4rz2 and 4rz3, respectively) [74]. Additionally, the *P. aeruginosa* homolog,

FleN, has itself been structurally characterized [93,94]. For a summary of FlhG interaction partners and domain organization see **Figures 7 and 5.**

1.2.6.2. FlhF

FlhF has been structurally characterized only in *Bacillus* species. It is an SRP-like GTPase with similarities to both Ffh and FtsY, the other members of this class. Additionally, it has been discovered that the GTPase activity of FlhF is stimulated by FlhG, specifically via the N-terminal activator helix [82,86]. FlhF possesses a natively unstructured basic domain (B-domain) at its N-terminus, which has been directly implicated in flagellar assembly; this domain is involved in the recruitment of FliF to the pole in *V. cholerae* [95]. From a structural point of view, FlhF can be present either as a monomer (inactive, apo state/GDP bound) or a dimer (active, GTP bound). The GTP hydrolysis induces a dissociation of the homodimer (which is promoted by the interaction with the activator helix of FlhG). The NG domain of FlhF is the catalytically active one (with the GTPase motif), and also the one with SRP homology [82,86]. The domain architecture of FlhF and FlhG is shown in **Figure 5** below. For an overview of the role of FlhF in different organisms, and the establishment of different flagellation patterns, please see section **1.4** of the thesis.

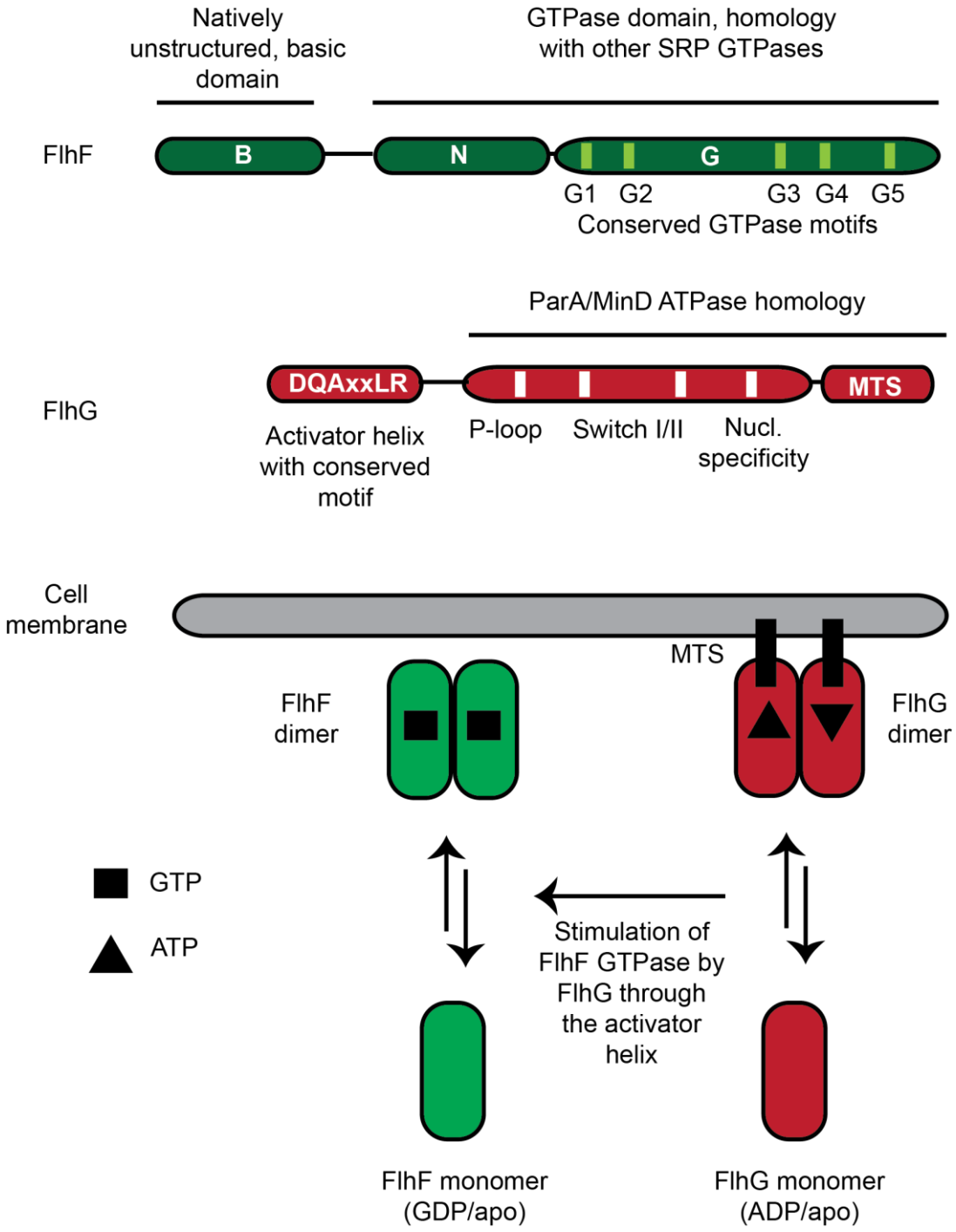

Figure 5: Structure and interplay of FlhF and FlhG Top panel: domain architecture with conserved regions indicated. Bottom panel: nucleotide, dimerization and membrane-dependent interactions of FlhF and FlhG. Inspired by references [29,96] .

1.2.6.3 FlrA

FlrA is an enhancer-binding protein (EBP), which is a master regulator for the transcription of flagellar assembly genes, and accomplishes this by binding to promoters of flagellar and biofilm-related genes [97,98]. FlrA belongs to the broad family of NifA/NtrC EBPs [99,100], but possesses significant differences to the typical member of this protein family. It does not have a corresponding sensor kinase protein, and it

lacks two strongly conserved residues that are typical for NtrC family proteins; these are Asp54 and Lys104. FlrA (FleQ) was first investigated as a protein that controls adhesion and flagellar assembly-relevant proteins in *P. aeruginosa* [100] .

The DNA-binding interaction of FleQ/FlrA has primarily been explored in *P. aeruginosa*, where a consensus sequence for promoter binding has been identified, and a model for binding to DNA has been proposed. In this organism, FleQ is essential for switching between free-swimming (planktonic) and biofilm-based lifestyle changes [97,101]. FleN (FlhG) and the second messenger cyclic-di-GMP are important factors in this. Overall, high cyclic-di-GMP levels lead to a decrease in transcription/expression of flagellar genes, and an increase of production of genes from *pel/psl* operons, which contains biofilm genes [102]. **Figure 6** below shows how FlrA/FleQ binds DNA – conformational rearrangements occur in the presence of c-di-GMP and absence of FleN/FlhG, which allows the FleQ hexamer to unblock one of the two DNA sequence "boxes" located in a given promoter region. The FleQ hexamer basically bends DNA between the two binding regions when it is bound to both of them, and then straightens it again when it is interacting with only one of the regions. The model investigated the binding of FleQ to biofilm genes in *P. aeruginosa (*see **Figure 6**).

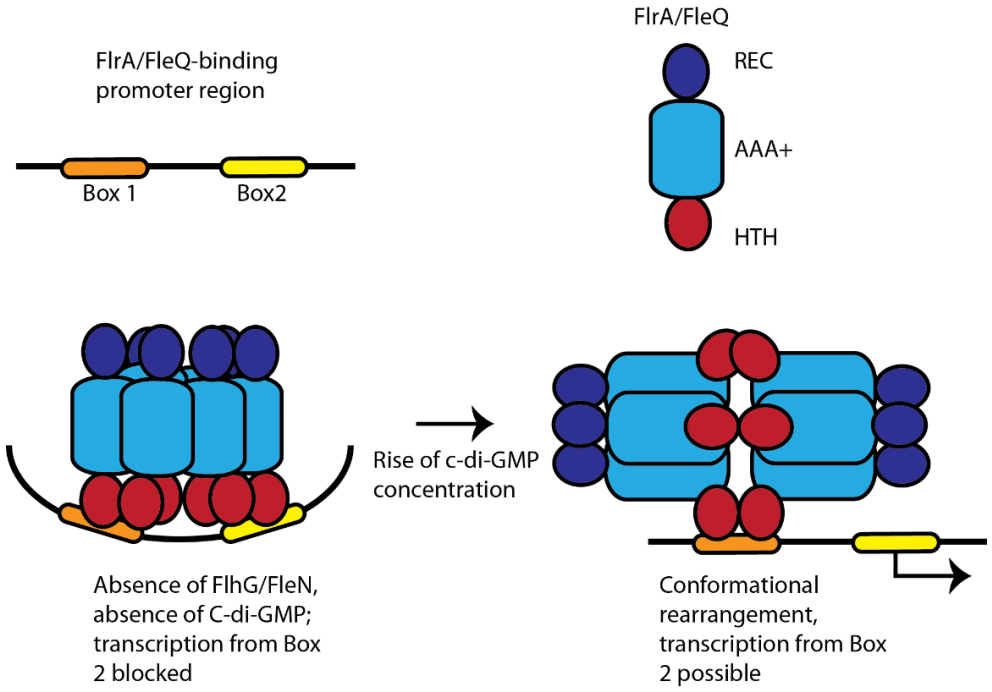

Figure 6*: model of the FleQ/DNA binding interaction*. Diagram inspired by references [101,103].

FlrA itself is made up of three domains (see **Figure 7**), the FleQ-like domain (also called Rec), the AAA+ ATPase middle domain, and the C-terminal DNA-binding HTH domain. The Rec domain is primarily involved in mediating dimerization [104]. The ATPase domain is capable not only of ATP hydrolysis, but also of cyclic-di-GMP binding. The binding of this signalling molecule has been shown to have a regulatory function in *P. aeruginosa*, where it affects the FleN/FleQ interaction [102,103]. The *S. putrefaciens* homologs of FleN and FleQ would be FlhG and FlrA, respectively. On top of this, the AAA+ domain is involved in a hexamerization interaction [103]. The last of the three domains, the HTH domain (helix-turn-helix) is involved in the binding of DNA, which enables FlrA/FleQ to carry out its role as a transcriptional activator.

In *P. aeruginosa*, FlhG reduces the intrinsic ATPase activity of FlrA; the effect is even more prominent when both cyclic-di-GMP and FlhG are both present [102,103,105]. Additional research demonstrates that FlhG decreases the ATPase activity of full-lengh FlrA, and that the initial ATPase activity of FlrA is 5-fold higher than that of FlhG [93].

Structural information is only available so far on the *P. aeruginosa* homolog FleQ, which itself is missing the HTH domain (example PDB ID structures include 4wxm, 5exx, 6jdi, and others [88,103,104] . It has previously been shown that the interaction of *P. aeruginosa* FleQ and FlhG(FleN) is ATP dependent, and that FlrA binds to promoters of FleSR and FlhA [89,102]. A combination of structural and biochemical methods have allowed a better understanding of how FlrA might bind DNA, and how this is related to its oligomerization state. The **Figure 6** previously shown indicates how FlrA hexamers (in the presence and absence of c-di-GMP) bind DNA.

Overall, it has been determined that FleQ/FlrA is found only in species of gammaproteobacteria that have polar flagellation patterns (monotrichous/lophotrichous species). This is a clear contrast to FlhG, which is, for example, also present in *Bacillus, Helicobacter and Campylobacter* species [29]. Interestingly, a single point mutation in the FlrA homolog FleQ in a pathogenic Pseudomonas aeruginosa strain is enough to completely abolish flagellar formation (G240V), highlighting the essential role of the protein in flagellar biosynthesis, and is located in a conserved Mg^{2+} binding site [106].

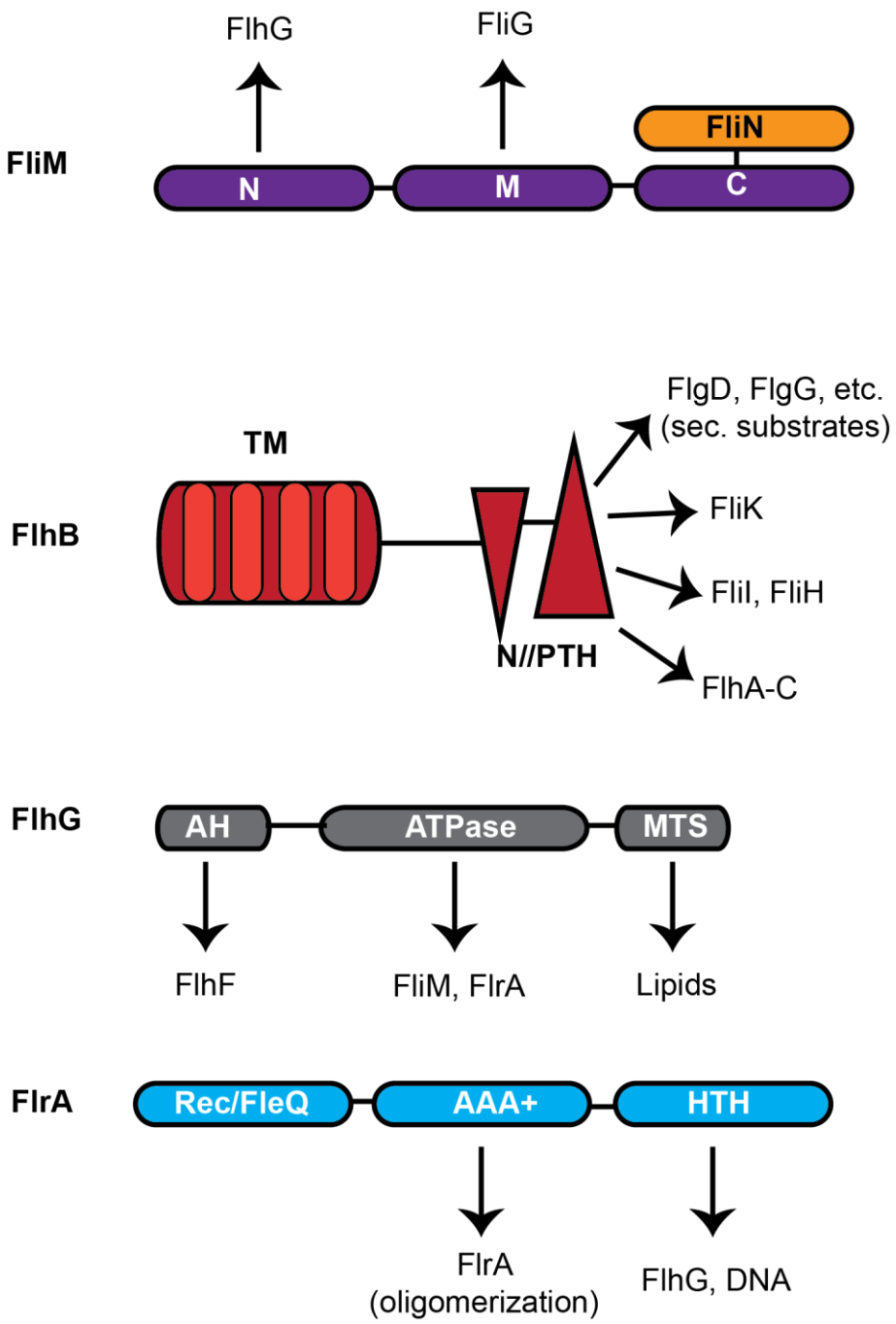

Figure 7: **Overview of domains and known interaction partners for key proteins of interest – FlhG, FlrA, FliM and FlhB**.

1.3. Chemotaxis

Bacteria base their movement upon detection of different compounds in the environment – with a biased random walk, they will move towards nutrients or other chemicals they require (together called chemoattractants), and away from toxic and harmful chemicals (together called chemorepellents). Changing the direction of

movement depends on the direction of flagellar rotation (alternating between clockwise (CW) and counterclockwise (CCW)); in *E. coli*, CCW rotation of flagella leads to forward movement, while a switch to CW rotation causes cells to tumble. The overall process and its regulation are together called chemotaxis [107–109].

In addition to the role of moving towards nutrients and away from toxins, which is particularly important in low nutrient and inhospitable environments, chemotaxis has more recently (2019) also been suggested as a tool promoting proliferation of cells in high-nutrient surroundings. According to [110], chemotaxis also allows bacterial cells (in the case of this study, *E. coli*) to spread further out in soft agar conditions (using what they named "navigated range expansion"), and to already navigate towards more profitable areas, even before the nutrients in their current position are fully depleted [110].

Additionally, and in a more applied context, chemotaxis is an important system to consider when investigating the usability of bacteria to degrade toxic compounds themselves, to be used in a bioremediation role (e.g., environmental cleanup and restoration of damaged ecoystems)[111–113]. It has been discovered that different toxic compounds can still be used as energy sources or nutrients by specific and adapted bacterial species [114]. Examples include toluene and chlorinated ethenes that are chemoattractants for *Burkholderia cepacia* and different *Pseudomonas* species [115,116]. Overall, such adaptations allow different bacteria to survive in highly inhospitable environments, or in specific ecological niches, to gain advantage over other organisms.

Despite the vast variety of chemoattractants and chemorepellents themselves, the signalling system that controls chemotaxis is almost ubiquitously present in prokaryotes, and it has been determined that it likely evolved from a less complex two-component system, similar to those that control bacterial transcription [117].

Despite being so common, there is a high diversity within the signalling proteins involved in chemotaxis, particularly in the receptor proteins themselves (likely due to the significant substrate variety, as discussed). This is particularly true for the ligand-binding domains ("LBDs"), where close to a hundred different ones have been discovered to date [118]. In this context, experiments were additionally performed

showing that a chimera/hybrid receptor assembled from components of different species can still possess functionality, and enhance the chemotaxis pathway of the original organism; this approach, utilizing components from *Pseudomonas putida* and *Bacillus subtilis* chemotaxis systems that detect amino acids, was successfully used in combination with *E. coli* receptors [119].

The whole chemotaxis system possesses a high degree of complexity, with many more different proteins involved. The most well studied, and one of the least complex in comparison with other species, is the *E. coli* chemotaxis system. Briefly, chemotaxis depends on the detection of chemical compounds through integral membrane receptors called methyl-accepting chemotaxis proteins, which are associated with CheA, a histidine kinase, and CheW, an adaptor protein [107,108]. CheY controls the switch of the direction of flagellar rotation in response to chemical gradients. It is active in its phosphorylated form (and triggers clockwise rotation), and it is dephosphorylated by the CheZ phosphatase (which triggers counterclockwise rotation) [108]. CheY itself is also a known interaction partner of the C-ring proteins FliM and FliN; in *E. coli*, a GFP-CheY did not bind to flagellar motors that lacked FliM/FliN, and association of CheY-P directly with FliM and FliN was also observed in the same organism [120,121] . After the rapid initial response to the detection of a chemical gradient (and the CheY/CheZ interplay), four conserved glutamate residues in the MCPs are methylated and demethylated, respectively, by CheR and CheB, which modulates the response. A graphical summary of the chemotaxis system is shown in **Figure 8.**

The MCPs themselves are not distributed overall across the cell surface but are rather arranged in bundles or clusters – this allows much faster response due to the rapid enhancement of the signal by the accessory and interaction proteins discussed in the previous paragraph. MCPs also interact with each other in a cooperative manner, which leads to better integration of the signals received by the cell. During ligand binding and methylation of specific residues, conformational changes and displacements within the receptors occur, particularly in the so-called “HAMP” domain, which contains several amphipathic helices and is also involved in dimerization interactions [122,123].

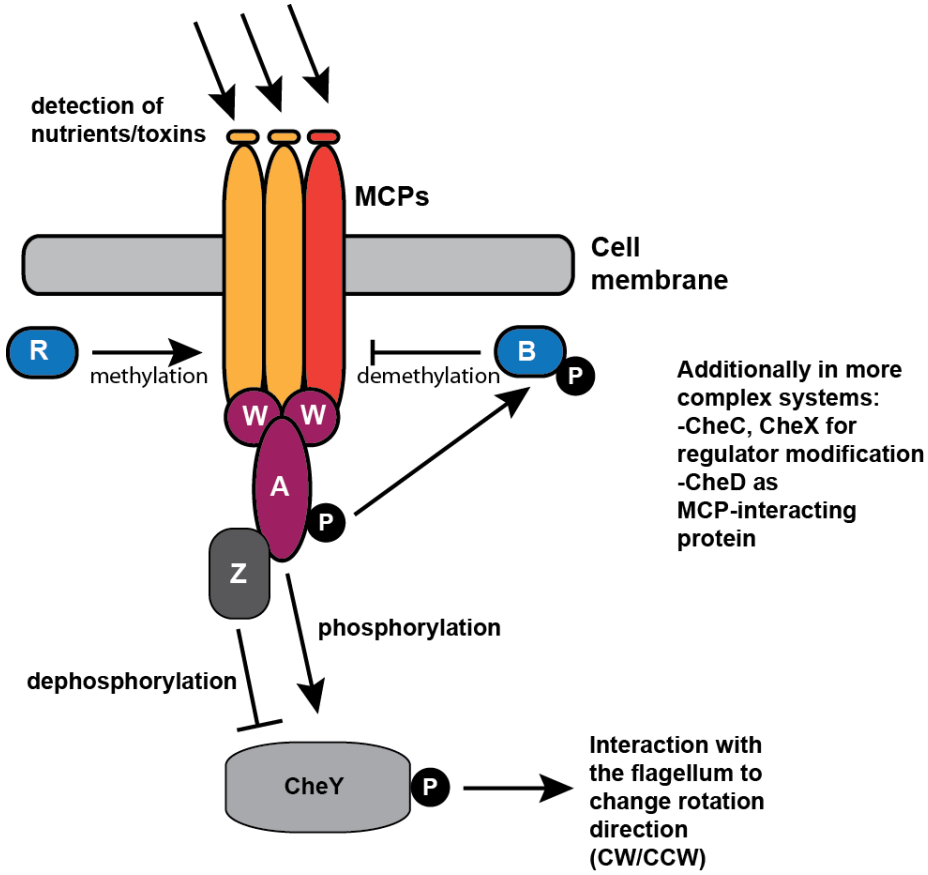

Figure 8: Overview of chemotaxis-involved proteins. Inspired **by references** [108,117]. R-CheR, B-CheB, Z-CheZ, P-phosphorylated site, W-CheW, A-CheA, MCP-methyl accepting proteins.

1.4. Bacterial flagellation patterns and the importance of the FlhF/FlhG pair

Flagellation is essential for bacterial cells that are freely swimming, whether this is in a pathogenic context of a bacterium targeting a host cell, or bacteria migrating together to form a surface-attached biofilm. Depending on the bacterial environment, interaction with its surroundings, and the evolution of different species, a flagellated bacterium can have a variety of different flagellation patterns. Overall, the structure of the flagellum is relatively well conserved, although differences particularly in regulation of number and positioning, as well as other components, can exist. Despite the enormous variation in the factors outlined above, only four main types of flagellation patterns exist (with some exceptions discussed later in this chapter): peritrichous, monotrichous, lophotrichous and amphitrichous (see **Figure 9**), [29,124,125]. Overall, an increased number of flagella is better suited to a

more viscous environment. Regarding different bacterial species, examples for peritrichous flagellation would include *B. subtilis* or *E. coli, H. pylori* for lophotrichous flagellation, *P. aeruginosa*, *C. crescentus* and *S. putrefaciens* for monotrichous, and *C. jejuni* for amphitrichous flagellation [29] . In many organisms with different flagellation patterns, a very important regulatory system involves the proteins FlhF and FlhG. Their importance is discussed later in this chapter, particularly in terms of their effects on the flagellar number and positioning, as well as their role in pathogenicity, if applicable. Structural and organizational aspects of FlhF and FlhG have already been discussed in the chapter **1.2.6.**

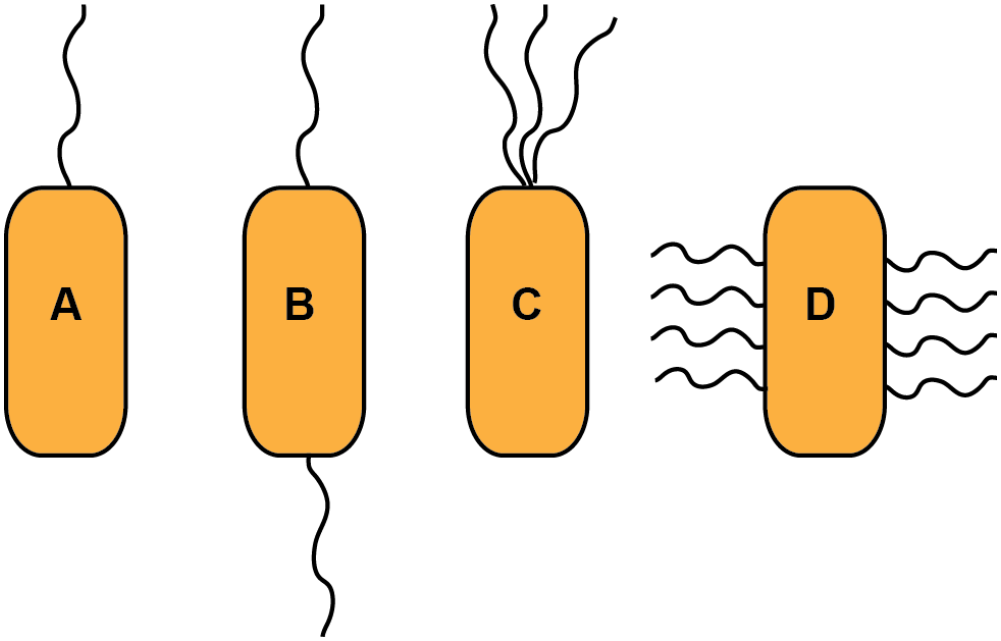

Figure 9: overview of different primary bacterial flagellation patterns. A – monotrichous flagellation B – amphitrichous flagellation C – lophotrichous flagellation D – peritrichous flagellation

1.4.1. Peritrichous, gram-negative (species lacking FlhF and FlhG)

E. coli and *S. typhimurium* are important model organisms which have been used in a number of studies on flagella, motility in general and chemotactic processes. Both of these organisms share the lack of FlhF and FlhG as regulatory proteins for flagellar positioning and number, as well as a peritrichous flagellation pattern. Both organisms normally possess 5 to 6 flagella. There are no identified "landmark" proteins that would control the positioning of flagella in these organisms, based on the current understanding [29].

In *Salmonella* species, the presence of the flagellum is essential for pathogenesis, and a lack of motility significantly reduces or abolishes virulence [126,127]. It has additionally been determined that even upon encountering a surface (and transitioning to swarming mode), *Salmonella* cells do not increase the "density" of flagella. This means that they do not produce more of them while maintaining the same cell size, they rather increase the cell length while inhibiting cell division, which leads to the formation of new flagella as the cell grows, linearly proportional to the increase in cell length. The flagellation pattern therefore stays unmodified [128].

In *E. coli*, flagella are distributed non-randomly and unevenly on the lateral sides of the cell. It has been observed that a greater proportion of flagella is located at the side corresponding to the old cell pole after cell division, leading to an asymmetric distribution; the same is true for chemotactic receptors, which accumulate at cell poles continuously. Hence, an uneven distribution of flagella may be beneficial for chemotaxis [129]. In *E. coli* it has also been observed that the movement of individual flagella in the same cell occurs in a coordinated manner, where a switch of rotation direction (from CCW to CW) in a single flagellum introduces a tumbling motion of the cell. This is termed the "simple veto model" , and has such a strong effect because a group of flagella are normally bundled together to push the cell forward [130]. Using further analysis and with the help of mathematical modelling, it is now known that a tight relationship exists between the presence of phosphorylated CheY (CheY-P) and the switching of flagella to CW rotation. At high concentrations of CheY-P, several flagella can actually switch their rotation direction at once, which increases tumbling even more [131].

1.4.2. Monopolar flagellation (dependent on FlhF and FlhG)

As opposed to *E. coli* and *Salmonella* species discussed in the previous chapter, gram-negative species with monopolar flagellation depend strongly on FlhF and FlhG, as well as other accessory and regulatory proteins for the control of the number and positioning of flagella [29,96].

In monotrichous polar flagellates (see chapter **1.5** for more details on *S. putrefaciens*), FlhF and FlhG are joined by two additional proteins that coordinate flagellar positioning and their number. One of these proteins is HubP, which was initially

discovered in *Vibrio* species, where it functions as an important interaction partner of proteins involved in different cellular processes by recruiting them to the pole. These include proteins that are involved in binding of the chromosomal origin, chemotaxis machinery and, finally, the flagellum. HubP is polarly localized for most of the cell cycle, but migrates to the middle of the cell before cell division occurs [132]. While HubP was determined to interact with FlhG and recruit it to the pole in *V. alginolyticus* [133], it interacts primarily with FlhF in *S. putrefaciens,* as well as the phosphodiesterase PdeB [134,135]. Additional interaction partners of HubP still need to be identified. The second protein of key importance in monotrichous polar flagellates is FlrA (FleQ), which has been discussed in more detail in chapter. **1.2.6.3.**.

Returning back to FlhF and FlhG themselves, their roles performed in monotrichous polar flagellates are strongly conserved; FlhG usually controls the number of flagella, and FlhF controls their positioning. In *Pseudomonas* and *Vibrio* species, respectively, an FlhG deletion results in a hyperflagellation phenotype, which in *Pseudomonas* leads to a flagellar bundle at the pole. A deletion of FlhF in *Vibrio alginolyticus* causes loss of flagella [84,87]. Historically, FlhF was first identified roughly 20 years ago in *Pseudomonas putida*, where it was determined to have a role in flagellar positioning, as well as stress response. A lack of FlhF resulted in a delocalized, random flagellar positioning, and its role was further hinted at due to its location in the motility gene cluster [136].

1.4.3. Peritrichous, gram-positive (dependent on FlhF and FlhG)

Flagellation in peritrichous, gram-positive species has been most closely studied in *Bacillus* organisms. In *B. subtilis,* the arrangement of flagella is non-random; the structures are positioned in a grid-like pattern, and absent from the poles. Mutations to FlhF lead to an increased amount of flagella being present at each pole, while mutations to FlhG result in an aggregation of basal bodies, and several flagella growing out of the same position [137,138]. Compared to, for example, monotrichous flagellates, FlhG does not regulate the number of flagella. In *B. subtilis*, this is accomplished by inhibiting the degradation of SwrA, which is a key regulator of flagellar genes in this organism. More specifically, this pathway is regulated by the AAA+ protease LonA, which can only degrade SwrA together with another protein – swarming motility inhibitor A [139]

In another *Bacillus* organism*, B. cereus,* FlhF has been implicated in pathogenicity, since levels of different virulence factors are altered (both positively and negatively, depending on the factor) in the absence of FlhF [140]. For example, a component of the BL hemolysin (L2) is recruited by FlhF to the plasma mebrane, where it gets secreted, and a lack of FlhF significantly reduces the secretion of the L2 component [141]. This would suggest that FlhF could possess a role in indirectly coordinating infection behaviour (swarming motility and secretion of virulence factors), and not only flagellation and flagellar positioning in *B. cereus* [140–142].

1.4.4. Other

In addition to the common patterns discussed in the above chapters, there are also bacterial species which possess flagella at both poles, have periplasmic flagella, or even a single primary lateral flagellum. An example of an organism with a single lateral flagellum (also called a "medial flagellate") is *Rhodobacter sphaeroides*, a purple photosynthetic bacterial species [143,144]. This is a highly unusual flagellation system since a single lateral flagellum normally carries out a secondary role, and is not constantly present (see the chapter on *S. putrefaciens´* dual flagellar system, for example).

A representative organism for amphitrichous flagellation (one flagellum at each pole, see **Figure 9B**) is *Camplyobacter jejuni.* The amphitrichous flagellation pattern provides the organism a distinct motility type, called "darting motility"; this is essential for its colonization of human and animal hosts [145]*.* This organism contains both FlhF and FlhG, although the ATPase domain of FlhG is not involved in the control of flagellar number, as in monotrichous flagellates like certain *Vibrio* and *Shewanella* species. FlhG regulates flagellar number with distinct regions not found in homologs from monotrichous flagellates. In *C. jejuni*, a deletion/mutation of both the C- and N-termini of FlhG result in hyperflagellation, although the effects are more pronounced when the N-terminus is altered [81]. Additionally, FlhG also interacts with FtsZ, and represses its role in the triggering of cell division; it also acts together with components of the flagellar motor to prevent cell division starting at cell poles. In the absence of FlhG, cell division can therefore start at cell poles, rather than in the midcell region, as is commonly observed [145].

In *C. jejuni*, FlhF has been found to play a key role in pathogenesis. An inactivation of FlhF affects various abilities of the bacterium that are essential for successful host colonization, such as formation of biofilms, adhesion to host cells, and the ability to invade host cells. Furthermore, FlhF has been determined to have an increased rate of expression throughout the process of infection, and a lack of its function also results in the downregulation of different genes which are not involved in flagellar biosynthesis, such as the Fed group of proteins ("flagellar coexpressed determinants")[146]. In *C. jejuni*, FlhF has also been determined to be an important factor in the initiation of flagellar assembly, since FlhB, a component of the fT3SS´s core secretion system, no longer localizes to the poles in the absence of FlhF [147]

While possessing a single polar flagellum, *Caulobacter crescentus* is controlled completely differently than the monotrichous polar flagellates covered in 1.4.3. (which belong to the gammaproteobacteria). Being an alphaproteobacterium, *C. crescentus* does not regulate its flagellation through FlhG and FlhF, but rather the TipN and TipF protein pair, which are both membrane proteins [148–150]. TipN is a so-called landmark protein which is transferred from the old to the new cell pole during the cytokinesis stage of the cell cycle, which signals that the flagellum should be assembled at that position. When TipN is lacking, flagellar delocalization occurs [149,151].

Regarding TipF, it is a cyclic-di-GMP binding protein that responds to an increase in the levels of this second messenger (this occurs at the transition from the G1 to the S phase of the cell cycle). TipF can then localize to the pole where the TipN landmark protein is already present. TipF, in turn, can recruit flagellar building blocks to the cell pole. TipF is then removed from the relevant pole as soon as the c-di-GMP levels start do decrease [150].

Borrelia burgdorferi (the causative agent of the deer tick-transmitted Lyme disease) belongs to the spirochete class of bacteria, and possesses between 7-11 periplasmic flagella. Such flagella contain a structure called the "collar", not observed in any other type of bacteria. A deletion of the collar protein FlcA causes a decrease in flagellar number, length and angle relative to the cell body [152]. The periplasmic flagella are also highly unique because they serve a role not only in motility, but also in maintaining cell shape, being involved in external stress resistance and having a

cytoskeletal role [153]. Recently, it has been discovered that flagellation in *B. burgdorferi* is even controlled by an FlhF homolog, which has an overall similar structure and enzymatic properties as counterparts from other organisms. A deletion of FlhF leads to a decrease in flagellar number, as well as a lack of normal cell morphology, the flat-ribbon shape. FlhF in *B. burgdorferi* has been implicated in the localization of FliF, and in the number and positioning of flagella [154].

1.5. Shewanella putrefaciens, the organism

1.5.1. Living environments and pathogenicity of *S. putrefaciens* and *Shewanellaceae*

Shewanella putrefaciens is a gram-negative, rod-shaped bacterium, with a variety of living environments, closely related to *Shewanella alga.* It is chiefly found in different water bodies (seawater, but also freshwater, as well as sewage), and was additionally found to exist in the vicinity of oil and natural gas deposits [155 156]. It was the first *Shewanella* organism to be discovered, already in the early 20th century (1931), but was initially named *Pseudomonas putrefaciens.*

The *Shewanella* genus contains roughly 40 different bacterial species, all of which are monotrichous polar flagellates, together belonging to gamma-proteobacteria, classified as facultative anaerobes [157]. A characteristic of *Shewanella* organisms is that they have a strong tolerance of cold temperatures; most species are able to grow at temperatures under 5 degrees Celsius, although the temperatures for optimal growth exceed 16 degrees [157]. The species *S. frigidimarina, S. gelidimirina* and *S. livingstonensis* have even been isolated from coastal areas of the Antarctic, and are particularly resistant to cold temperatures [158,159].

S. putrefaciens specifically is not usually pathogenic to humans in its own right, although different cases have been reported where infections of soft tissues, eyes and skin can occur [160–162]. Additionally, the bacterium is problematic in industrial-scale food production because it causes spoilage of seawater fish [163], as well as different types of meat products [156,163]. It has also been identified in biofilms on stainless steel surfaces, and contributes to food spoilage by secreting trimethylamine and volatile sulfides [164].

Different *Shewanella*, including *S. putrefaciens*, are capable of using a variety of different final electron acceptors in the electron transport chain, as alternatives to oxygen. *S. putrefaciens* is capable of iron reduction [165] as well as manganese reduction [166]. Regarding the potential use of *S. putrefaciens* for radioactive cleanup, experiments have shown that Technetium 99 can be reduced by the bacterium, which removes the material from solution, as the reduced form is much less soluble and primarily stays associated with cells after it is used as an electron acceptor [167]. *S. oneidensis* is also capable of using Technetium 99 as an electron acceptor, where results show that a reduction of Tc(VII) to Tc(IV) by the bacterium leads to the formation of black aggregates on the surface of colonies, which contain the reduced, insoluble Technetium [168].

1.5.2. Dual flagellation and its control

S. putrefaciens is a polar monotrichous bacterial species, but it also has an inducible lateral flagellum, which is encoded in a separate gene cluster, and primarily contains proteins unique to it [73,169]. Also other species, in addition to a variety of *Shewanella* organisms, have a closely related polar/lateral flagellar system: these include *Aeromonas, Vibrio, Azospirillum* and *Rhodobacter* bacteria [8,170].

In *Shewanella*, the polar and lateral components have high sequence similarity, but are still distinct. Whether and to what extent some of the components can undergo crosstalk interactions, or are interchangeable, is still being explored. Only the polar flagellum is chemotaxis-controlled [169]. The first (=polar) flagellar gene cluster contains genes 2556-2605, among those a number of additional genes compared to the lateral cluster, hence being longer (see **Figure 10, top panel**). Among other genes, FlhF and FlhG, for example, are not found in the second (=lateral) gene cluster, which otherwise contains genes 3447-3485 (see **Figure 10, bottom panel**) [73]. This is an indication that the positioning and number of the lateral flagellum are not controlled in the same manner as those of the polar flagellum (with the FlhFG pair), and the control of lateral flagellation in general is less strict.

A small number of genes are also found as “orphans”, meaning that they are located outside of their main designated flagellar cluster. These genes are PomAB (related to

MotAB, and motor components of the polar flagellum), as well as MotXY. For *S. putrefaciens* specifically, the gene expression from the polar cluster is controlled primarily either by FlrA/RpoN, or by FliA (in the context of FlgM). There are, however, still a number of flagellar genes the control of which is unknown, or has not been experimentally determined [73].

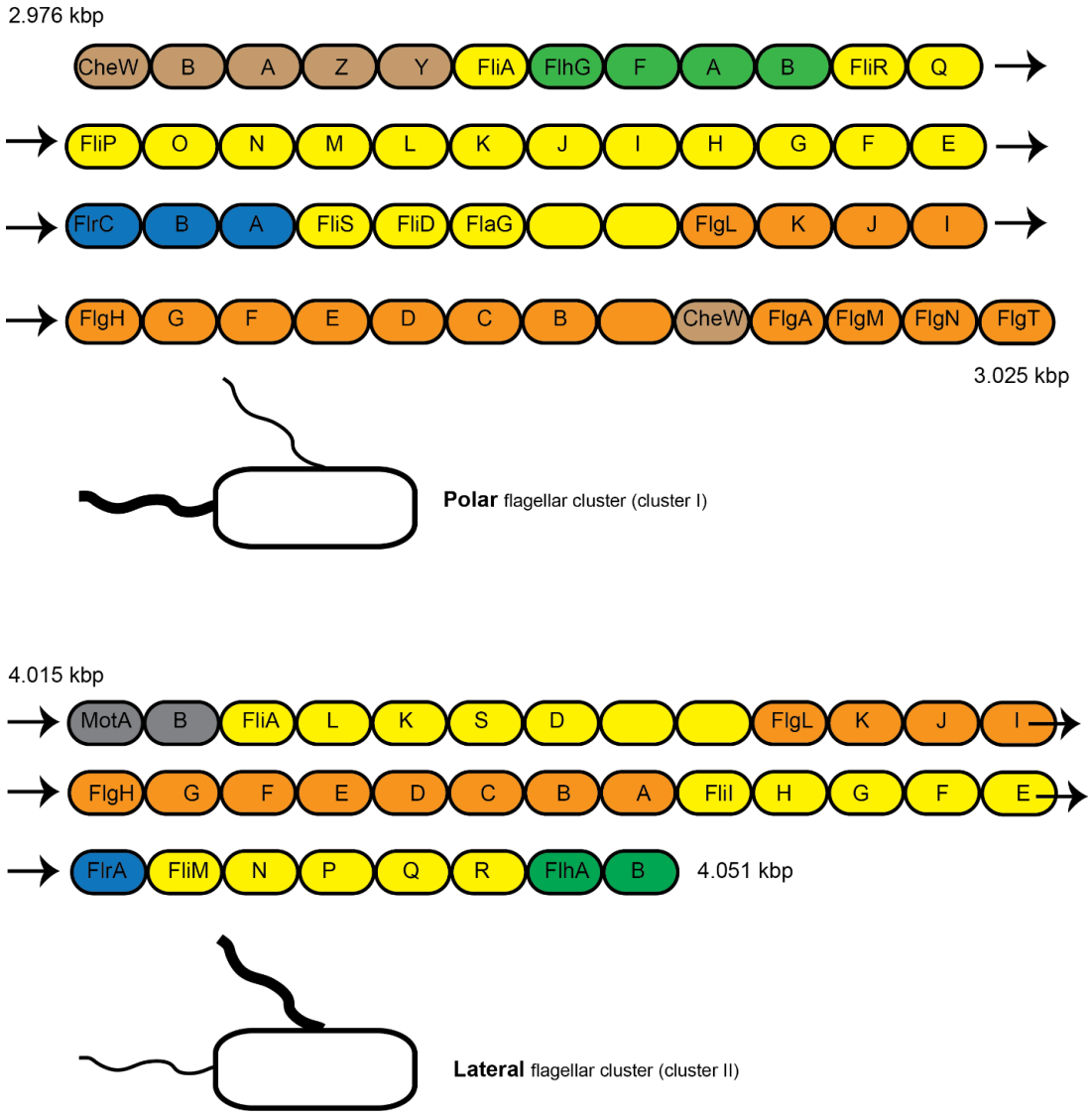

Figure 10: **Primary and secondary (polar and lateral) flagellar gene clusters in *S. putrefaciens*** (based on [73], Supplemental information). Start and end basepair counts are indicated for both clusters, rounded to the nearest kbp value. Colours indicate a general classification of the role of the proteins; grey – motor proteins, blue – FlrA-mediated transcription control, green – spationumerical regulation and FlhAB proteins, brown – chemotaxis, yellow and orange – various roles from C-ring, rod and hook proteins, T3SS.

In the past, the conditions leading to the expression of both flagellar systems were investigated, using FliF1 and FliF2 proteins as reporters. It was determined by Bubendorfer and coworkers [73] that it is not only the swimming mode, but also the nutrient availability that determines the expression of the lateral flagellar system, as a clear expression of FliF2 was still occurring in free-swimming (planktonic) cells. In nutrient-rich media such as LB, the lateral flagellum is induced in the exponential phase of planktonic growth. Up to three lateral flagella can form, which are randomly distributed over the cell surface. It should be pointed out, however, that a deletion of the first (polar) flagellar cluster also resulted in significantly decreased expression of the lateral flagellar components [73]. There is a significant difference when it comes to the role of the lateral flagellar cluster in minimal versus nutrient-rich medium – in minimal medium, mutants lacking the lateral flagellar cluster showed no difference in terms of motility to WT strains, whereas in nutrient-rich medium, motility was decreased when the lateral flagella could not be expressed [73].

In a second study investigating *S. putrefaciens* flagella [169], it was shown that another difference between strains with both flagellar clusters and those with only the polar one, is that those with both can spread further on soft agar plates and in medium-filled channels. The study showed that wildtype cells have higher "directional persistence", which is caused by them needing to introduce smaller corrections to their angle of movement (realignment angle), compared to cells lacking lateral flagella [169]. It is therefore the polar flagellum that is the key driving motor for the locomotion itself, while the lateral flagellum´s main role is to control the swimming direction and assists in viscous environments.

There has been another key protein discovered in *Shewanella*, which is a homolog of *V. cholerae* HubP [135]. The flagellar localization depends on FlhF, but the chemotaxis-controlling system (and the chromosome segregation machinery) is localization-controlled by HubP. The chemotaxis machinery, containing 37 methyl-accepting sensor proteins (MCPs), was found to localize to the pole in fluorescence microscopy experiments. [135].

In *S. putrefaciens* it was shown that FlhG stimulates the ATPase activity of FlhF (3-5 fold), and it was additionally discovered that a deletion of the first 20 residues of FlhG

(the N-terminal activator helix) in *S. putrefaciens* results in hyperflagellation, believed to be due to a decrease in FlhG stimulation of FlhG GTPase activity [135]. FlhF itself has been shown to localize to the pole without any additional flagellar components being present in *V. cholerae* [95], while FlhF from *Vibrio alginolyticus* expressed in *E. coli* was also found to localize to the pole [87]. The data from *Vibrio*, which is closely related to *Shewanella* and *Pseudomonas,* therefore hints at the intrinsic ability of FlhF to localize to the cell pole. Back to FlhG, only the polar FliM contains an EIDAL motif, which allows an FlhG/FliM interaction, and allows polar localization of FliM [74]. A graphical representation of the flagellar positioning/number regulation system discussed in this chapter, relevant to *S. putrefaciens,* can be found in **Figure 11.**

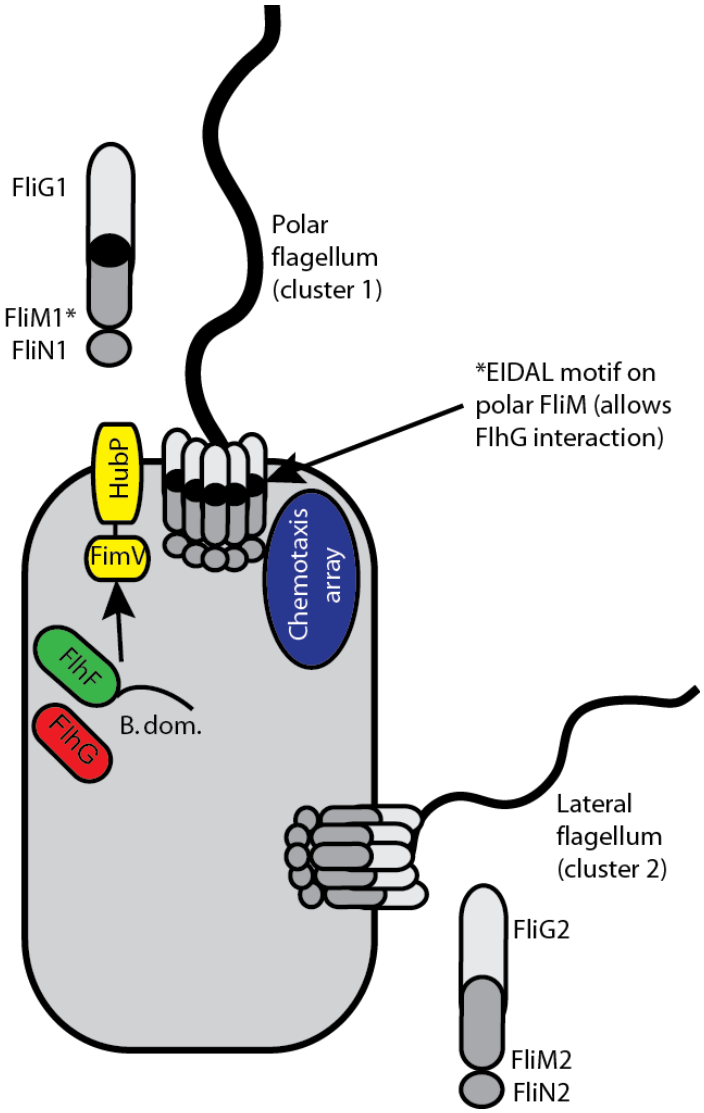

Figure 11: overview of control of the flagellation pattern in S. putrefaciens The diagram depicts the polar (top) and lateral (bottom right) flagella in *S. putrefaciens*. C-ring proteins and the cell itself are shown in grey, FlhF in green, FlhG in red. The polar determinant HubP and its FimV domain are shown in yellow. Chemotaxis array shown in blue. Only the polar flagellum is shown to be under control of FlhF/FlhG.

Shewanella putrefaciens has also been an important model organism for the investigation of how the composition of flagella (e.g. the flagellins themselves) can affect bacterial motility in different environments [171]. The research on this topic has shown that two flagellins in *S. putrefaciens*, called FlaA and FlaB, are arranged differently depending on which region of the flagellar filament they are located in. FlaA, which is used in the part of the filament closest to the cell, confers rigidity and stability to the filament (and is suitable for a variety of environments), while FlaB is used in the top of the filament, and confers more flexibility, allowing the filament to wrap itself around the cell, which is useful in complex and obstacle-rich areas (such as in soil or mucus for pathogenic bacteria). Such a wrapping event allows cells to "reverse" out of tight pockets or traps, which has been studied with *Shewanella* cells [171,172]. The coiling of flagella around the cell is not unique to *Shewanella*, though, and has also been investigated in another class of gram-negative, monotrichous polar flagellates – *Pseudomonas* (more specifically, *P. putida*) [173].

2. Aim of this work

The main purpose of this work is to build on existing foundations to further delineate the roles of FlhB, FlhG and their respective interaction partners in *S. putrefaciens,* relative to the polar flagellar system. Previously, both FliM and FlrA had already been identified as interaction partners of FlhG, in *S. putrefaciens* this was shown in the PhD thesis of D. Mrusek and the Schuhmacher 2015. et al, PNAS article, reference [74].

This work aimed to structurally characterize FlhB in *S. putrefaciens* (particularly the CCT region/PRR motif, which had never before been structurally characterized in any FlhB homolog) and to investigate the potential differences in binding behaviour of FlhB interacting proteins upon introducing a non-cleaver mutation in FlhB, or upon a deletion of the PRR motif, in comparison with WT FlhB-C. On top of this, shining more light onto the *in vivo* role of the PRR motif in the context of flagellar assembly was also a key objective.

Regarding FlhG, this work aimed to further delineate the FlhG/FlrA interaction, in particular the ATP hydrolysis kinetics of FlhG in the presence and absence of the FlrA-HTH domain, importance of key regions/residues in FlrA for the FlrA/FlhG interaction both *in vivo* and *in vitro,* and the effects of different nucleotide concentrations on the ability of the HTH domain of FlrA to bind FlhG. Additionally, the role of FliM in the context of FlhG nucleotide binding needed to be investigated (fluorescent Mant-ADP experiments, HDX, FlhG-based ATP hydrolysis kinetics profile in the presence of FliM).

Furthermore, the FliM/N//FlhG interaction was to be examined in the context of FlhB, to determine whether concurrent binding of FliM/N to FlhG as well as FlhB is still possible. Other putative interaction partners of FlhB were also a point of interest, to further delineate its position in the complex sequence of events that control flagellar assembly and the production of flagellar building blocks in particular. The C-terminal (cytoplasmic) region of FlhB was of particular interest.

3. Results

3.1 FlhG and its interaction partners, FliM and FlrA

3.1.1 Delineating the FlhG binding site on FlrA

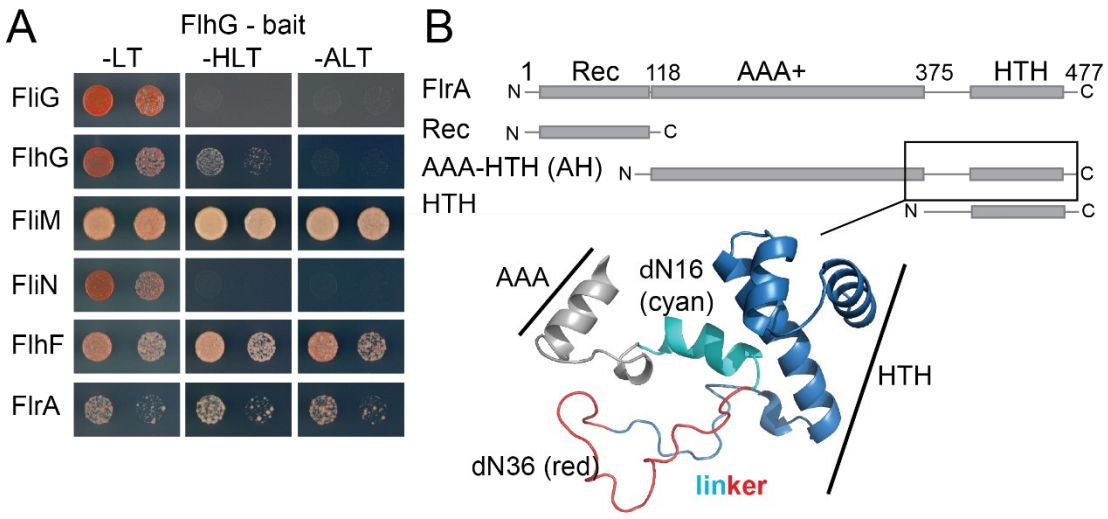

Figure 12: FlrA constructs and interaction partners of FlhG identified in Y2H experiments. A - summary of FlhG interaction partners previously identified with Y2H experiments (Y2H experiments performed by Dieter Kressler, who kindly provided the original image. An extended version of part A was also contained in the thesis of D. Mrusek) B - Overview of the FlrA constructs employed (constructs were GST-tagged) and a visualization of the loop region between the HTH and AAA domains.

Pulldowns were carried out to investigate the binding of FlhG to different regions of FlrA. For this, different GST-constructs of FlrA truncations were used (see **Figure 12B**.). The pulldowns showed that FlhG D58A (in the absence of any additional nucleotides) and FlhG WT (in the presence of 1 mM ATP) bound to GST-FlrA-HTH and GST-FlrA-AAA-HTH, but not to GST-Rec domain (see **Figure 13A, B**). The binding to the HTH domain alone appears to be stronger, judging from the FlhG band intensity. Due to the instability of the AAA domain, constructs of GST-Rec-AAA or GST-AAA could not be successfully purified or used in GST-pulldowns.

Additional pulldowns were carried out with both GST-FliM-N and GST-FlrA-HTH, to investigate the effects of different concentrations of ADP and ATP on the binding of WT FlhG to both interaction partners (see **Figure 13E, F**). The results show that the GST-FliM-N interaction with FlhG occurs in the presence of both nucleotides (the

interaction occurs in the presence of 0.1, 0.5, 1.0 and 2.5 mM ADP/ATP), although the binding is considerably stronger in the presence of ADP than ATP (**Figure 13F**). In contrast, the GST-FlrA-HTH/FlhG interaction is crucially ATP dependent (and is observed at 0.1, 0.5, 1.0 and 2.5 mM ATP, **Figure 13E**). The difference in the range of concentrations did not seem to have a significant effect on the binding in any of the cases.

To further investigate the exact binding site of FlhG on FlrA, an additional pulldown was carried out with a full-length GST-FlrA-HTH construct, a dN16 HTH and dN36 HTH construct (see **Figure 13C**). While binding of WT FlhG (in the presence of 1 mM ATP) occurred in the case of GST-HTH and GST-HTH dN16, the binding was not observed in the case of the GST-HTH dN36 construct. A related experiment had been performed by D. Mrusek in his thesis, which used only FlhG D58A instead (without added ATP), and observed similar results. Overall, this demonstrates *in vitro* that it is the loop region between the AAA and the HTH domains that contains the FlhG binding site on FlrA (requiring the presence of ATP with WT FlhG), specifically the region between residues 389-409. In addition to the GST pulldown in **Figure 13C**, the role of this region was studied in greater detail *in vitro* through qPCR/Western blotting (**Figure 20**), in further GST pulldowns (**Figure 21**), and *in vivo*, using fluorescence microscopy studies (**Figure 19**). The conservation of the region was also investigated with Consurf (**Figure 18**). Concerning the binding site of FlhG on FliM, on the other hand, as mentioned in the discussion, a conserved EIDAL motif (contained in the polar FliM in *S. putrefaciens*, and in FliY in certain other organisms, for example *B. subtilis*) is responsible for the interaction with FlhG [74].

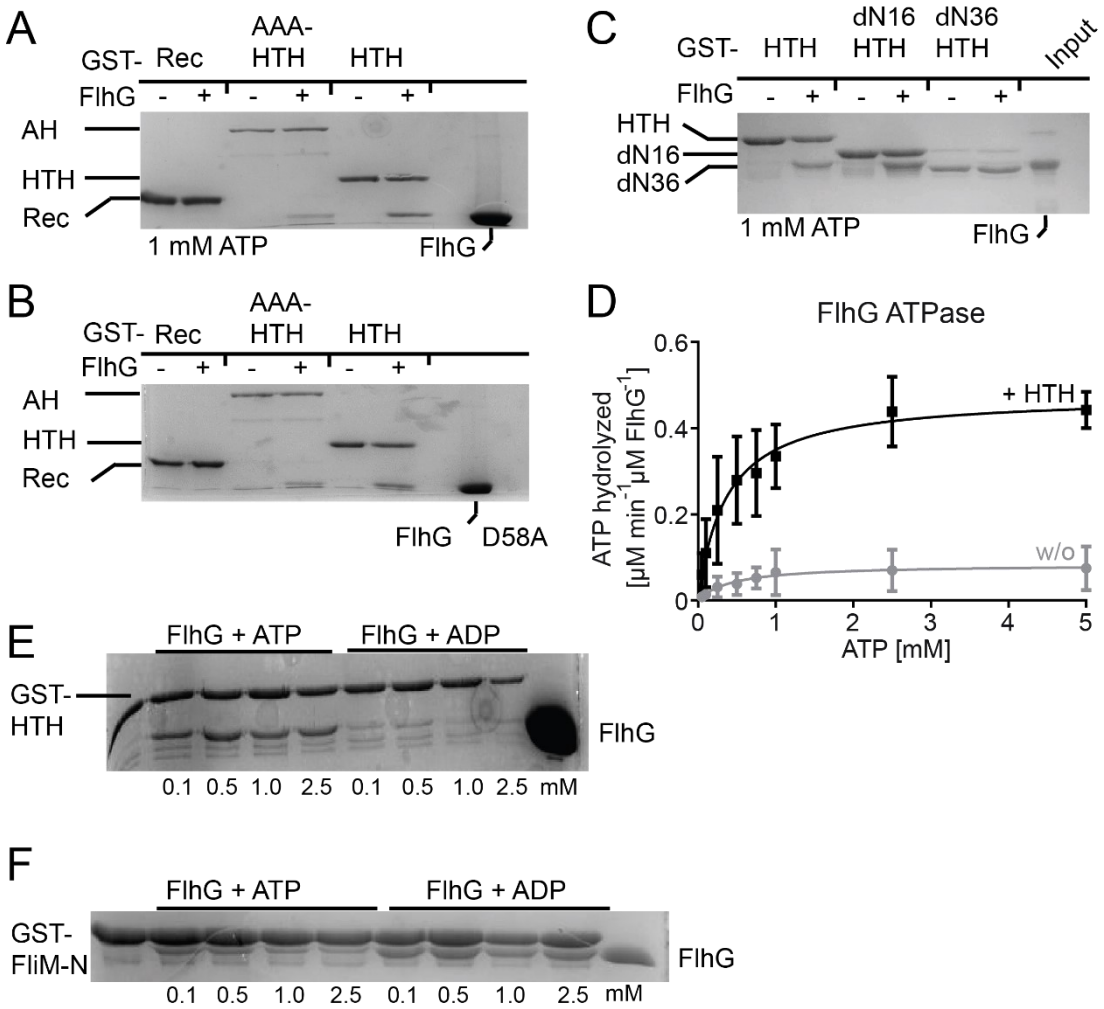

Figure 13*:* **FlhG-involving *in vitro* GST pulldowns and FlhG kinetics**. A - Pulldown of FlrA truncations with WT FlhG in the presence of 1 mM ATP; B - Pulldown of FlrA truncations with FlhG D58A in the absence of nucleotides; C - Pulldown of FlrA-HTH truncations with WT FlhG in the presence of 1 mM ATP; D - FlhG and FlhG+HTH ATP hydrolysis assays over a range of different ATP concentrations - error bars show standard deviation values; data analyzed and kinetics graph prepared by Dr. Wieland Steinchen; E - Pulldown of FlrA-HTH with FlhG WT in the presence of different concentrations of ATP and ADP; F - Pulldown FliM-N with FlhG WT in the presence of different concentrations of ATP and ADP.

3.1.2. ATPase assays with FlhG and FlrA

To further investigate the interaction of FlhG and FlrA in terms of the stimulation of the ATPase activity of FlhG, the kinetics profile of ATP hydrolysis by FlhG in the presence of the HTH domain of FlrA was investigated. It was determined that a strong increase of ATP hydrolysis occurs upon the addition of equimolar amount of GST-FlrA-HTH to FlhG (see **Figure 13D above**). The activity was tested with FlhG alone, and with equimolar amounts of FlrA-HTH, over a range of different ATP concentrations

(from 0.125 mM to 5 mM). The ATPase activity of FlhG alone was determined to have K_m and V_{max} values of 0.45 ± 0.34 mM ATP. Additionally, 0.08 ± 0.02 µM ATP was hydrolyzed per minute per µM FlhG, respectively. The presence of FlrA-HTH increased V_{max} by approximately a factor of 5 (0.48 ± 0.04 µM ATP hydrolyzed per minute per µM FlhG) with an unchanged K_m (0.36 ± 0.12 mM ATP). Calculation performed by Dr. Wieland Steinchen. This stimulating effect of FlrA on the ATPase activity of FlhG would in turn likely lead to a dissociation of the FlhG homodimer, since the ATP required for the presence of a dimer has been hydrolyzed.

The next part discusses endpoint measurement ATP hydrolysis experiments with different full-length FlhG and FlrA constructs (also see **Figure 14**).

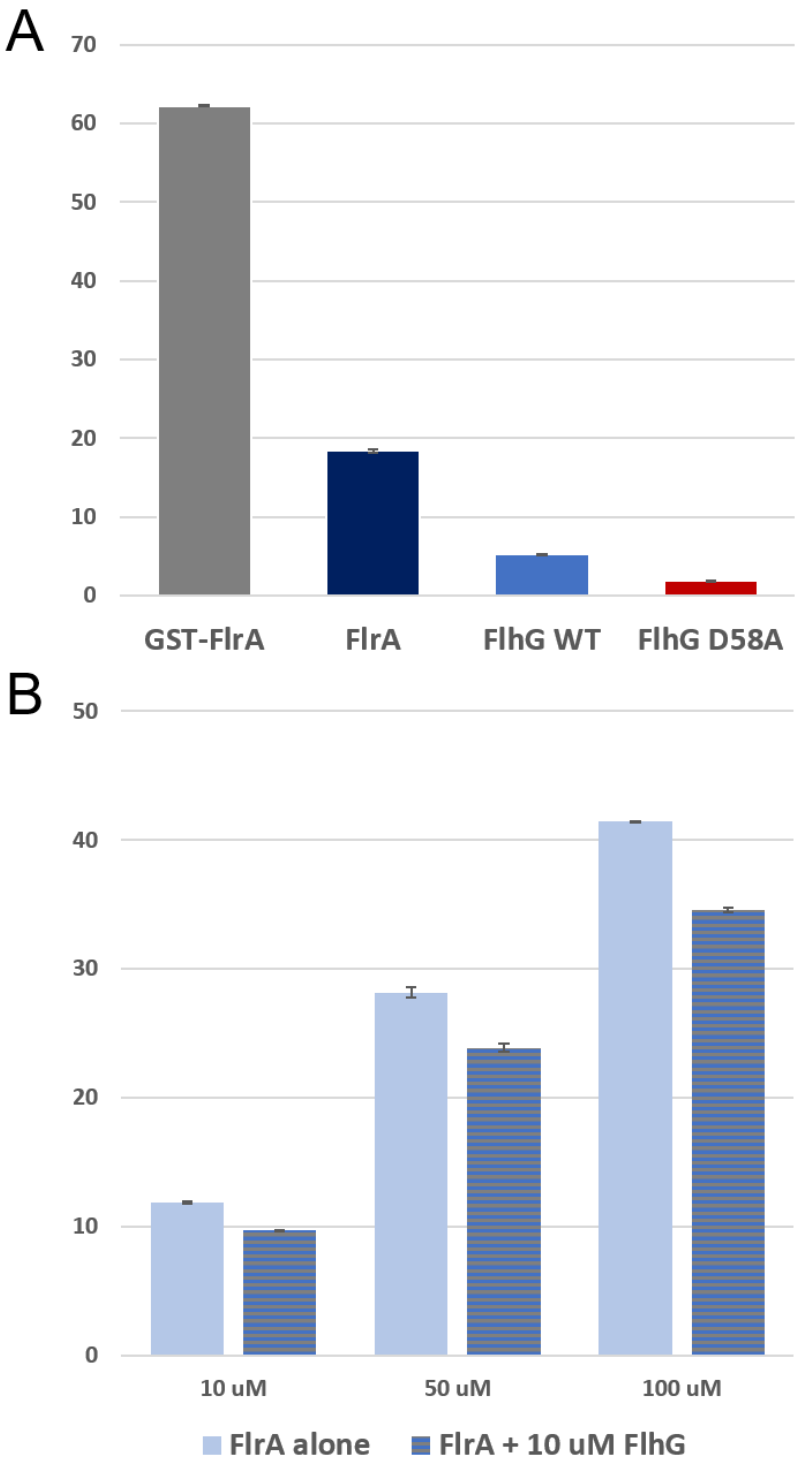

Figure 14: Endpoint measurements of full-length FlrA and FlhG construct ATP hydrolysis. A - Comparison of GST-FlrA, His-FlrA, FlhG WT and FlhG D58A ATPase activity; B - Investigation of the effects of addition of constant (10 uM) FlhG to an increasing concentration of FlrA. The concentrations written under the graph refer to FlrA concentrations. Y-axis in both panels shows %ATP hydrolysis. Error bars refer to standard deviation values.

Regarding individual, full-length proteins, it has been determined that the ATPase activity of equimolar amounts (10 uM) of FlrA and FlhG are very different (FlrA significantly more active). Such a result is in good agreement with experiments that were performed in [93] with *P. aeruginosa* homologs (FleQ was significantly more active, and in the article, a 5-fold higher concentration of FleN was used). It can be observed in *S. putrefaciens* that, using 1 mM ATP as substrate, the ATPase activity of full-length FlrA alone is approximately 3 times as high as the activity of FlhG (in other experiments, only the HTH-domain of FlrA was used, which has no intrinsic ATPase activity) (see **Figure 14A**). The ATPase activity of FlhG D58A (a mutant that binds but does not hydrolyze ATP) was substantially lower in comparison; some residual activity is believed to remain due to potential contamination of the sample (see **Figure 14A**). Interestingly, the GST-FlrA construct had a roughly 3.5-fold activity of the His-FlrA; this is unexpected, but it is possible that the GST tag either stabilizes the FlrA protein, and a greater proportion of it is active as a result, or that the enforced dimerization (GST proteins form dimers) plays a role in this.

What has also been performed are experiments identifying the effects of having both FlrA (full-length) and FlhG in solution at the same time (see **Figure 14B**). The total ATPase activity of FlrA+FlhG was observed to be somewhat lower compared to the activity of FlrA alone – this would also be in accordance with previous *P. aeruginosa* experiments where full-length FlhG was shown to inhibit FlrA, but the difference is less pronounced in *S. putrefaciens.* In these experiments, the concentration of FlhG was kept constant, with increasing concentration of FlrA being added (from equimolar 10 uM, up to 100 uM). The proportional decrease in total activity appears to be relatively constant (see **Figure 14B**). Activity of FlrA+FlhG is always lower than that of FlrA alone, which would hint at some degree of inhibition by FlhG. This degree, however, is not nearly as pronounced as in *P. aeruginosa*, as already stated.

3.1.3. Purifications and purification optimizations for FlhG and FlrA

Both FlhG and FlrA are ATPases, and relatively unstable during purification. For FlhG, employing the D58A mutant simplifies the purification significantly, while this is not the case for FlrA D233A; both the D58A FlhG mutant and FlrA D233A mutant allow the binding (but not hydrolysis) of ATP. Both FlrA WT and FlrA D233A are less stable during purification compared to both FlhG constructs, and show both significantly

greater precipitation rates, poorer expression, as well as lower overall purification yields. Precipitation can be reduced by adding small amounts of ATP during the Ni-affinity step.

Initially, purification of both FlhG and FlrA was attempted with standard buffer B (see Methods section), which contains an imidazole concentration of 500 mM. Since high imidazole amounts, as well as low salt concentrations, frequently have a negative effect on unstable proteins, alterations to the imidazole concentration in buffer B were performed. This was done by carrying out different gradient elutions to determine the optimal range where FlhG/FlrA elute from the Ni-NTA column, before it starts to precipitate.

Both FlhG and FlrA were eluted in 50 mM imidazole steps, and significant amounts of protein were already detected in much lower imidazole concentrations than the usual 500 mM; the only exception to this is the FlrA D233A, which still elutes primarily at 500 mM imidazole. Both FlhG variants, however, already eluted primarily at 100-150 mM imidazole (see **appendix 7.3.**). The presence of lower amounts of imidazole in the elution buffer lead to decreased amounts of precipitation (although FlrA was still significantly more unstable than FlhG).

3.1.4. Is FliM a factor promoting ADP release from FlhG?

Mant-ADP is a fluorescent ADP analogue that retains properties of normal ADP (e.g., can be degraded to AMP, binds efficiently to ADP-binding pockets, etc.), but in this case, allows tracking of the fraction of bound ADP over time. An experiment was carried out where FlhG alone, and FlhG in complex with FliM/N had normal ADP exchanged for Mant-ADP, to determine whether a change of fluorescence occurs. Even though a minor decrease in Mant-ADP fluorescence was observed when FlhG and FliM/N were in complex, compared to FlhG alone, this behaviour does not explain the role of FliM as an interaction partner of FlhG. Provided FliM was promoting the release of ADP, this would be more clearly observable in this experiment, and the difference would be more pronounced (see **Figure 15** below).

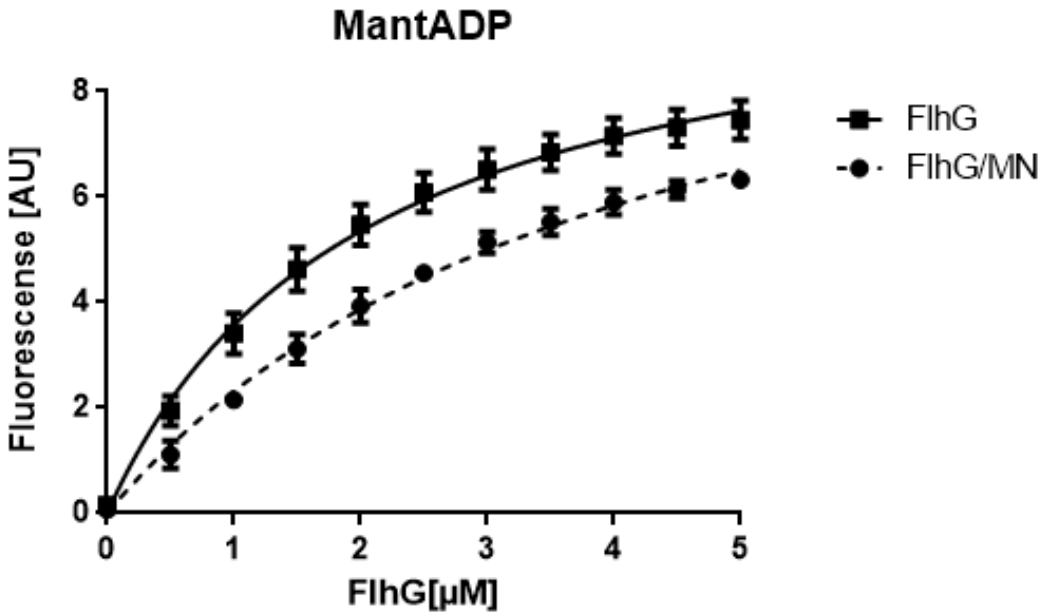

Figure 15: **fluorescence Mant-ADP experiment**. Showing data referring to FlhG alone and FlhG in the context of the FlhG//FliM/N complex. X-axis showing increasing concentration of FlhG, Y-axis shows fluorescence units. Measurements performed and image kindly provided by Dr. Wieland Steinchen.

3.1.5. Hydrogen-deuterium exchange mass spectrometry experiments investigating the binding interfaces of FliM and FlrA on FlhG

HDX-MS [174] was used to investigate how the pattern in protection from H/D exchange changes depending on whether FlhG is in solution alone, or with one of its interaction partners. HDX involves the incubation of proteins of interest in deuterated buffer either with or without their respective binding partners, which allows an exchange of amide hydrogens to deuterium. After the proteins of interested are proteolytically digested, the resulting fragments are analysed with mass spectrometry, and changes (to either higher or lower protection from exchange relative to the target protein alone) are mapped to a model of the structure of the protein of interest. From the change in behaviour (and depending on the location of the fragments within the overall structure), HDX can be used to identify either conformational changes or binding events with interaction partners.

The HDX experiments were performed at the HDX-MS facility at Philipps University in Marburg, by Dr. Wieland Steinchen. The binding sites for FlrA and FliM were identified.

In **Figure 16** below, part A shows the H/D exchange behaviour observed upon incubation of FlhG D58A with FlrA-HTH, compared to FlhG D58A alone. Additionally, 1 mM ATP was supplied during incubation of the samples. A number of regions incorporated less deuterium when FlrA-HTH was also present, including helices 6 and 7 of FlhG, as well as the region involving beta sheet 2 and alpha helix 4. Other regions with increased protection from exchange, such as loops connecting beta strand 1 and alpha helix 2, and those connecting alpha helix 5 with beta strand 5 are likely involved in dimerization interactions (**Figure 16A**).

A related experiment was performed with a complex of FliM/N and FlhG (**Figure 16B),** which again showed a behaviour consistent with FliM/N binding to FlhG. No nucleotides were added during incubation. Interestingly, FliM/N was also shown to cause increased protection from exchange and to bind to helices 6 and 7, like FlrA-HTH previously, which would hint at an overlapping binding site. The region containing alpha helix 4 and beta strand 2 of FlhG, however, did not show a reduction in HDX, which could be used to understand why FliM can interact with the monomeric form of FlhG and FlrA-HTH only interacts with the homodimeric form. It was also observed that there are additional secondary structural elements with increased HDX present in the presence of FliM/N, found at the C-terminal end of alpha helix 2, and beta-strands 2, 3 and 4 (this does not include the loops between them). The HDX data also suggests that a partial unfolding of secondary structure occurred upon FliM/N binding, which was not observed with FlrA-HTH. Taken together, the results point towards the fact that FliM and FlrA share an overlapping binding site on FlhG. Both parts of figure 16 were also published in reference [175].

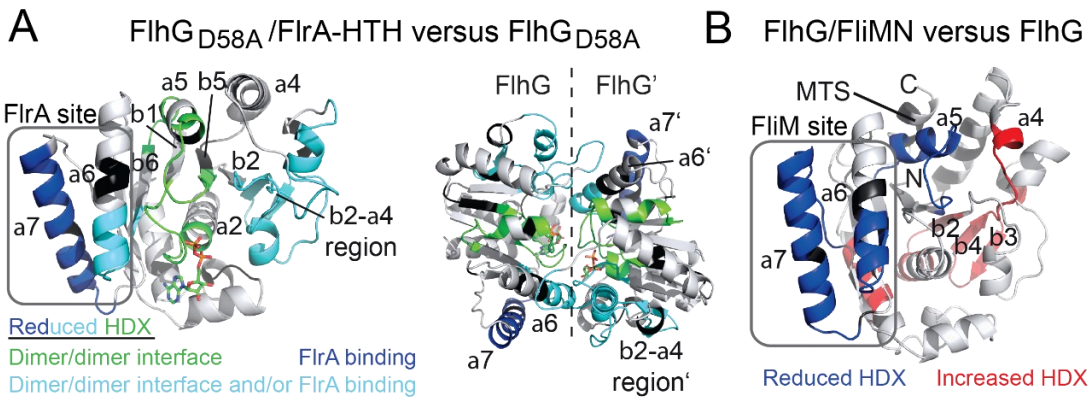

Figure 16: **HDX data on the interactions of FlhG with FlrA and FliM** A – FlhG D58A/FlrA-HTH HDX data with binding site on FlhG indicated in left panel, FlhG-FlhG´ dimerization interface in the right panel. HDX experiment performed by Dr. Wieland Steinchen using proteins purified by former AG Bange Master student Sabrina Henche; data obtained/analyzed by Dr. Wieland Steinchen, who kindly provided the images, which were also published in [175]. B - HDX data on the FlhG//FliM/N interaction identifying the FlhG/FliM binding site. HDX experiments performed and data obtained/analyzed by Dr. Wieland Steinchen, who kindly provided the image, which was also published in [175]. For both parts, the grey frame indicates helices α6 and α7 and the overlapping binding site.

An additional set of experiments was carried out to investigate whether a difference in hydrogen/deuterium exchange occurs on FlhG, comparing its apo- and ADP-bound states. The behaviour of FlhG alone was compared with FlhG in the context of the FlhG/FliM/FliN complex, and ADP was selectively added (see **Figure 17 below**). In the upper half (**parts A and B**), the difference in HDX between the FlhG/FliM/N complex and FlhG alone is shown. **Figure 17A** depicts the data from the apo state (without ADP), and **Figure 17B** depicts the data with ADP added. Yellow/red indicate the regions where the H/D exchange in the FlhG/FliM/FliN complex was higher than with FlhG alone. Blue regions indicate regions where the exchange was lower in the complex (e.g., protected regions; the binding sites). For the HDX colour scale, please see the lowest panel of **Figure 17**, far right.

In the lower half (**parts C and D**), the H/D exchange values for FlhG (alone or in complex) without ADP present are subtracted from the H/D exchange values for FlhG with ADP present. Essentially, the difference in exchange that is a consequence of ADP binding is determined. In **Figure 17C**, data for FlhG alone is shown (exchange with ADP minus exchange without ADP), and in **Figure 17D**, data for the FlhG/FliM/FliN complex is shown (again, exchange with ADP minus exchange without

ADP). Blue in this case refers to regions where H/D exchange with ADP is lower than the H/D exchange without ADP; in other words, regions that see more protection from exchange in presence of ADP. From this, conclusions about changes in the protein that occur during ADP binding can be drawn. The regions involved in ADP binding were mapped onto a model of *Sp*FlhG (created with Swissmodel [176,177]) in **Figure 17E**. Figure **17F** depicts the regions R1-R6 of FlhG, as indicated in the rest of **Figure 17,** mapped onto the model of *Sp*FlhG.

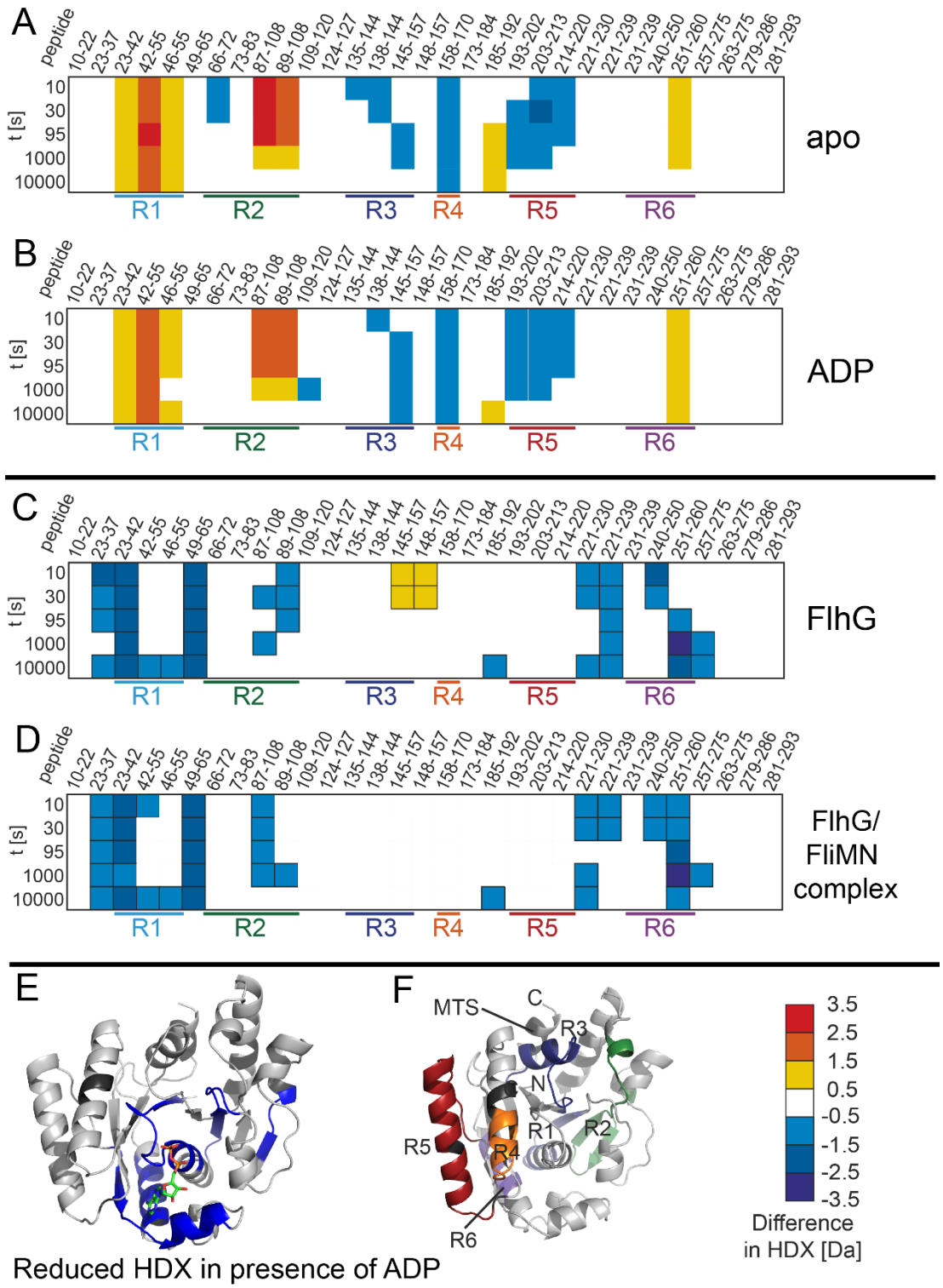

Figure 17: **HDX data of FlhG with and without FliM/N in the context of ADP binding.** Top panel: Difference between HDX of SpFlhG/FliMN and FlhG alone in absence (A) and presence of ADP (B). Middle panel: Difference between HDX in the presence and absence of ADP ("without ADP" subtracted from "with ADP") for FlhG alone (C) and as part of SpFlhG/FliMN complex (D). Lower panel: (E) shows areas with reduced HDX upon ADP binding mapped to a structural model of FlhG . (F) The colour markings of important FlhG regions, R1-R6, are shown mapped to the FlhG model structure. On the far right of the lower panel, the HDX colour scale relevant for parts A-D is

depicted. HDX experiments performed and data obtained/analyzed by Dr. Wieland Steinchen. Figure modified from images kindly provided by Dr. Wieland Steinchen.

3.1.6. Consurf, sequence analysis and structural models of FlhG, FliM and FlrA

In order to discover additional information regarding the conservation of different important regions in the three proteins of interest, structural models of each were first made using Swissmodel [176,177]. For FlhG, the chosen template was the crystal structure of *G. thermodenitrificans* FlhG from Schuhmacher et. al [74], and for FlrA, , NtrX *from Brucella abortus* (5m7n PDB ID) [178]; for FliM, there were no structures available that could be used to model the far region of the N-terminus, which contains the EIDAL motif. Hence, structural models were only used as Consurf templates in the case of FlrA and FlhG (**Figure 18A and B**, respectively). The conservation score scale is also shown in **Figure 18**, with light blue representing low conservation, white intermediate conservation, and purple high conservation scores. As a sidenote, the reason why no *P. aeruginosa* FleQ structures (of which several exist, but contain the Rec and/or AAA domain only [88,179]) were used as templates for the Consurf analysis is because none of those structures contained the HTH when the analysis was performed. NtrX was the best match at the time to cover the entire FlrA sequence.

The Consurf analysis firstly confirmed previous findings based only on sequence alignments (D. Mrusek in his PhD thesis) that the FlhG residues involved in the interaction of FlhG with FliM and FlrA are indeed highly conserved. These residues are K175, K205 and F213 (indicated as groups of spheres in **Figure 18B** and stars in **Figure 18C**). Surprisingly, however, the FlrA region involved in FlhG binding (389-409) was shown in its entirety as poorly conserved or highly variable (indicated in **Figure 18A, C**). The EIDAL motif in FliM, involved in FlhG binding, is extremely highly conserved, with each of the five residues receiving the highest possible conservation score in Consurf (indicated in **Figure 18C**), also higher than K205 or F213 in FlhG, for example.

A pairwise sequence alignment (Emboss Needle) calculated the sequence identity of *S. putrefaciens* FlrA with *P. aeruginosa* FleQ as 52.0 % (see **Appendix 7.5.4.2**). It also

demonstrates that the region of *Sp*FlrA involved in binding FlhG (389-409) has lower sequence identity with *Pa*FleQ than the rest of the protein, which could indicate a key difference between *S. putrefaciens* FlrA and its *P. aeruginosa* homolog (see **Appendix 7.5.4.2.**). The identity of *S. putrefaciens* FlhG with *P. aeruginosa* FleN was 59.0% (see **Appendix 7.5.4.1.**). Overall, the sequence identities would indicate a high degree of similarity.

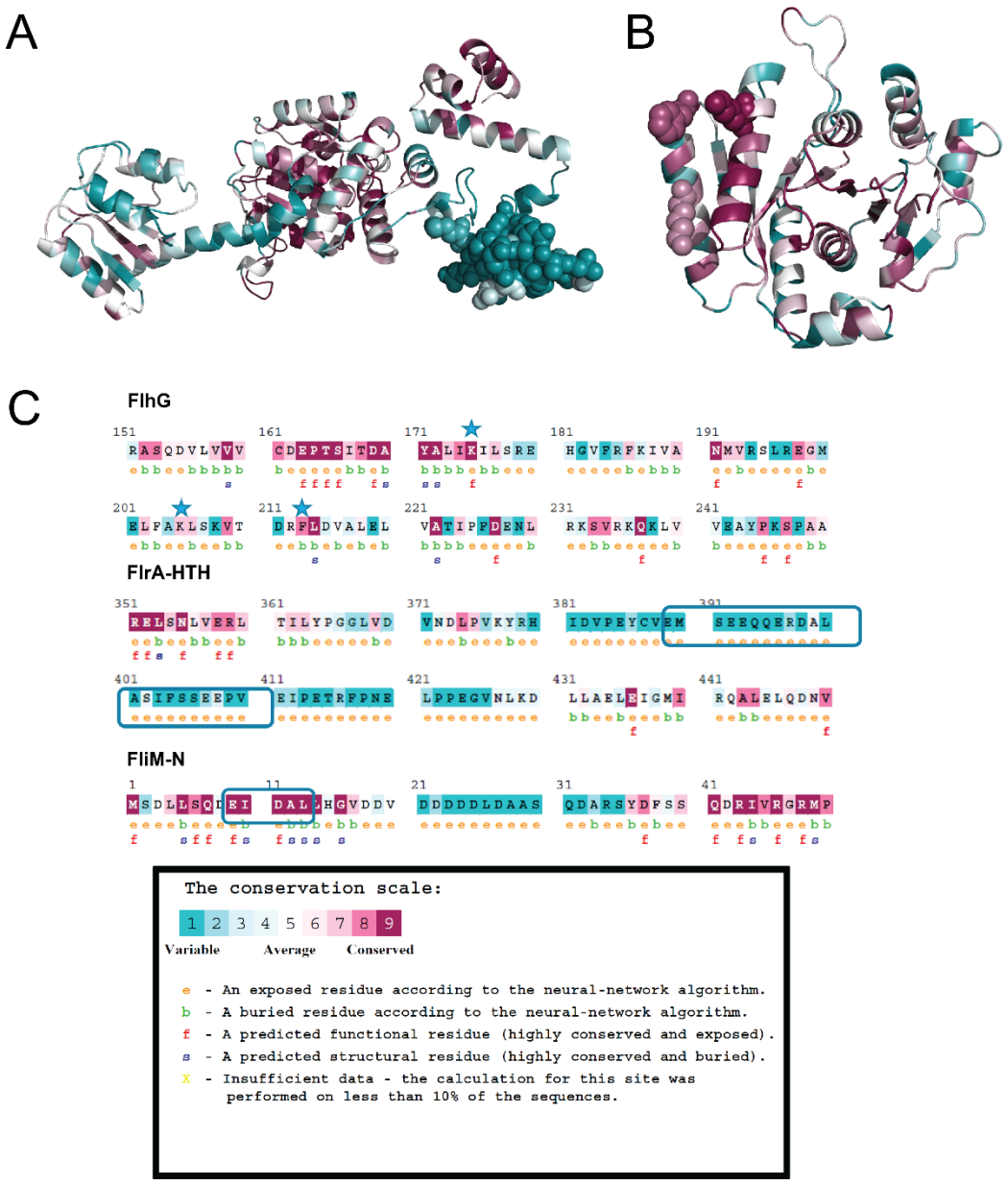

Figure 18: **Consurf analysis of FlhG, FlrA and FliM with residues colour-coded for conservation scores.** A - structural homology model of FlrA, showing the FlhG interacting region as spheres; B - structural homology model of FlhG, showing K175, K205 and F213 as spheres; C - selected sequence regions of FlhG, FlrA and FliM showing Consurf conservation scores; key regions identified with starts (FlhG) or frames (FlrA-HTH, FliM-N).

3.1.7. Physiological and *in vitro* effects of mutations in the FlhG binding site on FlrA on *S. putrefaciens*

As it had been shown in the GST pulldown comparing different truncations of the FlrA HTH domain, binding of FlhG to FlrA is disrupted, provided that enough residues are deleted in the linker region between the AAA and the HTH domains (**Figure 13C**, experiment performed with WT FlhG and 1 mM ATP). As the next step, different *in vivo* fluorescence microscopy experiments were carried out to further investigate this region.

Firstly, the entire 389-409 region was deleted from the *flrA* gene, having previously been identified as the essential region of the HTH domain where FlhG binds to FlrA.

Secondly, a number of experiments were carried out to investigate different single residues that were identified as potentially significant (based on Consurf and sequence alignments with *P. aeruginosa* FleQ and other NtrC-class EBPs). Several residues were identified as very strongly conserved in *Shewanellaceae*, based on an alignment of sequences obtained from ProteinBlast (https://blast.ncbi.nlm.nih.gov). Using *S. putrefaciens* CN-32 numbering, E392, E393, ERDALA (396 to 401), F405 were found to be universally conserved in the tested entries (alignment not shown). These identified residues were then suggested to Meike Schwan, who performed fluorescence microscopy experiments.

Meike Schwan tested five mutations, and of those, only one resulted in a significant phenotype change – the FlrA L400E mutation (the remaining mutations were FlrA E393R, R397E, D398R and additionally E408R). For the remaining mutations that showed no phenotype changes compared to the WT FlrA, the fluorescence images can be seen in **Appendix. 7.6**.

The observed phenotype, a delocalized, hyperflagellation state resembles the delta 389-409 FlrA phenotype, as well as a deletion of FlhF and FlhG (see **Figure 19A** below). The WT strain has only one polar flagellum, the same is observed in the empty vector control (EVC). An overexpression of FlrA (pBTOK FlrA) leads to a hyperflagellated but not delocalized phenotype (lophotrichous flagellation), while an overexpression of FlhF and FlhG leads to a suppression, and complete lack of flagella. Additionally to

the filament-visualising experiments, the same mutant and control strains were subjected to hook-visualisation experiments as well, which confirm the research findings shown in **Figure 19A** below. For the hook-visualisation fluorescence microscopy experiments, please see **Appendix 7.6.** Fluorescence microscopy data obtained in collaboration with Meike Schwan and John Hook, AG Thormann.

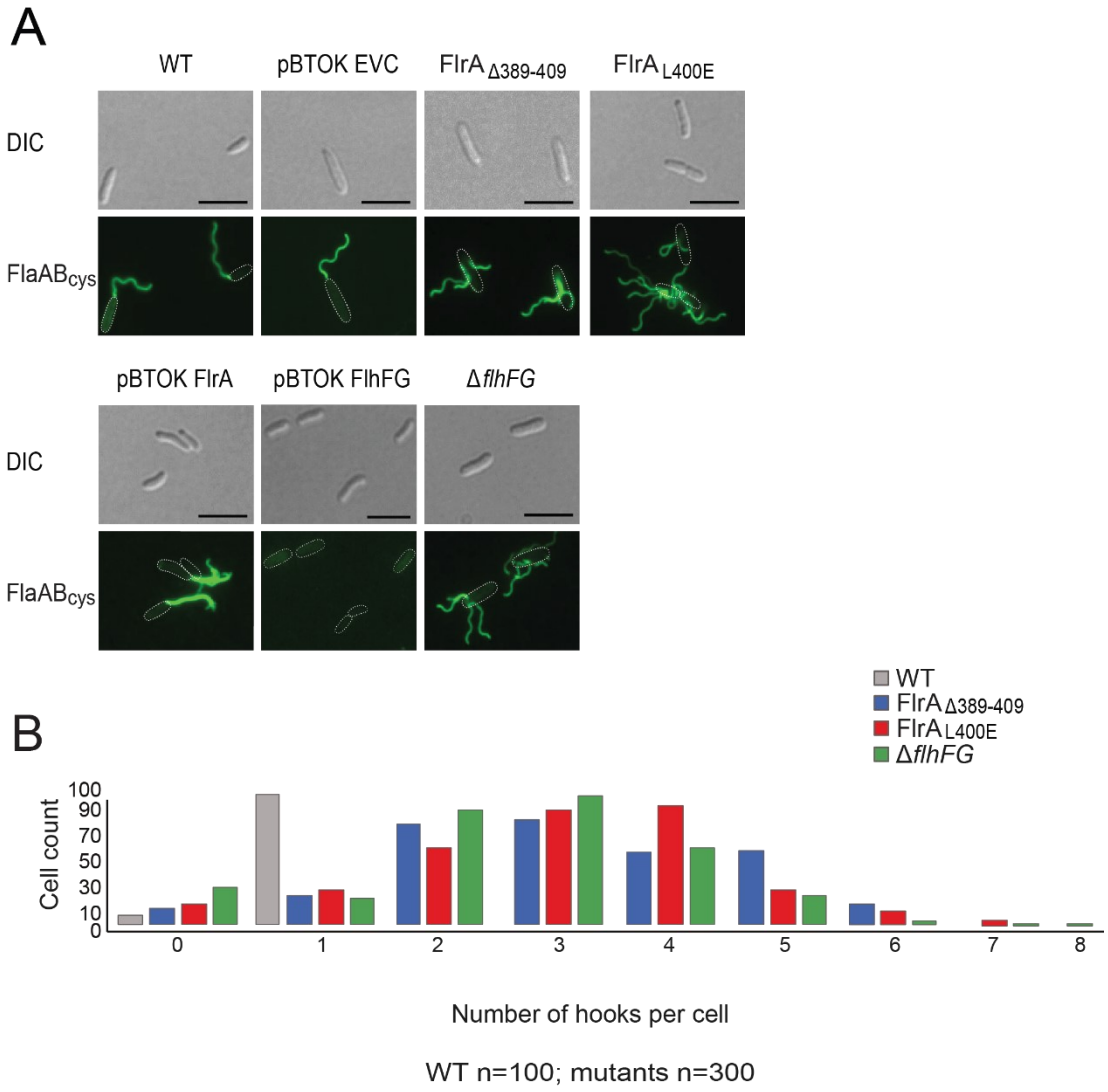

Figure 19.: Fluorescence microscopy data on the FlhG/FlrA interaction. A – fluorescence microscopy images demonstrating the flagellation pattern in response to mutations in the FlhG binding site on FlrA, in comparison with controls B – number of hooks formed per cell in different strains(for A and B, data obtained in collaboration with Meike Schwan and John Hook, AG Thormann and published in [175]). Scale bar 5 µm.

For both strains with mutations in the FlhG binding site in FlrA, a quantification for the number of flagella formed in comparison with the WT *S. putrefaciens* was also carried out in collaboration with John Hook from AG Thormann in Gießen. The results

(**Figure 19B** above) show that a noticeably different population of cells can be observed, with a large proportion of those having 2-5, or even 6 or more flagella on the far end of the spectrum, when either the 389-409 region in FlrA is deleted, or the L400E mutation is used. Only a very small proportion of these cells has a WT phenotype (single flagellum).

In addition to the fluorescence microscopy experiments, additional qPCR and Western blot experiments were carried out to investigate the effects of altering the FlhG binding site on FlrA on protein transcription and expression levels (collaboration with Meike Schwan, AG Thormann) (see **Figure 20** below).

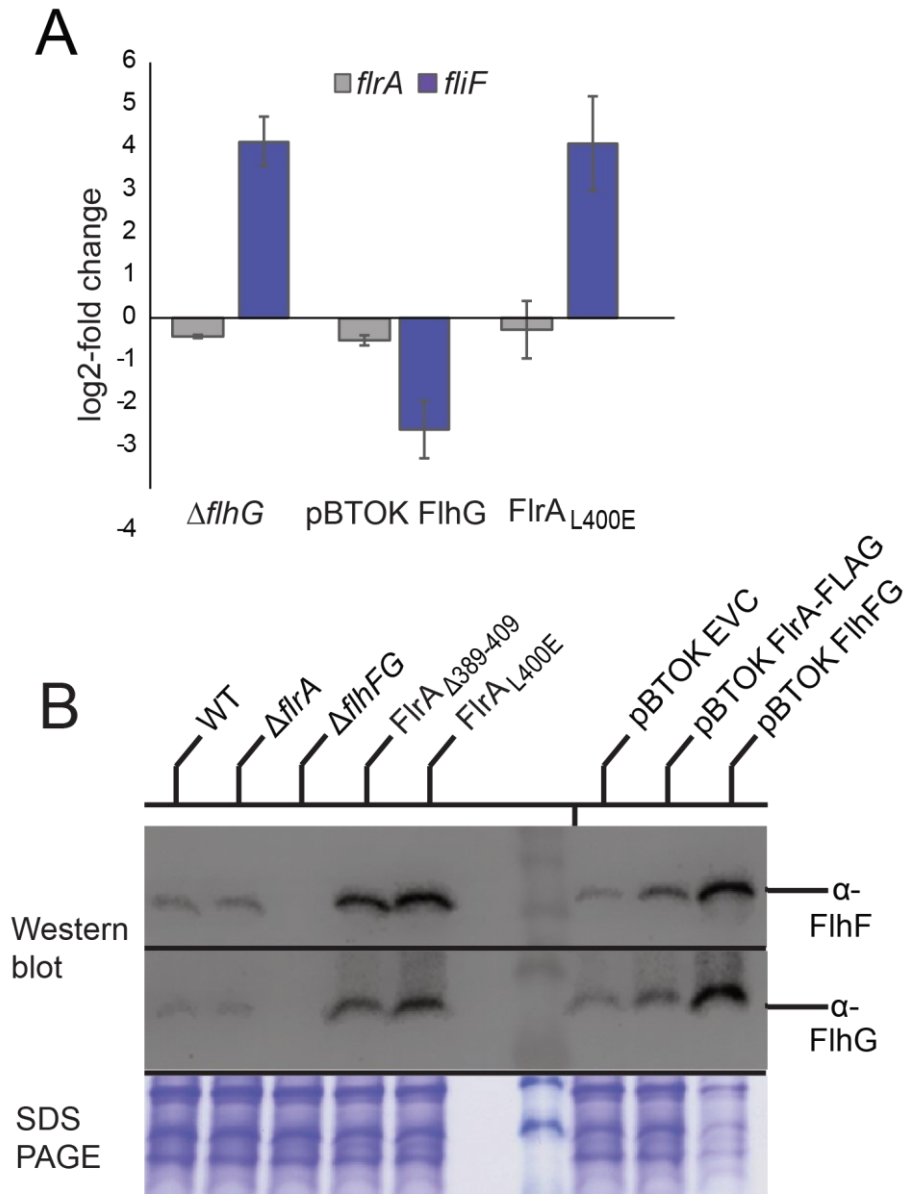

Figure 20: Transcriptional role of the interplay between FlhG and FlrA A - qPCR data showing the transcription rate of FliF and FlrA in a delta-FlhG, FlhG overexpression and FlrA L400E mutation strain; B - Western blot showing FlhF and FlhG levels in different strains (for both parts, data obtained in collaboration with Meike Schwan, AG Thormann, who kindly provided the images, which were also published in [175]).

With qPCR, transcription levels of FlrA and FliF were compared under different conditions; overexpression of FlhG (pBTOK FlhG), deletion of FlhG, and a FlrA L400E mutation. It can be observed from (**Figure 20A**) that while the transcription levels of FlrA are very similar across all three conditions, there is a significant increase of FliF transcription levels upon deletion of FlhG, or the FlrA L400E mutation, compared to an overexpression of FlhG. This indicates that FliF, which is under the transcriptional control of FlrA, is more strongly transcribed when FlhG is unavailable, or the FlhG/FlrA interaction is disrupted.

With Western blots (see **Figure 20B**), it has been determined that both the FlrA L400E mutation, as well as the deletion of the 389-409 region led to an increase in FlhF and FlhG levels. The levels of both are considerably higher compared to the WT and *flra* deletion strains, and similar to the overexpression control (pBTOK FlhFhG). Therefore, blocking the FlrA/FlhG interaction by disrupting the FlhG binding site on FlrA leads to a loss of control over the production of FlhF and FlhG, with significantly higher amounts of both being produced.

Regarding the FlrA/FlhG interaction *in vitro*, the mutations to the FlhG binding site on FlrA that had been already investigated using fluorescence microscopy experiments, were also tested with GST-pulldowns. It has been determined that, as expected, in the presence of 1 mM ATP, WT FlhG reacts with the unmodified HTH domains of FlrA, but not with the L400E HTH domain or the HTH domain containing the 389-409 fragment deletion. This again confirms that this whole region, and the Leucine 400 in particular, are crucial for establishing the FlhG-FlrA interaction. The same was observed when FlhG D58A was used (**see Figure 21 below**).

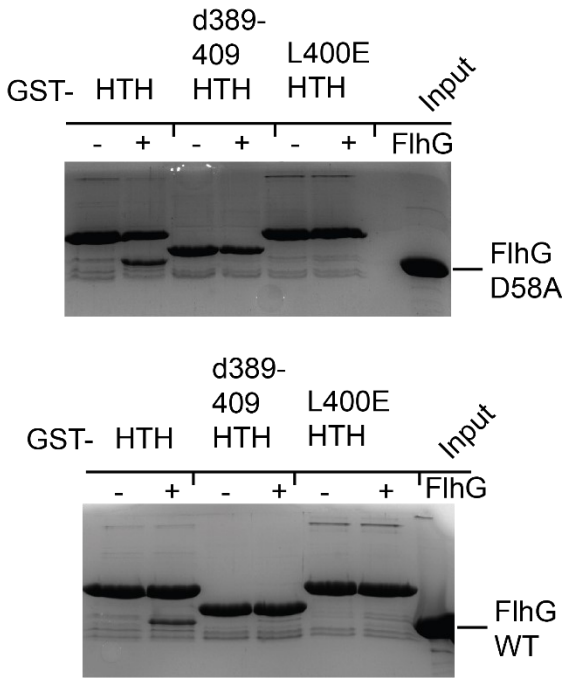

Figure 21: **Pulldown experiments investigating the FlhG binding site on FlrA**. GST-pulldowns of different HTH mutants against WT (lower panel) and D58A (upper panel) FlhG. The experiment shown in the bottom panel was performed in the presence of 1 mM ATP.

3.2. FlhB

3.2.1. FlhB-C WT and FlhB-C N269A

The WT FlhB-C and the N269A FlhB-C (non-cleaver mutant) run at the same elution volume on size-exclusion chromatography, as both FlhB-C WT fragments remain associated (**Figure 22A**), indicating that the two cleaved fragments of the wildtype retain affinity for each other (the solved structure in **Figure 24 and 25** also shows the FlhB-CC fragment still present despite the cleavage). The proteins were purified using His-tag affinity purification with a Ni-NTA resin column. For the His-tagged WT protein, however, only one band (roughly 14 kDa) is visible on the SDS-PAGE gel, not two bands (due to cleavage), as expected. The N269A does show a single band, at the expected size (roughly 19 kDa, see **Figure 22A**). Similar behaviour for the WT protein had previously been observed with *Salmonella* FlhB-C in Inoue et. al [54] and [48], for example; in [48], they postulate that the single band is actually a superimposition of the FlhB-CN and FlhB-CC bands, even though FlhB-CN is a significantly smaller fragment. This behaviour would explain why only a single band is also observed for the *S. putrefaciens* FlhB-C (His).

In order to further demonstrate that the WT FlhB-C protein indeed splits into two fragments (SDS gel bands) that retain affinity for each other after cleavage, an N-terminal GST-tagged FlhB construct can be used instead – in this case, the GST-FlhB-C-N269A runs as a large single band, while the GST-FlhB-C WT protein clearly shows two bands; a large band corresponding to the GST-FlhB-CN fragment, and a smaller band, which is the FlhB-CC fragment (**Figure 22C**). For more details on crystallization of FlhB-C, see **chapter 3.2.3.** together with **Figure 22B**.

Both the non-cleaver mutant and the wildtype protein migrated on size exclusion with the apparent molecular weight of a monomer, as indicated by the calibration standard molecular weights in (**Figure 22A**). This confirms that both fragments of the cleaved wildtype protein co-migrate together. The mutation of the Asparagine 269 does not in any way change the behaviour of the protein in terms of oligomerization.

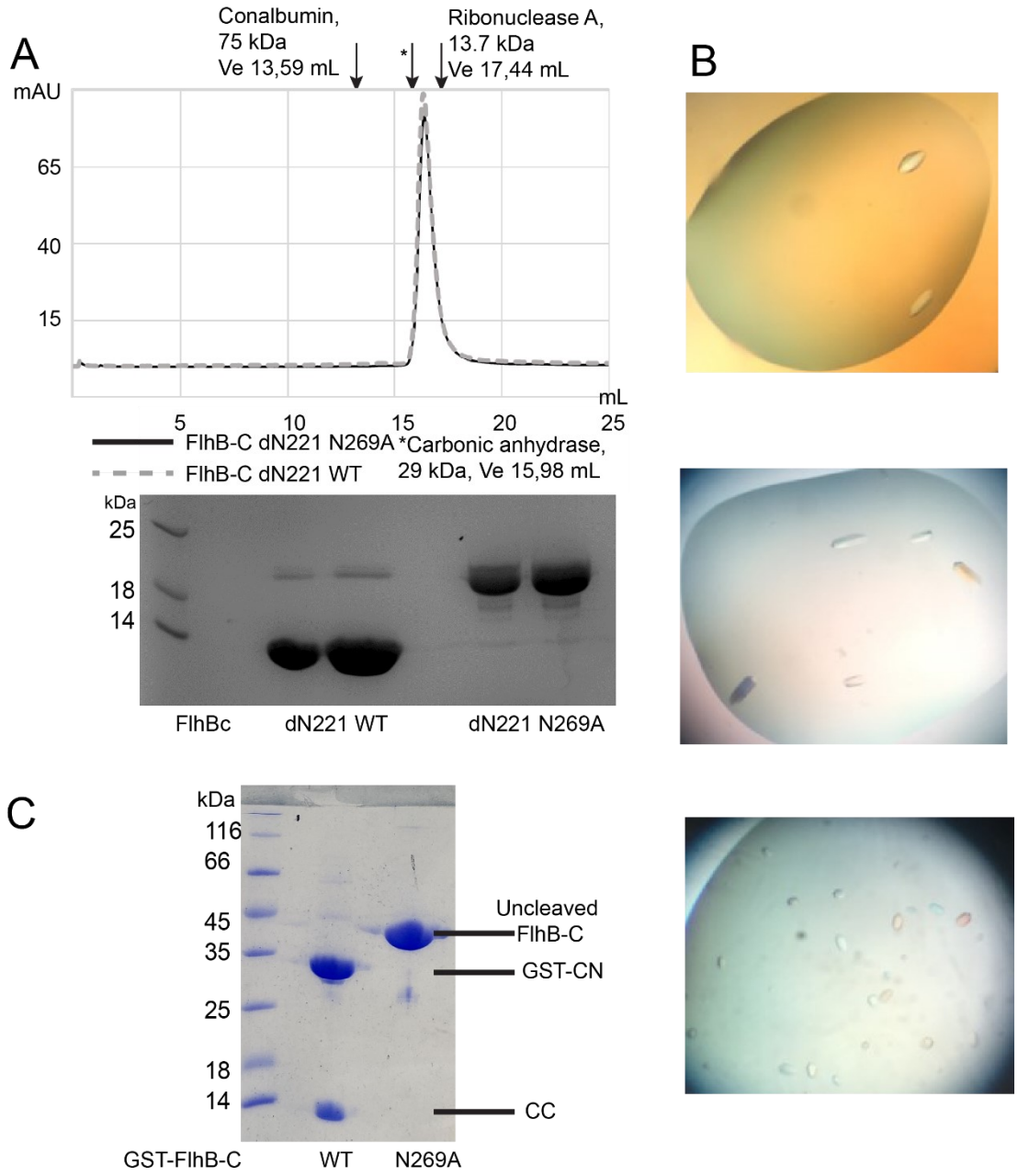

Figure 22 FlhB behaviour and crystallization. A - Analytical SEC runs of FlhB-C dN221 N269A and WT (upper panel) together with the corresponding SDS-PAGE gel (lower panel); B - Crystals of FlhB-C WT obtained in three different conditions (top to bottom: Core III B2, Core IV D5, Core Complex H6; for exact composition see Methods section),C - SDS-PAGE gel showing the difference between WT and N269A (non-cleaver) GST-FlhB purified proteins

Furthermore, additional experiments were performed in collaboration with John Hook of AG Thormann to determine whether the cleavage event is affected by mutations/deletions to FlhB-C (**Figure 23 below**). These experiments clearly confirm the already known result that a N269A variant of FlhB significantly represses the cleavage event and is primarily present as the non-cleaved version of FlhB. Interestingly, a deletion of the PRR motif also results in an increase in proportion of

uncleaved FlhB, in comparison with the wildtype protein. The Y376A mutant does not differ significantly from the wildtype protein in behaviour.

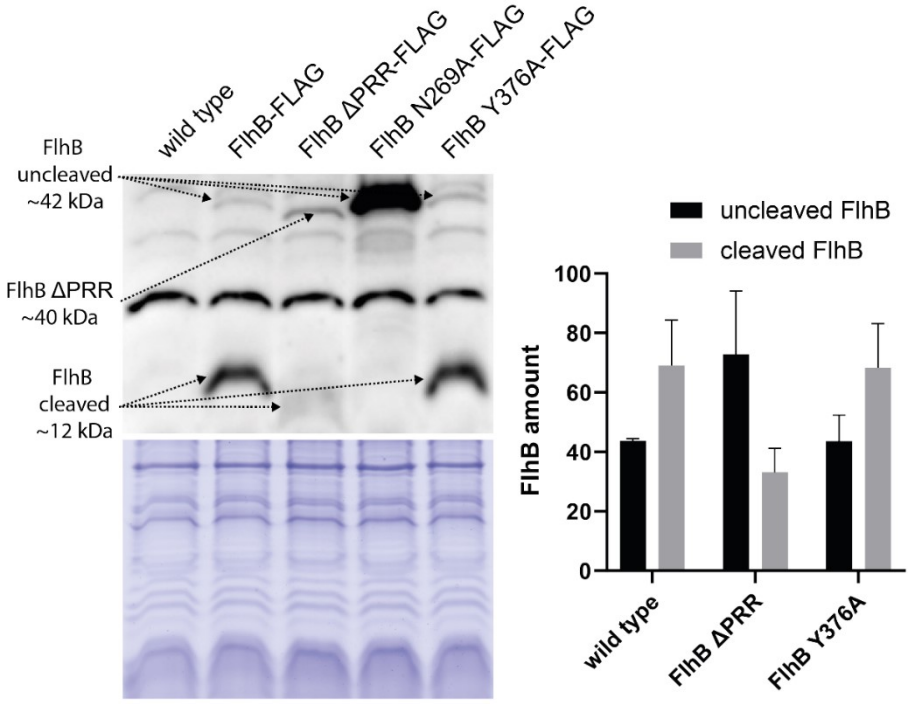

Figure 23 Western blots and analysis of FlhB mutants. The western blot (left panel) was used for detection of FlhB protein to observe and quantify cleavage behaviour of different constructs (right panel). Data obtained in collaboration with John Hook, AG Thormann, Gießen, who kindly provided the images, which were also published in [180].

3.2.2. Crystallization and structure of FlhB-C

Prior to successfully obtaining a crystal structure of the protein, FlhB-C WT and different non-cleaver mutants (N269A, P270A) were attempted to be crystallized. Despite successfully obtaining crystals, no quality data could be obtained, and hence the structure could not be resolved.

After further attempts, a crystallization of the WT protein was successful, leading to crystals being observed in three different conditions (see **Figure 22B**) (JCSG Core III B2, 0.2M Lithium sulfate, 0.1M Tris pH 8.5, 1.26 M ammonium sulfate; JCSG Core IV D5, 0.1 HEPES pH 7.5, 1.5M Lithium sulfate; Core ProComplex H6, 0.1M MES pH 6.5, 1.6M Magnesium sulfate), three weeks after setting up crystallization plates. Only two of the conditions lead to crystals large enough to be harvested, which were then frozen in liquid nitrogen, and data was collected on them at the DESY synchrotron facility in Hamburg. Of the crystals that were tested, one dataset allowed structure determination to proceed successfully.

From this dataset, a final structure of FlhB-C containing residues 252-376 could be obtained and refined to the final resolution of 2.1 A (**Figures 24C**). The structure was resolved using molecular replacement, where the structure of *S. typhimurium* FlhB-C was used to perform MR (PDB structure 3B0Z). The structure was additionally compared to *A. aeolicus* FlhB (3B1S; both structures obtained from reference [37] (**Figure 24B**). The structures are highly structurally similar and share the overall fold, containing a central four-stranded beta sheet, as well as four surrounding alpha helices. In accordance with previously available FlhB-C structures, the cleavage event could also be observed in the *Sp*FlhB-C structure (**Figure 24C**), leading to the formation of two subdomains that remained tightly associated with each other (CN and CC domains containing residues 252-269 and 270-376, respectively). The C-terminal region sequences of *S. typhimurium* and *S. putrefaciens* are shown in **Figure 24A.**

In contrast to the many similarities, there are also two important differences between the *Sp*FlhB-C structure and the previously solved FlhB-C structures (**Figures 24 B, C**). The first one being the N-terminal part of the first alpha helix, which was not successfully resolved in the *Shewanella* case (but clearly takes the form of a longer alpha helix in other structures). In the second case, the *Sp*FlhB-C structure managed to show for the first time the very C-terminal part of FlhB-C, which was termed the PRR. This region contains residues 356-376, many of which are located in close proximity to alpha helices 3 and 4, to the latter in particular. To analyze the binding interface between the core domain of FlhB-C and the PRR, the LigPlot software was used, which identified specific residues participating in hydrophobic interactions and hydrogen bonding (see **Figure 27** and chapter **3.2.5.**).

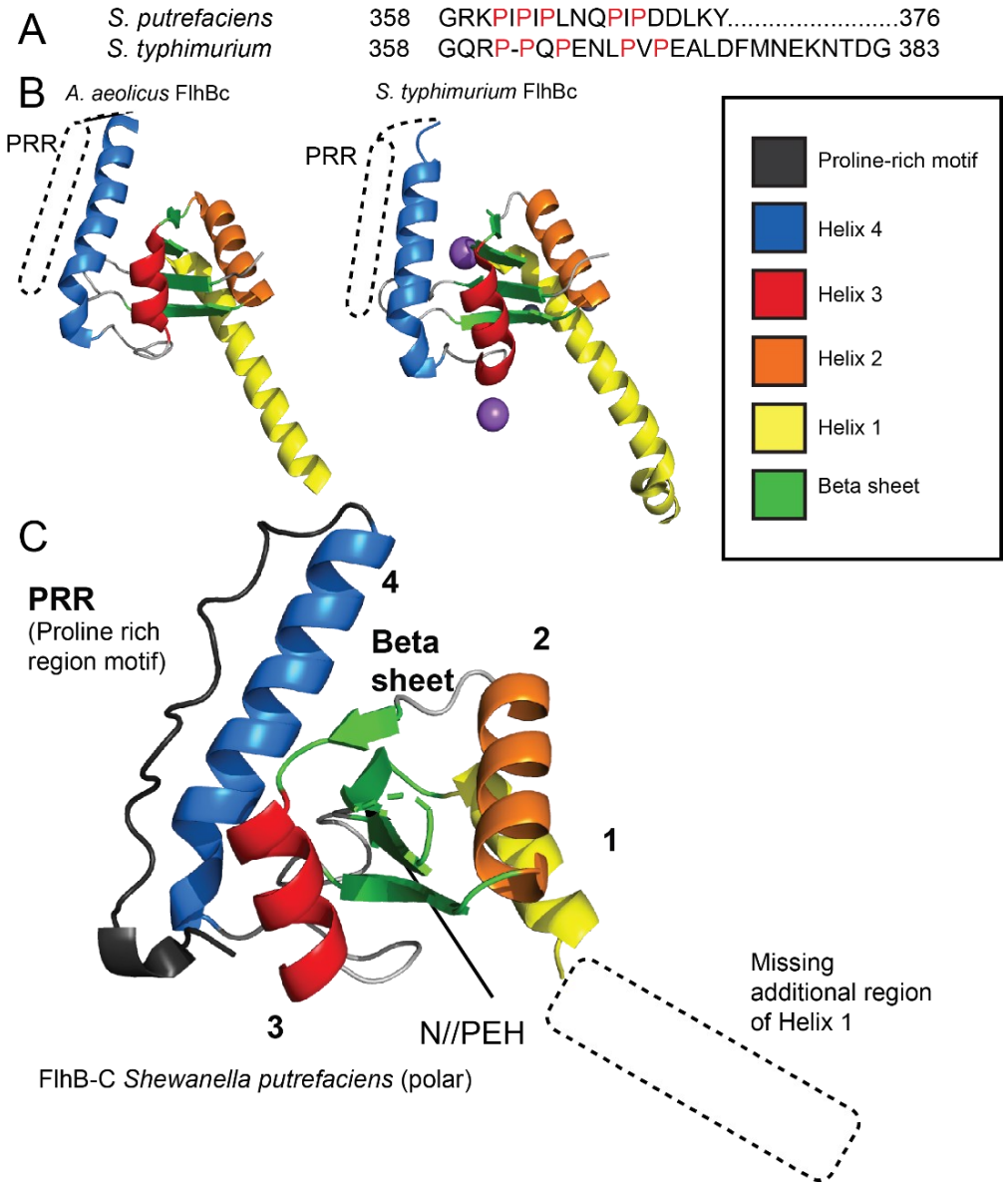

Figure 24 Structure analysis of FlhB-C . A - Comparison of C-terminal sequences of *S. typhimurium* and *S. putrefaciens;* B - Structure of FlhB-C from *A. aeolicus* and *S. typhimurium* ([37]) indicating the missing PRR motif; C - S*. putrefaciens* FlhB-C structure indicating the region of Helix 1 that is present in AA and ST structures. Helices have been colour coded for easier identification between different structures (see part B, right side). Images of structures prepared with Pymol software.

3.2.3. Consurf analysis of FlhB-C

The Consurf analysis of the solved *Shewanella* FlhB-C structure discussed in **3.2.2.** (which was provided as template/input to the Consurf server) has shown that the *S. putrefaciens* cytoplasmic domain of FlhB is overall relatively well conserved. This is particularly true for the cleavage site and the region immediately adjacent to the cleavage site (**Figure 25C, E**), as well as a number of residues identified by [181](in

Salmonella) as essential for interactions with flagellar secretion substrates, see **1.2.2.1** (the numbering in **Figure 25** is referring to the FlhB-C structure only, so residue 251 is residue 1, for example). Most of the PRR motif (**Figure 25D, E**), at least according to Consurf, is overall relatively poorly conserved, and in any case less conserved than most other regions of the protein. This is in accordance with data presented in **Figure 29**., since the PRR is primarily specific to gamma- and beta-proteobacteria. The Consurf conservation score, as presented in **Figure 25E**., displays the least conserved residues as a full cyan colour, and the most conserved ones as burgundy/dark red, with intermediate conservation scores having a white colour. Figure **25A** shows the conservation of the C-termini of various representative species with different flagellation patterns compared to the FlhB-C PRR.

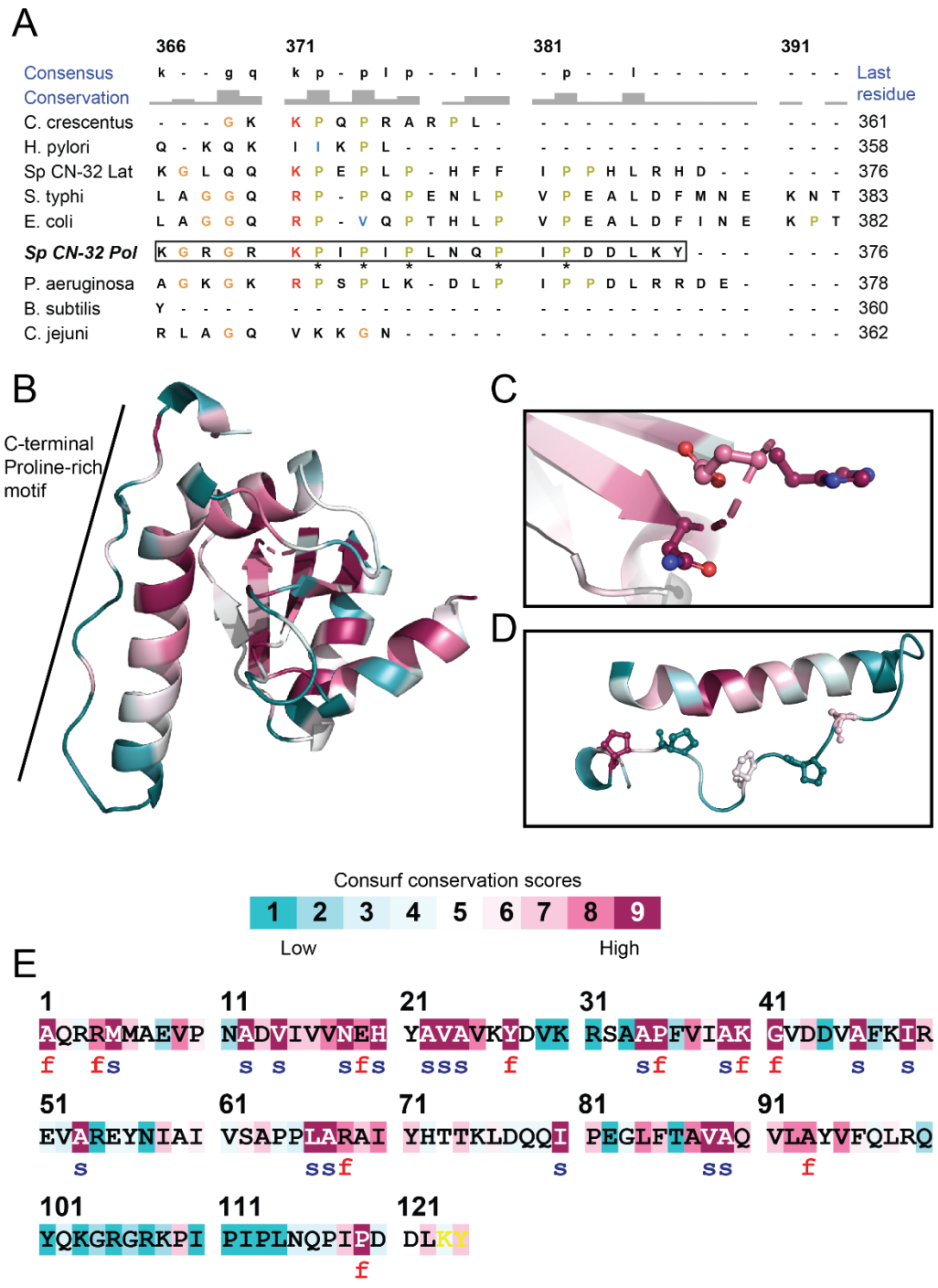

Figure 25 : **Consurf analysis of FlhB-C**. A - alignment of the C-termini of representative FlhBs; B - consurf conservation scores (E) projected onto the SpFlhB-C-Pol structure; C - zoom-in onto the strongly conserved NPEH cleavage site; D - zoom-in onto helix 4 and the PRR motif; E - Conservation score scale and the colour coded FlhB-C residue sequence. For additional explanation of conservation scores please see **Figure 18**. Images of structures prepared with Pymol software.

3.2.4. Further FlhB structure analysis in context of Evans et. al 2013 and Inoue et. al 2019

The two articles (references [54,181]) mentioned in the title of the chapter had previously delineated the role of several residues in FlhB-C, which were found to perform distinct roles. The researchers did so focusing on the *S. typhimurium* FlhB and its structure. The authors of these articles identified several residues in the cytosolic domain of FlhB that form a surface hydrophobic patch, which is important for interactions with hook and rod flagellar substrates (later tested with FlgD and FlgG, respectively)[54] These residues are A286, P287, A341, L344 (which actually retain their numbering and are fully conserved also in the *S. putrefaciens* polar FlhB, see **Appendix 7.5.1.**). In the published *S. putrefaciens* FlhB-C structure [180], the PRR region, which was never structurally resolved before, is not directly interacting with these residues making up the hydrophobic patch (see **Figure 26A, red residues**). It is therefore not the role of the PRR to interfere with flagellar substrates interacting with this region.

Additionally, the article [54] was also investigating the role of additional residues, this time involved in an intra-FlhB-C interaction, providing a hydrophobic interaction network to stabilize the cytoplasmic domain of the protein (these residues from *Salmonella* were again compared to equivalent *S. putrefaciens* residues, see **Appendix 7.5.1**). These residues were also visualized in Pymol, and, in contrast to the hydrophobic patch mentioned earlier, some of the residues could potentially face in the direction of the PRR. One of them is located close to the Evans et. al [181] hydrophobic patch and could potentially be facing in the direction of the PRR (sand coloured, V340 in **Figure 26A**). **Figure 26B** visualizes the whole hydrophobic patch region from [181](plus V340), but in a zoomed-out view. Judging from this side, A341 is also potentially facing the PRR, but is likely not directly interacting with it. A341 was also not identified as an interacting residue (between the PRR and helices 3 and 4) in the LigPlot data, **Figure 27.**

Other residues from Inoue et. al [54] are visualized in **figure 26C**; A311, L350, L318-322. The only residue potentially facing the PRR region is R320 (bottom residue of the indicated red region). To sum up, only R320/V340 ([54]) or perhaps A341 ([181]) could be in a position to weakly interact with the PRR, but none of them are found in direct

proximity to it, just facing in its general direction. The PRR is then likely not involved in the intra-FlhB-C hydrophobic interaction network, or in regulating the hydrophobic patch residues.

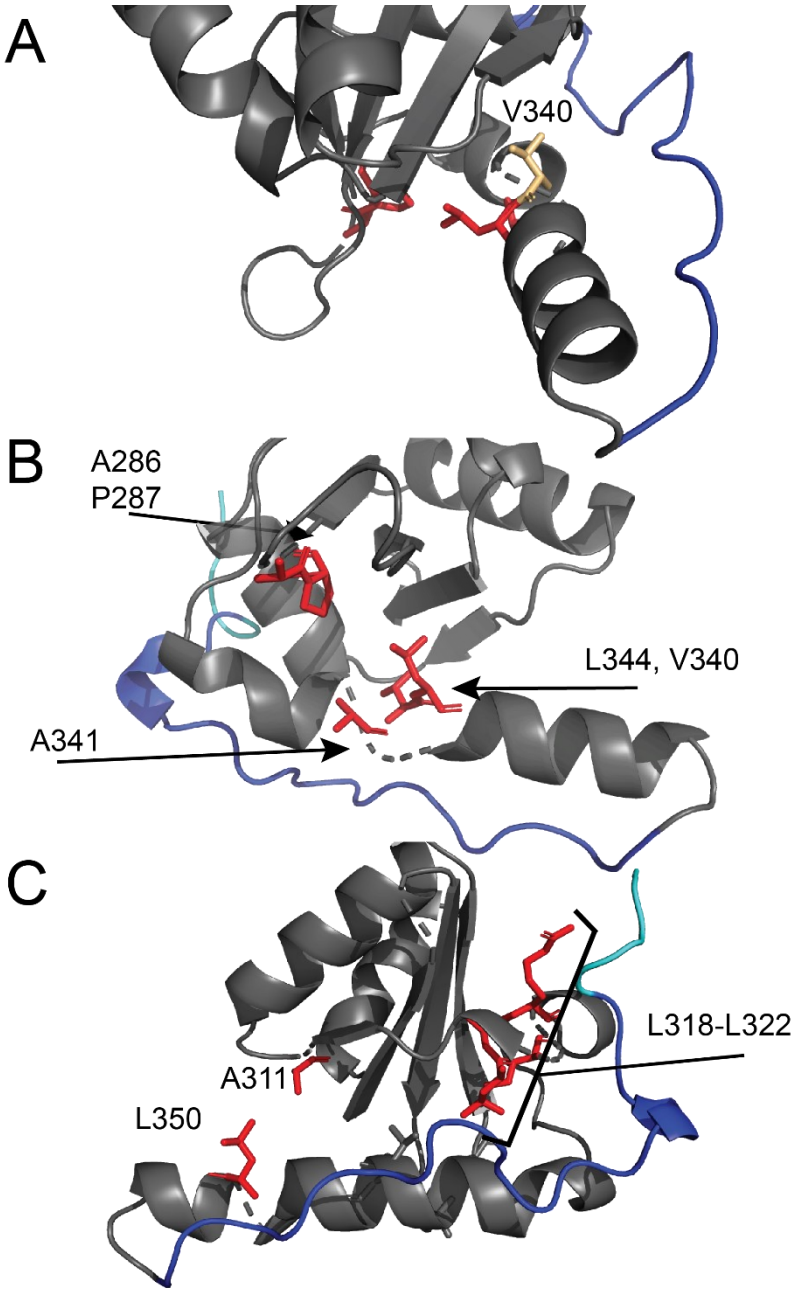

Figure 26: **Visualisation of different residues in S. putrefaciens FlhB-C**. Performed to analyse their proximity to the PRR motif. A – identified in [181] hydrophobic patch residues (red), V340[54] (sand), PRR (blue), zoomed in to visualize V340; B - hydrophobic patch [181], all residues (zoom out view); C - residues involved in intra-FlhB-C hydrophobic networks [54] (red), His tag (cyan), PRR (blue). Images of structures prepared with Pymol software.

3.2.5. LigPlot analysis of FlhB-C

An additional analysis of the interactions between the PRR and the core domain of FlhB was carried out with the help of LigPlot [182,183]. This software allows the identification of hydrogen bonding interactions and hydrophobic interactions between residues in close proximity from a provided PDB file. LigPlot automatically generates interaction diagrams for protein-ligand and protein-protein interactions. In this case, the interactions between helices 3/4 and the PRR were investigated (the former containing residues 312-356 and the latter 357-376). Based on the data produced by LigPlot, the following hydrogen bonding interactions take place between the PRR and the core domain of FlhB (PRR residue always written first): K360 with Y353, G358 with Q349 and Q352, R359 with Q349, R357 with Q352. Additionally, Q368 with Q342 and A339 (see **Figure 27**). All of the residues from the core domain participating in hydrogen bonding with the PRR are found in helix 4. Other residues that are only involved in the formation of hydrophobic contacts with surrounding residues are also identified by LigPlot; looking at the residues themselves, the extreme C-terminal part of the TRR is located in proximity to helix 3 (**Figure 27** panel 3). The **Figure 27** below depicts the interaction interface as defined by the DIMPLOT module of LigPlot [182,183] .

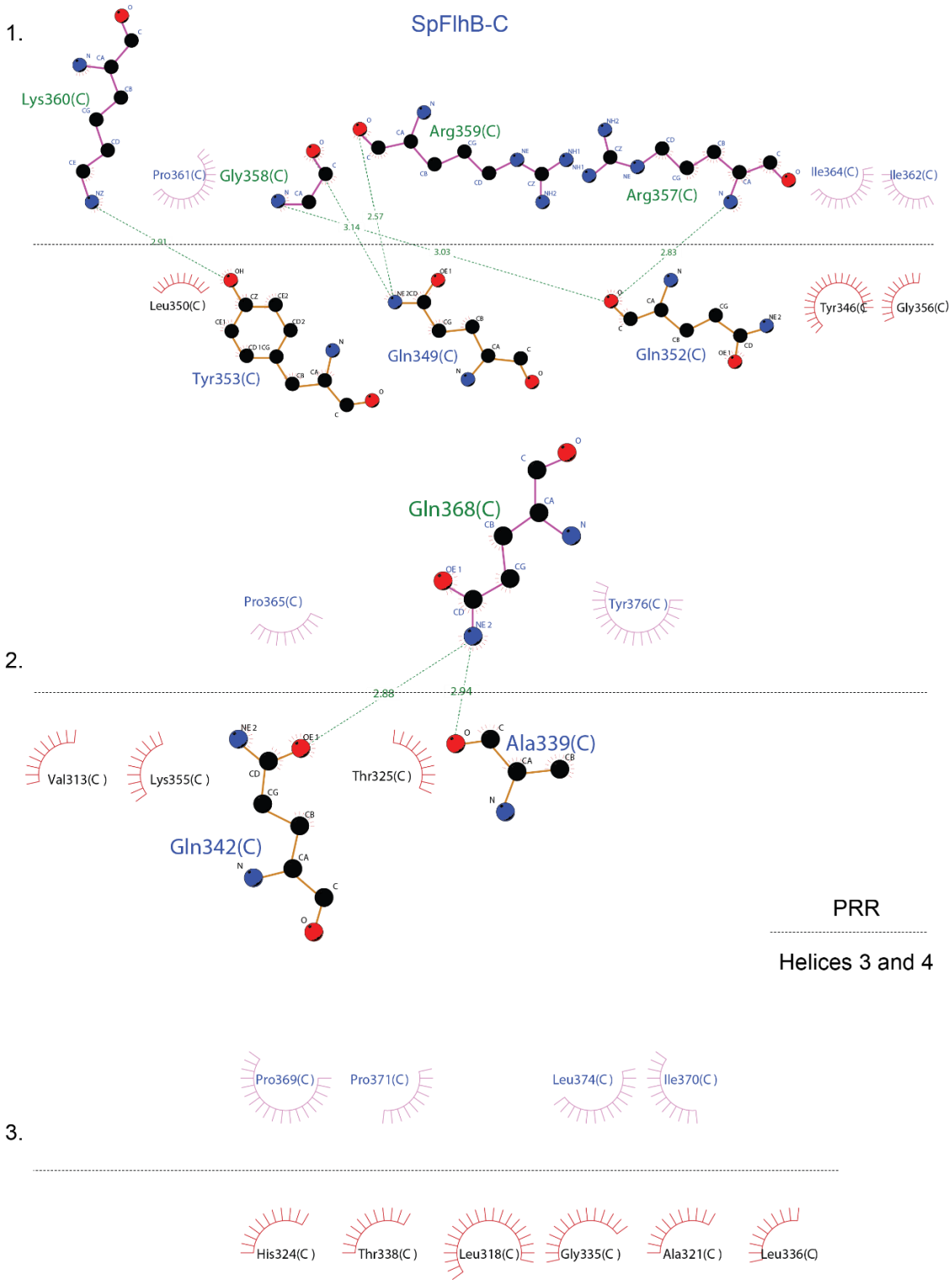

Figure 27: LigPlot DIMPLOT data output. Residues directly interacting with one another through hydrogen bonding are fully depicted, with interacting atoms indicated. Residues forming hydrophobic contacts only are depicted by name and residue number. The residues on the top half of panels 1, 2 and 3 are those contained in the PRR (357-376); those in the bottom half of all panels, under the dotted line, are residues from helices 3 and 4 of FlhB-C (residues 312-356). Data originally obtained as single horizontal image but rearranged to fit into a vertical layout. Figure and legend text also used in Supplementary data of [180].

3.2.5. Deleting the last 20 C-terminal residues of FlhB leads to a decrease in flagellation

Since FlhB is essential for assembly of the flagellar secretion system, a deletion of FlhB led to a complete lack of flagellation in cells (this was confirmed both by hook and filament visualisation methods). Wildtype *S. putrefaciens* cells were classified as having a polar flagellum in 56% of hook stains and 67% of filament stains (the rest of cells appeared to be non-flagellated, see **Figure 28A, B**). The number is likely lower than the actual percentage due to method inefficiency – it can also be observed that the hook-stain method is less effective than the filament-stain method.

In the strains that had the PRR motif of FlhB deleted, the number or position of the polar flagellum did not change, which hints that the spatial and numerical regulation isn´t disrupted by this alteration. The percentage of flagellated cells, however, was noticeably lower in the strains missing the PRR motif. This percentage reduction was 31 ± 7% in filament-stained and 26 ± 10% in hook-stained cells (see **Figure 28A, B**). The results undoubtedly show that the PRR motif is important for efficient flagellar assembly, and that it affects both hook and filament assembly (see **Figure 28A, B**). A deletion of FlhB fully abolished flagellation.

Additionally, the role of deleting the PRR in C-ring assembly was also investigated. It was determined that the deletion does not affect the assembly of the C-ring, as FliM1 still localized to the pole even in the delta PRR strain. Additionally, 32 +/- 5% of the FlhB deletion strain still had flagellar C-rings (evidenced by the polar localization of FliM1), even though no hooks or filaments could be detected (**Figure 28C**). Based on these results, it can be concluded that the PRR motif of FlhB is important for the functioning export of flagellar substrates but not basal body formation.

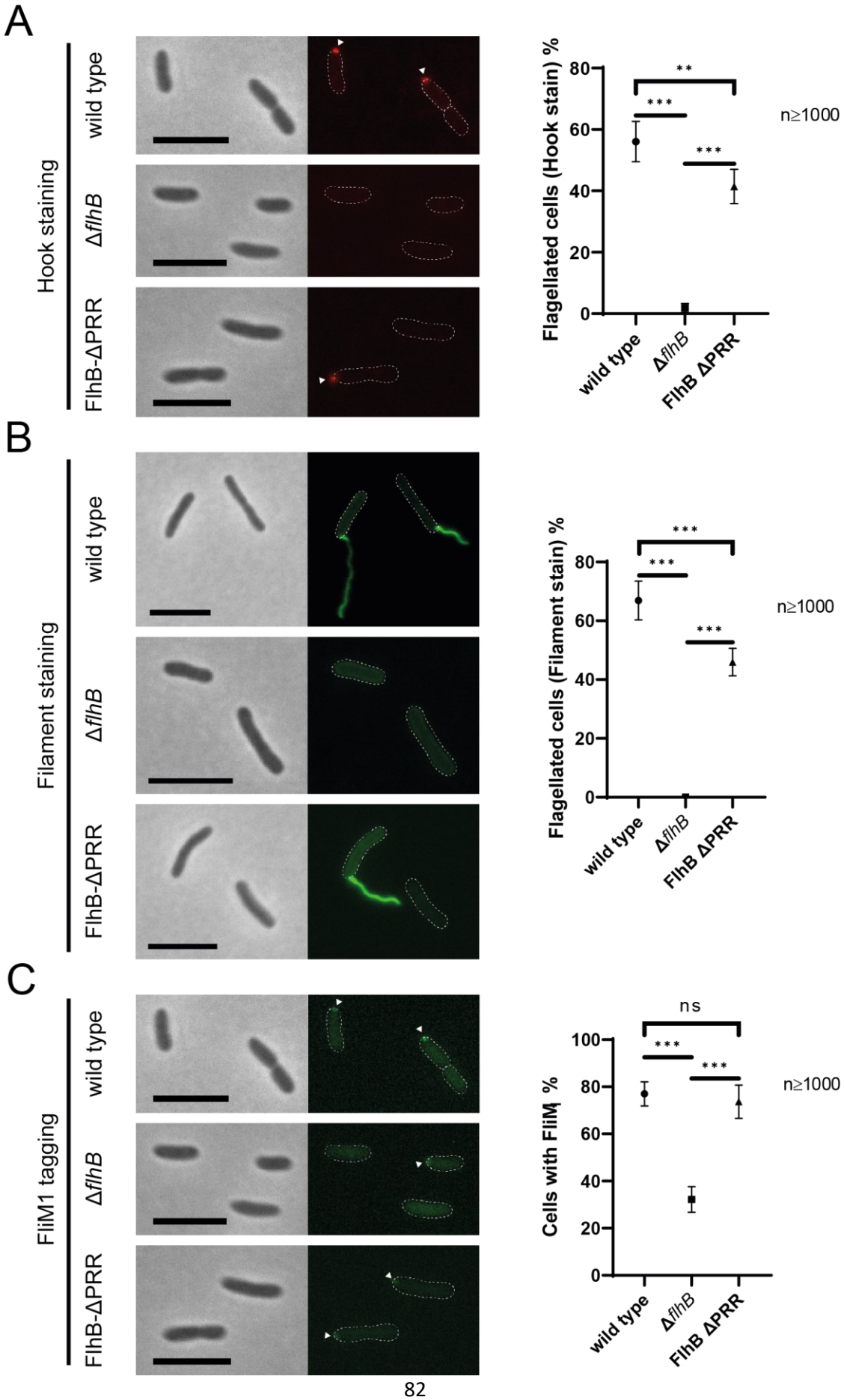
A
Hook staining
wild type
ΔflhB
FlhB-ΔPRR
Flagellated cells (Hook stain) %
n≥1000
wild type
ΔflhB
FlhB ΔPRR
B
Filament staining
wild type
ΔflhB
FlhB-ΔPRR
Flagellated cells (Filament stain) %
n≥1000
wild type
ΔflhB
FlhB ΔPRR
C
FliM1 tagging
wild type
ΔflhB
FlhB-ΔPRR
Cells with FliM %
ns
n≥1000
wild type
ΔflhB
FlhB ΔPRR

Figure 28 Microscopy and quantification analysis of SpFlhB ΔPRR effects in comparison to wildtype and a ΔflhB mutant. A - Microscopy images of hook-stained cells and comparative quantification of hook formation; B - Microscopy images of filament-stained cells and comparative quantification of filament formation; C - Microscopy images of $FliM_1$ localization in cells and comparative quantification of $FliM_1$ localization. Scale bar: 5 µm. ✱✱✱ ≙ P = <0.0001. ✱✱ ≙ P = <0.001 (data obtained in collaboration with John Hook, AG Thormann , Gießen, who kindly provided the images)

3.2.6. Phylogenetic analysis of FlhB

The phylogenetic analysis of the proline-rich region was performed in collaboration with Dr. Jan Pane-Farre of the Bange lab, who kindly provided **Figure 29** (which was also published in [180]).

Due to the additional structural information now gained on the PRR, the occurrence of the PRR itself (and its conservation) in different groups of bacteria was investigated. First, a comparison of the sequences of various representative FlhB proteins from the major bacterial phyla was carried out (see **Figure 29A** for the different species). This showed that FlhBs (including their proline-rich regions) from beta and gammaproteobacteria are closely related to each other, but also that there is an additional domain (called Pfam Bac_export_2, see **Appendix 7.5.3**) which is contained in beta and gammaproteobacteria, as well as actinobacteria, which contains 30 to 60 residues.

BLAST searches were then performed to further investigate the presence of PRR motifs within gamma and betaproteobacteria (see **Figure 29B**). As the query sequences, PRR regions (far-end C-termini of FlhB) identified in the phylogenetic analysis were used. The results indicated that the motif from the *S. putrefaciens* polar FlhB can primarily be found within gammaproteobacteria (Alteromonadales, Vibrionales and Pseudomonales). Additionally, there were two other proline-rich regions which were found in enterobacterales and different betaproteobacteria groups (Neisseriales, Burkholderiales and Nitrosomonadales)(see **Figure 29B**).

Even though slight differences exist, there are four key points that summarize the common elements of the PRR elements found in the groups of bacterial species outlined above. These are: a) a highly conserved N-terminal glycine b) five or less

proline residues, which can variably be separated by 1-4 residues c) a hydrophobic/bulky valine or isoleucine directly before the fourth/fifth proline of the PRR in beta/gammaproteobacteria respectively d) residues with negative charge found close to the last proline residue of the PRR.

At last it should also be stated that the proline-rich motif is not found in any of the investigated sequences of FlhB homologs found in injectisomes. It can then therefore be summarized that the PRR is unique to FlhB proteins found in flagellar systems of gamma and betaproteobacteria.

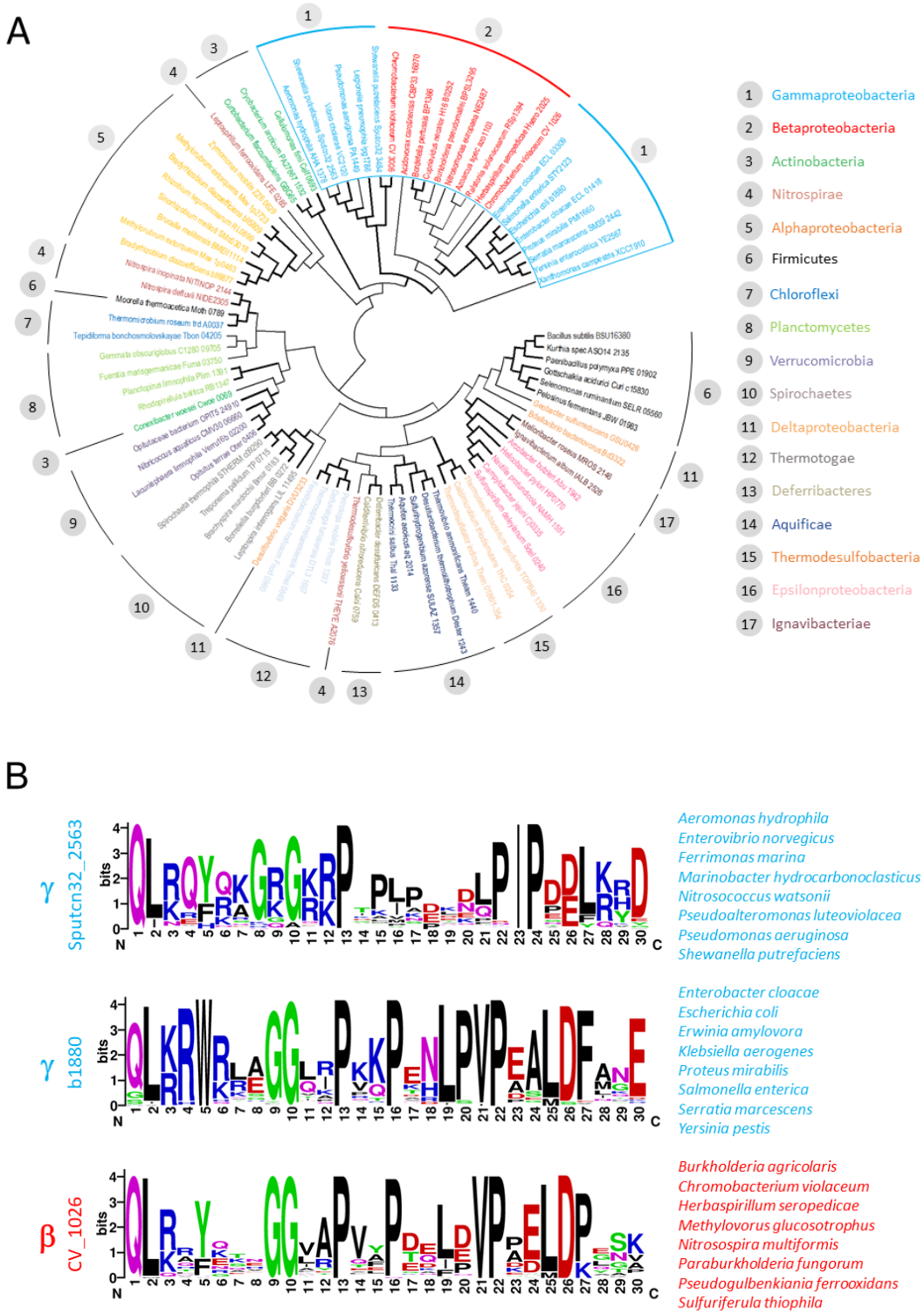

Figure 29 Occurrence of PRR within the g- and b-proteobacteria. Prepared by Dr. Jan Pane-Farre. A - Phylogenetic analysis of FlhB sequences. Bifurcations supported in 50% or greater proportion of bootstrap replicates depicted bold; B - Sequence logo depictions of the PRR relative to the two gamma- and one beta-proteobacterial cluster as indicated. The locus tag of the query used for PRR identification shown on the left side of Part B, species names on the right side. The figure was also published in [180] and kindly prepared by Dr. Jan Pane-Farre.

3.2.7. Additional interaction partners of FlhB in *S. putrefaciens*

With a Y2H experiment, different potential interaction partners of the *S. putrefaciens* FlhB were screened, with the experiment showing a clear interaction between the polar FliM and polar FlhB (performed by Dieter Kressler, see **Figure 30A**). To further investigate these findings, GST-pulldowns were carried out to determine whether FlhB-C can also bind to FliM *in vitro.* Even though the Y2H experiment did not show interactions with FlhA-C or FliK, pulldown experiments were still performed to probe for interactions in *S. putrefaciens*, since FlhA and FliK are known interaction partners of FlhB from other organisms ([39,40]).

The pulldown in **Figure 30B** shows that FliM/N strongly binds to GST-FlhB-C WT, with a fainter FlhA band visible in the absence of FliM/N (FliM and FlhA-C bands overlap in size on the SDS-PAGE gel). The FliM/N binding to FlhB is in accordance with the previous Y2H data. Reversing the pulldown (immobilizing GST-FlhA, see **Figure 30C**) shows that FliM/N is only seen to strongly bind to FlhA if FlhB is also present (**Figure 30, lane 3**). This would suggest that there is no strong direct interaction possible between FliM/N and FlhA, and that FlhB acts as a bridging partner between them (FlhB/FlhA interactions have also been identified and confirmed previously in other organisms, such as *S. typhimurium,* in the literature [39,40]). In **Figure 30D**, both FlhB-C WT and FlhB-C N269A are shown binding moderately to a GST-FlhA-C construct, but only very faintly to a negative control (an unrelated protein, the first 20 residues of PomX from *M. xanthus*, fused to a GST tag). Overall, the binding between FlhB-C and FlhA-C does not seem to be particularly strong when they are present alone.

Regarding the importance of the PRR motif (or lack thereof), another experiment was performed to probe the interactions of GST-FlhB-C WT, GST-FlhB-C dC20 (lacking most of the PRR motif), and GST-PRR itself with FliK. No interactions could be identified with any of the constructs, however (**Figure 30E**).

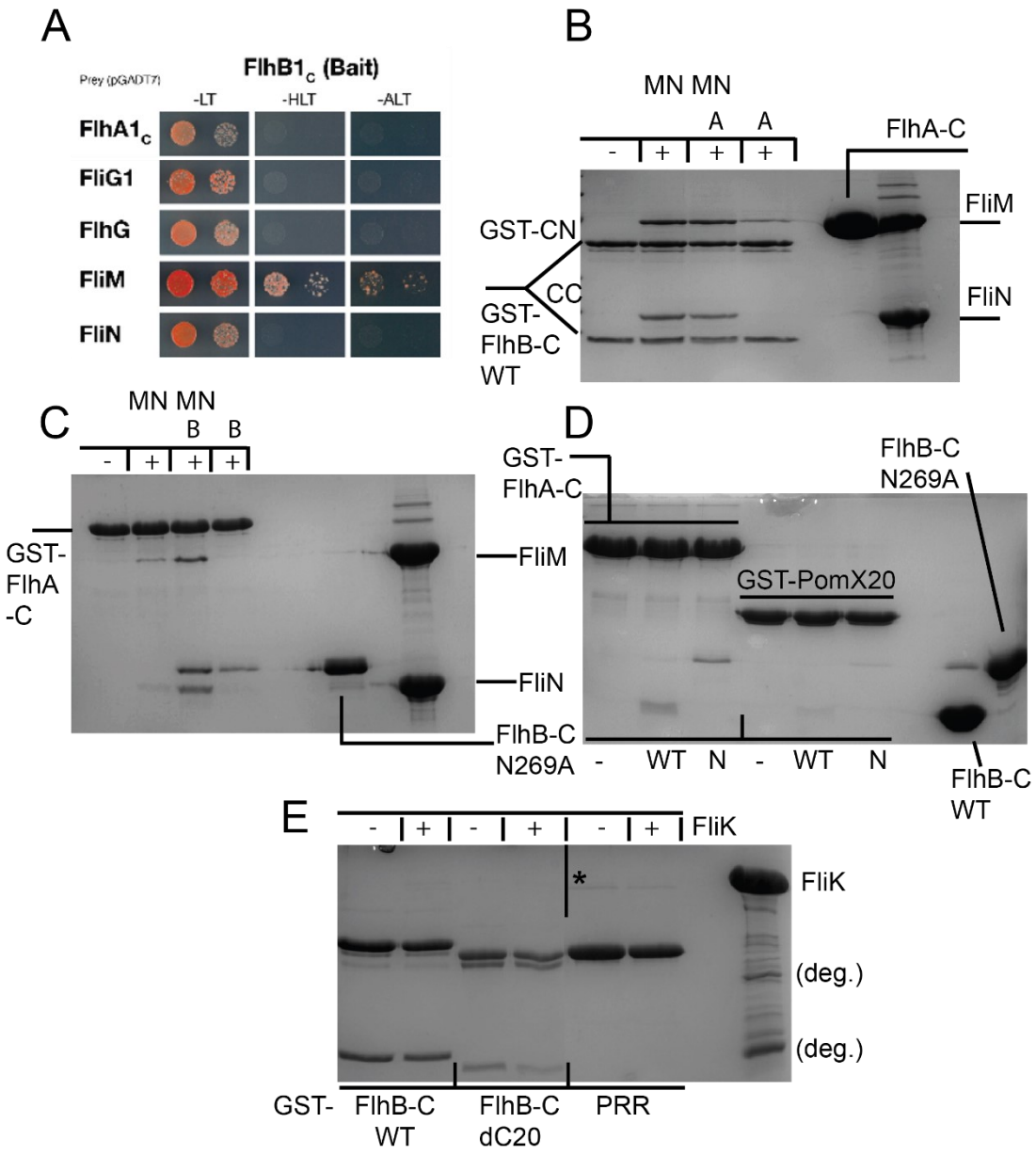

Figure 30 Additional interaction partners of FlhB-C in S. putrefaciens. A - Y2H experiment showing an identified interaction between FliM and FlhB-C, but not showing interactions with FliG, FliN, FlhG or FlhA. Experiment performed and image provided by Dr. Dieter Kressler; B - GST-pulldown testing interactions between GST-FlhB-C and FliM/N, FlhA-C; C - GST-pulldown testing interactions between GST-FlhA-C and FliM/N, FlhB-C N269A; D - GST-pulldown testing interactions between GST-FlhA-C, an unrelated GST-control peptide and FlhB-C N269A, FlhB-C WT; non-specific interactions with the control are significantly weaker and barely detectable based on bands intensity; E - different GST-FlhB-C constructs tested for binding against FliK; there was no binding observed with any of the constructs. (*in part E refers to a lane in the gel being cropped out; sample in lane 4 was loaded twice by accident).

4. Discussion

4.1. FlhG and its interaction partners

As outlined already in the introduction, it has been determined previously that FlhG is a key regulatory protein present in a variety of bacterial species with different flagellation patterns. It was also known that it functions as a negative regulator of flagellar number in monotrichous polar flagellates (which also include *S. putrefaciens*). FliM and FlrA themselves have also been identified as interaction partners of FlhG in the past, although their interplay in controlling the rate of flagellar assembly remained poorly understood to a significant degree. Proteins assembled into different flagellar substructures are not all expressed and assembled at the same time – rather, an intricate control system exists to ensure that this occurs stepwise, and that (in a wildtype situation) the next "batch" of proteins only starts being produced, when assembly of the previous flagellar stage has been completed. Flagellar genes are normally separated into class I, class II, class III and class IV genes, depending on their hierarchy. The figure below (**Figure 31**) shows the hierarchy of flagellar genes in *Legionella pneumophila*, which is (like *S. putrefaciens*) also a gram-negative gamma-proteobacterium with a single polar flagellum.

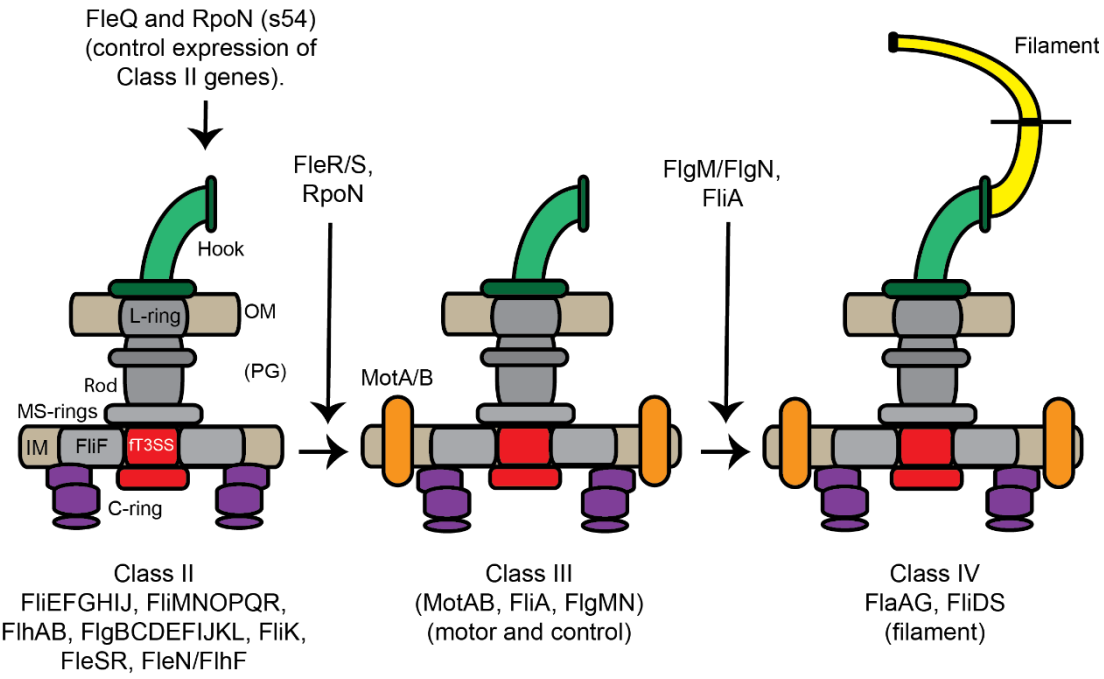

Figure 31 Summary of different flagellar gene classes and their control. It is taking into account the overall structure of the flagellum and its assembly apparatus at each of the stages. OM – outer membrane; PG – peptidoglycan; IM – inner membrane. Regulatory proteins for each stage indicated. Inspired by reference [184] .

With the results presented in this thesis, the step that was of key interest is the regulation of Class II flagellar genes, which, among others, include C-ring proteins (FliGMN), components of the secretion system (FlhAB, FliOPQR), and many others (including FlhG and FlhF themselves). In *S. putrefaciens*, this step is controlled through FlrA, which is, in addition to being an interaction partner of FlhG, also a transcriptional activator. The main question to be answered in this part of the discussion is: what are the roles of FlhG and FliM, directly or indirectly, in the regulation of expression of class II flagellar genes, and later on in the transition to the expression of class III genes?

In *S. putrefaciens,* FliM has already been identified as an interaction partner of FlhG in the past (Schuhmacher et. al [74] , D. Mrusek PhD thesis); the same is true for FlrA (D. Mrusek PhD thesis).

It has been presented in this (V. Blagotinsek) thesis, based on HDX data (see **Figures 16 and 17**), that both FlrA and FliM bind to roughly the same region of FlhG, with binding sites overlapping in helices 6 and 7. Previous data from the thesis of D. Mrusek also supports these findings, employing three different point mutations within these helices in FlhG to show that FliM and FlrA no longer bind upon their alteration (see **Figure 17D** for a visualisation of these residues in FlhG). As seen from the experiments presented in this (V. Blagotinsek) thesis, FliM is also not a factor promoting ADP release from FlhG (see **Figure 15**), and the conformational changes in FlhG occurring in ADP-bound and *apo* states were also investigated (the latter with HDX-MS experiments, see **Figure 17**). It is worth mentioning again that FlrA is only bound to FlhG when FlhG is a homodimer (therefore, as D58A, or in the presence of ATP), while FliM does not seem to prefer either state (and can also bind in the absence of added nucleotides); see **Figure 13.**

The *in vitro* binding behaviour of both interaction partners has also been investigated by using a variety of ATP and ADP concentrations. Using GST pulldowns, (see **Figure**

13E, F), it has been shown that while the FlrA/FlhG interaction essentially depends on the presence of ATP (using WT FlhG), this is not the case with FliM/FlhG. In the latter case, binding occurs in the presence of ADP and ATP, and appears stronger, judging by band intensity, in the presence of ADP; this is true for a concentration range between 0.1 and 2.5 mM ATP/ADP. Also, from this thesis, it can be seen that the FlrA-HTH domain stimulates the ATPase activity over a range of different ATP concentrations, with FlhG and FlrA-HTH both being present in equimolar concentrations (10 uM each) (see **Figure 13D)**. This fits into the model because the stimulation of hydrolysis of the ATP that is bound to FlhG would lead to dissociation of the FlhG homodimer. End-point ATP hydrolysis measurements from *S. putrefaciens* FlhG and FlrA were also used to investigate the behaviour of both full-length proteins, showing that FlrA has a significantly higher intrinsic ATPase activity compared to FlhG (see **Figure 14**).

The **Figure 32** below graphically summarizes key findings, specifically the effects of different mutations on the behaviour of FlhG, FlrA and FliM, and their phenotypic effects in regard to flagellar number and positioning in *S. putrefaciens.* The experimental results have been presented and discussed earlier in the text, but for easier orientation through the figure below, a short text overview of the various stages shown in the figure (A-I) follows (after **Figure 32**).

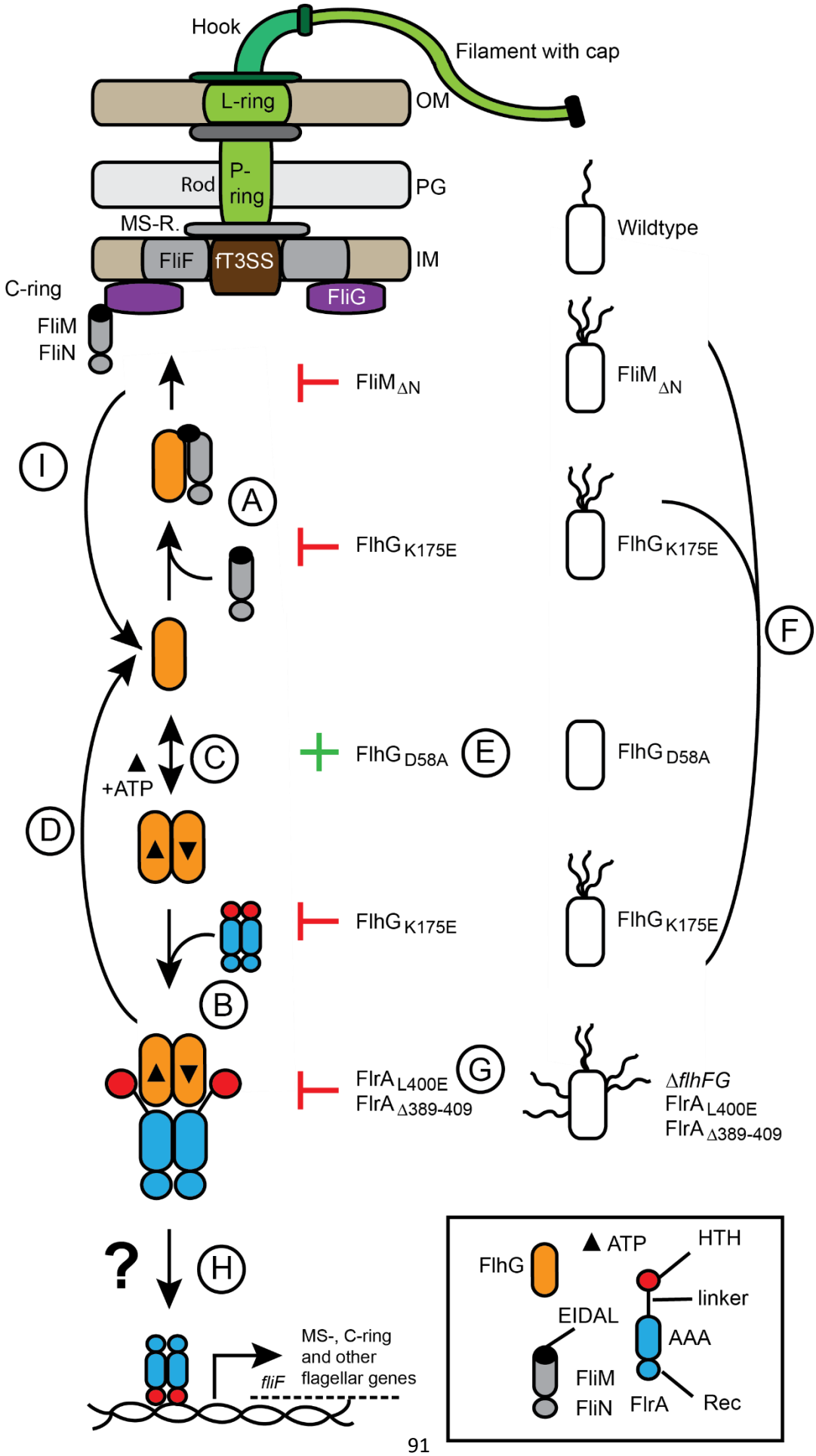
Hook
Filament with cap
L-ring
OM
Rod
P-ring
PG
MS-R.
FliF
fT3SS
IM
C-ring
FliG
FliM
FliN
Wildtype
FliM ΔN
FlhG K175E
FlhG D58A
ΔflhFG
FlrA L400E
FlrA Δ389-409
+ATP
A
B
C
D
E
F
G
H
I
?
MS-, C-ring
and other
flagellar genes
fliF
ATP
HTH
linker
EIDAL
AAA
Rec
FlrA

Figure 32: **Summary of the roles of FlhG, FlrA and FliM in the context of transcriptional control and C-ring assembly**. Figure also published in [175]. Figure depicts different stages in the interactions of FlhG, FliM and FlrA (left) and corresponding mutant phenotypes (right). A – FliM/N binding to FlhG; B – FlrA binding to dimeric, ATP-bound FlhG; C – equilibrium between monomeric and dimeric FlhG; D – release of FlhG after binding to FlrA; E – FlhG D58A mutation leads to lack of flagellation; F – different mutations lead to lophotrichous flagellation; G – disruption of the FlhG binding site on FlrA or deletion of FlhG and FlhF leads to a delocalized hyperflagellation pattern.

A) FlhG (in a nucleotide independent manner) interacts with FliM, and is recruited to the cell pole, where FliM gets incorporated into the growing C-ring. The FlhG K175E mutant acts at this stage, preventing a FliM/FlhG interacting through the mutation in the FliM/FlrA binding region on FlhG (helices 6 and 7). The result of this is a lophotrichous flagellation pattern.

***B)** FlrA (most likely as a dimer) interacts with strictly dimeric FlhG (either WT FlhG in an ATP-bound state, or an ATP-non-hydrolyzing mutant, FlhG D58A). This step, just like step A, is also prevented by an FlhG K175E mutation. The result of this mutation is a lophotrichous flagellation pattern.*

***C)** FlhG is in a monomer-homodimer equilibrium, where the homodimer is ATP-dependent.*

***D)** The FlhG/FlrA interaction ends after FlhG ceases existing as a dimer, and the ATP is hydrolyzed. Free FlhG returns into circulation.*

***E)** In relation to C), the FlhG D58A variant shifts the equilibrium to a purely homodimeric state. The result of this is a lack of flagellation.*

***F)** A lophotrichous phenotype (several flagella at the cell pole) can occur both through a disruption of FlhG/FliM or FlhG/FlrA binding by disrupting their binding site (which is identical) on FlhG, or by deleting the N-terminal region of FliM, which contains the EIDAL motif.*

***G)** A mutation of the binding site of FlhG on FlrA, either by deleting the whole binding region (389-409) or by the mutation L400E. This results in a delocalized hyperflagellation pattern.*

H) *FlrA is released from being sequestered by FlhG and is free to act as a transcriptional activator. The details of this interaction are still unknown.*

I) *FlhG that was interacting with FliM and recruited to the pole is released back into circulation as free monomeric FlhG.*

Complementing the already discussed data and **Figure 32** above, the **Figure 33** on the next pages additionally summarizes flagellar pattern and number together with the state of the FlrA/FlhG interaction, also taking into account (comparing them with) FlhFG overexpression and deletion phenotypes. The interplay between FlhG and FlrA which has an effect on the flagellation pattern, while also taking into account the various mutants, can be thought of as a spectrum. A spectrum that, on one side, shows a "strengthened" FlhG/FlrA interaction (when FlhG D58A is employed, which prevents FlhG ATP hydrolysis and hence dimer dissociation, see **Figure 32E**), which leads to a lack of flagella, and on the other side a "weakened" FlhG/FlrA interaction (which occurs by employing mutants in the interaction interfaces in either protein and results in hyperflagellation and delocalization of flagella, see **Figure 32G**). The WT situation is in between the two extremes, with a dynamic equilibrium between monomeric and dimeric FlhG, and hence free and FlrA-associated FlhG. The association of FlhG with FlrA, as discussed, also possesses implications for the oligomerization state of FlrA itself, but this needs to be investigated further, and is also not fully understood in other organisms (*P. aeruginosa*, for example).

A sensible follow-up question to this model would be, at which point during flagellar assembly FlhG actually becomes a dimer? Since its membrane-association is mediated by the MTS, there might be other unknown interactions at the membrane that FlhG is involved in, which occur after the recruitment by FliM. FlhG is required to be a homodimer to interact with FlrA, and because of transcriptional control, this needs to occur after enough flagellar building blocks have been synthesized. Hence, it is likely that FlhG first interacts with FliM, then dissociates from the pole, binds ATP/forms a dimer, and is ready to sequester FlrA. ATP hydrolysis then releases "free" monomeric FlhG. Such a model also makes sense because qPCR data (see **Figure 20**) show that a deletion of FlhG/FlrA L400E mutation result in an increase of transcription of FliF (which is part of the flagellar cluster under control of FlrA).

Because FlhG is binding to FlrA in FlrA´s linker region, which lies between the AAA+ ATPase domain and the HTH DNA-binding domain, it is so far unknown how exactly its effects are conferred on FlrA. FlhG´s binding could either prevent FlrA from binding DNA directly, or it could interfere with hexamerization, which occurs via the AAA+ domain [103]. Another layer of complexity lies in the ability of FlrA to bind to different promoters, which could be controlled in a variety of ways, including the oligomerization state of FlrA, or the conformational arrangement of the DNA-binding domains. [97,101]. It has actually been determined that in solution, FlrA can be present (in *P. putida*, at least) as a mixture of dimers, tetramers and hexamers and that the equilibrium between different oligomeric states is unaffected by c-di-GMP [185].

Another key question at this point remains why the FlrA d389-409 and the L400E mutant do not simply phenocopy an FlhG deletion mutant, but rather resemble an FlhFG deletion mutant (see **Figure 19**) (so, not a lophotrichous but a delocalized hyperflagellation phenotype). This would suggest that the behaviour cannot only be explained by the FlhG/FlrA interaction but requires FlhF to be considered as well. In previous studies, it has been determined that FlhG interacts with FlhF through the N-terminal activator helix (which stimulates the GTPase activity of FlhF) [86,135]. The FlhG/FlhF interaction might therefore also indirectly be affected by FlrA interacting with FlhG. The Western blots quantifying FlhG and FlhF levels in response to different mutations (**Figure 20**) support this theory. This means that the amounts of both FlhF and FlhG must somehow be controlled through the FlhG/FlrA interaction. This in turn means that both of the alterations of the FlhG binding site on FlrA (deletion of the region and the L400E mutation) cause greater amounts of FlhG to be produced. A consequence of this is that FlhF is then stopped from establishing the cell pole as the site of flagellar synthesis. The overall message is that the flagellar number depends on the equilibrium between FlhG and FlrA, and the availability of FliM, since FlhG interacting with FliM is unable to sequester FlrA, and stop its oligomerization.

Regarding FliM, it has also been determined that the interaction with FlhG is essential to allow FlhG to be recruited to the cell pole (where flagellar assembly is taking place), since FlhG cannot become localized to the pole if FliM is lacking the EIDAL motif ([175],

and D. Mrusek PhD thesis). This hints towards the conclusion that FlhG is not actively determining the pole at all, as it had been speculated in the past.

The recruitment of FlhG by FliM only increases the amount of FlhG present at the pole transiently, and likely when the C-ring is not assembled yet. After the assembly, or rather, at an unidentified point during it, as FliM is incorporated into the C-ring, FlhG dissociates. The mechanisms for this action is also presently unknown, but likely involves a conformational change that is caused by FliM associating both with other FliM monomers within the C-ring, and with FliG, located directly above FliM in the finished C-ring. At that point, association of FlhG with FliM would also be unlikely due to the hindrances presented by the already assembled C-ring components. Cryo-tomography experiments (not shown here but presented in [175]) also show that FlhG by itself is not required for the assembly of a functional and properly assembled C-ring.

Another point to mention is that FliM itself has also been determined to interact with CheY, an important chemotaxis regulatory protein [120,121]. This could be another connection linking flagellar assembly/localization with chemotactic control, but the point in time when FliM interacts with CheY is also unknown. Speculatively, this interaction likely takes place before the interaction with FlhG.

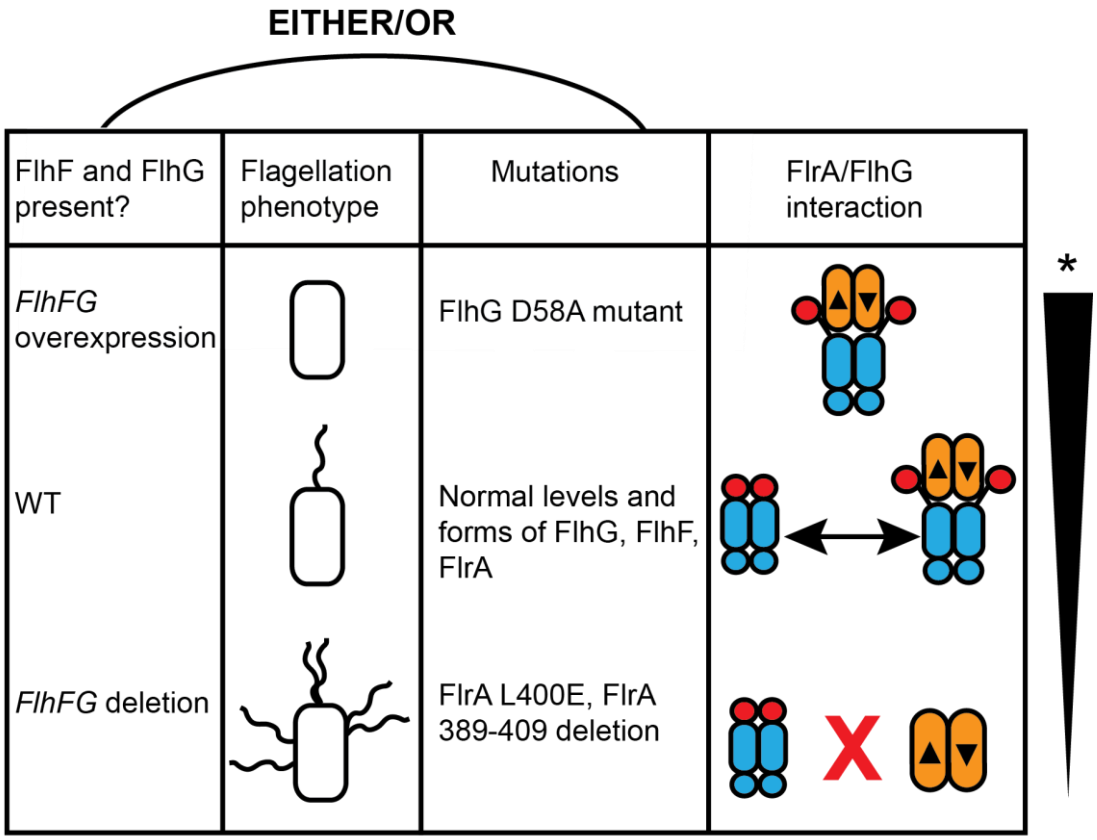

Figure 33*: Summary of key results and model information linking the FlrA/FlhG interaction to different flagellation phenotypes. Considered in relation to the degree/extent of the FlrA/FlhG interaction. From left to right: column 1 indicates the presence or absence of FlhF and FlhG; column 2 indicates the flagellation phenotype; column 3 indicates any implemented mutations; column 4 indicates the degree of FlhG/FlrA interaction. FlhG shown in orange with triangles representing bound ATP. FlrA shown in blue, with the HTH domain shown in red.

4.1.2. Considering the *S. putrefaciens* FlhG/FlrA pair in the context of previous studies done on *P. aeruginosa* FleN/FleQ

Since the FleN/FleQ pair have been studied in considerable detail in *P. aeruginosa*, I wanted to summarize some final conclusions of the similarities and differences between the two systems, which are found in two relatively similar, monotrichous polar flagellates.

Resembling the situation with *Shewanella* FlhG that has been demonstrated with GST-pulldowns for FlhG, HDX and MST measurements (MST measurements that were already presented in the PhD thesis of D. Mrusek, as well as in Blagotinsek et al 2020 PNAS, reference [175]), the *P. aeruginosa* FleN is also active in its ATP-bound form, and

interacts with (=inhibits) FleQ in its dimeric form [93]. As the available data demonstrates, *S. putrefaciens* FlhG does not interact with FlrA in the absence of ATP, when it is monomeric. In this part, the results match previously known findings from *P. aeruginosa.*

A pairwise sequence alignment (Emboss Needle, see **Appendix 7.5.4.2**) calculated the sequence identity of *S. putrefaciens* FlrA with *P. aeruginosa* FleQ as 52.0%. It also demonstrates that the region of *Sp*FlrA involved in binding FlhG (389-409) has lower sequence identity with the *Pseudomonas* FleQ than the rest of the protein, which could indicate a key difference between *S. putrefaciens* FlrA and its *P. aeruginosa* homolog. The Consurf data for FlhG/FlrA presented in this thesis (**Figure 18**) also shows that the FlhG-interacting region of FlrA is poorly conserved (being compared to 150 overall most similar sequences), which could be a potential indication for a difference in the relationship between the FleN/FleQ and the FlhG/FlrA (but this would need to be further investigated with full length FlhG and FlrA in *S. putrefaciens*).

Regarding the effects on transcription, the findings presented in this thesis are in accordance with the general consensus of previous publications investigating the roles of the two proteins in the polarly flagellated *P. aeruginosa,* regarding the inhibitory/negative activation role FlhG (FleN) has on FlrA (FleQ) [85,93,105]. Through qPCR and fluorescence microscopy experiments performed in collaboration with AG Thormann (**see Figures. 19 and 20**), it has been demonstrated that the L400E mutation in FlrA mirrors the results observed for a FlhG knockout (increased transcription of FliF in qPCR and a hyperflagellation pattern in microscopy experiments). An overexpression of FlhG, on the other hand, has the opposite effect in both cases – a reduction in FliF transcription (which is under control of the transcription factor FlrA), as well as loss of flagella.

An important difference between the organisms can be observed in the interplay between FlhG/FlrA, and how they affect each other´s ATPase activity. In *P. aeruginosa*, the ability of the HTH domain of FleN/FlhG on its own to stimulate ATP hydrolysis by FlhG has never been investigated, as they only ever considered full-

length FleN and FleQ. The findings show that full-length, WT FleN leads to a very significant decrease of ATPase activity in full-length FleQ [93], and that FleN alone has a significantly lower ATPase activity than FleQ alone. The second point is also true in *S. putrefaciens*, as shown in this thesis – full-length FlrA does indeed have a higher activity than FlhG of the same concentration (at 10 uM concentration of both, the difference is 3.5-fold) (**see Figure 14**). The former point, (that FleN strongly inhibits FlrA´s ATPase activity) does not seem to be the case, though. Keeping the concentration of FlhG constant and starting with equimolar FlrA, then adding up to 10-fold excess in concentration of FlrA results only in a very modest decrease in the total activity (see **Figure 14)**. Why the case is different in *Shewanella* compared to *Pseudomonas* still remains to be investigated further.

4.1.3. Future perspectives/outlook

So far, the 389-409 region has only been studied in the context of a deletion within FlrA, both *in vivo* and *in vitro*. Additionally, the 389-409 region of FlrA could be directly fused to a GST tag and used in *in vitro* pulldowns to determine whether this region in isolation is enough to still bind FlhG, or whether other regions perhaps have an accessory role in this interaction. Additionally, the L400E mutation can be introduced into the GST-389-409 construct. Both of the GST-fusions of FlrA-HTH, L400E and d389-409, should also be tested for the stimulation of ATPase activity; it is expected that no (or very minor) degree of stimulation would occur. This would further delineate the role of this region.

A more important topic to investigate further in the context of the FlrA/FlhG interaction is the oligomerization state of both proteins – in dependence of different nucleotides (ATP/ADP/AMPPNP), as well as the ATP-binding but non-hydrolyzing mutants of the two proteins; FlrA D233A and FlhG D58A. FlrA as such has been identified as existing in dimeric, tetrameric and hexameric states [88,179,185] . It would be interesting to investigate how different functional states of FlrA and FlhG affect their oligomerization. As a sub-topic of this, the effects of DNA binding on FlrA´s oligomerization state, as well as its capacity to bind FlhG, still need to be investigated further. FlrA could then be co-crystallized with an appropriate DNA fragment (e.g., a

part of the FlrABC promoter, as used in electrophoretic shift assay experiments by D. Mrusek in the past – PhD thesis, unpublished data).

On top of this, HDX experiments with full-length FlhG and FlrA proteins would further allow better understanding of interaction interfaces (and potential conformational changes) that are employed when full-length FlhG and FlrA are used; do these interfaces significantly differ in comparison to those identified between FlrA-HTH/FlhG?

The role of cyclic-di-GMP has not been at all investigated in the context of FlrA/FlhG in *S. putrefaciens,* but further study of its effects would allow a better understanding of differences between the two organisms and their flagellar systems (otherwise, *P. aeruginosa* and *S. putrefaciens* are relatively closely related, and both possess a single polar flagellum; additionally, *S. putrefaciens* was initially named *Pseudomonas putrefaciens*). For this, the binding of c-di-GMP to FlrA in *S. putrefaciens* would need to be investigated, together with the implications c-di-GMP presence has on the FlhG/FlrA interaction in the same organism.

Returning to FliM, further research is also necessary to better understand how exactly FliM is involved in flagellar localization, especially in the context of FlhG localization and how the nucleotide-bound state of FlhG influences its preference for either FliM or FlrA. It would need to be explored at which point (chronologically) during flagellar assembly FlhG interacts with either FliM or FlrA, and especially, what the role of lipids, and membrane interaction of FlhG is in this mechanism.

The current model (as shown in **Figure 32**) likely does not provide a detailed enough insight into the role of the membrane-targeting sequence (MTS) of FlhG, and whether a deletion of the MTS would have a discerning effect on FlrA/FliM binding. It is also possible that the FliM/FlhG interaction, which has now been shown to recruit FlhG itself to the cell pole in *S. putrefaciens*, in turn also affects the anchoring of FlhG to the membrane, and potentially its interactions with another crucial (and previously investigated) interaction partner, the SRP-like GTPase FlhF. Provided this is the case, further experiments would be necessary to examine the role of the FlhG-membrane interaction, which could be accomplished both *in vivo* by an alteration of the MTS

sequence, or *in vitro* by studying the association of FlhG and its interaction partners with artificial lipid vesicles.

Finally, it is now better understood how the interactions between FlhG/FlrA and FlhG/FliM link the correct flagellar localization to the timed production of flagellar building blocks, but it is still unknown how repeated flagellar synthesis is initiated, for example after the division of an old cell into two new cells. Based on the model presented in (**Figures 32, 33**), it could be stated that FlhG indirectly controls its own expression, which takes place by FlhG binding FlrA and blocking/inhibiting its activity as a transcriptional activator (which would in turn lead to less FlhG being produced). So far, the situation that has been investigated is related to FlhG and FlrA already being present in significant amounts. It is possible that a renewed start of flagellar synthesis (e.g., after cell division, as mentioned earlier) could be a consequence of a temporary short increase of FlrA expression, which would lead to an increase in the amount of "free" (from FlhG) FlrA. Judging from the hierarchy of flagellar gene expression, FlrA is expressed already before FlhG, which would mean that a gradual production of FlhG then slowly disrupts FlrA´s transcriptional activity, until so much FlhG is produced that all of FlrA is sequestered and inactive. This question is even more complex to answer, because even in a freshly divided cell, there is likely still some leftover FlhG from before-cell division (it would be interesting to know how FlhG is distributed around the cell right before the cell divides; whether a significant part of it is still pole-associated, or not).

4.2.1. FlhB

Even though FlhB has been investigated in a variety of organisms (most thoroughly in *S. typhimurium*), one of the key pieces of information that was still lacking – in order to further delineate the role of FlhB – was the structural characterization of the extreme C-terminus. This region was previously named the "CCT" region in *Salmonella* but referred to as the "PRR" in this work. The overall structure is, as outlined in the results section, very similar to the previously solved structures of FlhB homologs from *S. typhimurium* and *A. aeolicus* [37]. The main differences are a shorter

alpha helix 1 that was not successfully resolved in the *S. putrefaciens* case (likely due to poor crystal packing or high flexibility of the region), as well as the PRR region itself.

The role of the PRR in hook length control has been investigated by Inoue et. al [54] in *S. typhimurium.* The Inoue et. al study also determined that different truncations to the extreme C-terminus (PRR motif) of FlhB-C have a minor effect on the efficiency of self-cleavage of FlhB-C. The research has shown that an otherwise wildtype FlhB-C protein (e.g. with no mutations to the cleavage site, NP(E/T)H) with a truncation at residue 375 or 380 results in a 100% cleavage efficiency (as observed from Western blot experiments using an anti-FlhB antibody). In contrast, the cleavage was no longer 100% efficient with truncations at residues 355, 360, 365 and 370. A truncation of part or the whole PRR therefore results in a decreased cleavage efficiency. The authors suggest this is potentially occurring due to a change in the conformation of the NP(E/T)H cleavage loop. When it comes to the role of this region in binding flagellar secretion substrates (hook and rod type), a FlhB containing a deletion of the PRR (truncation at residue 353 in *S. typhimurium*) fused to a GST tag could still bind FlgD successfully (FlgD is a hook-type substrate otherwise shown to interact with an exposed hydrophobic patch on the surface of FlhB); this was investigated by [181].

Inoue et. al also tested the importance of the PRR *in vivo* – they observed that an increase in motility with *S. typhimurium* is present in strains with C-terminal FlhB truncations ending at residues 350, 355 or 360. A key point, however, is that this behaviour was only observed in the absence of FliK. When normal wildtype FliK is present and expressed, the PRR truncations lose their effect on the motility phenotype. With these same strains that were previously found to exhibit a different phenotype than the wildtype FlhB strains in the absence of FliK, a large variation in hook length was also noticed (present only in a small proportion of flagella, but leading to significantly longer hooks than average)[54].

Regarding the results in *S. putrefaciens*, the key findings regarding the link between flagellation and presence of the PRR are shown in the diagram below (**Figure 34**). Briefly, data in this thesis supports the model that a deletion of the PRR leads to both a reduction in flagellation, as well as a significant decrease in cleavage of otherwise wildtype FlhB (no mutations to the cleavage site) (see **Figures 23 and 28)**. This could,

to a degree, be related to the findings of Inoue et. al [54], as described earlier in the discussion (a reduction in cleavage of FlhB-C when the PRR region was deleted in *Salmonella*). It is unclear exactly how a removal of the PRR motif leads to decreased flagellation, and why this effect is not more pronounced – this shows that this region of FlhB-C undoubtedly plays a role, but it is still not fully clear which mechanism is employed to reach the observed phenotype.

Additionally, it has been discovered that the PRR motif is primarily restricted to beta and gammaproteobacteria, which contain a variety of diverse species with varied flagellation patterns; on one hand, the relatively closely related *Vibrio, Pseudomonas* and *Shewanella* groups of organisms, which are all FlhF/FlhG possessing monotrichous polar flagellates, to *E. coli*, a peritrichous organism lacking the pair. Therefore, there isn´t an immediately detectable link between the presence of the PRR motif, and the flagellation pattern. It is perhaps an old conserved motif that had a defined function already in the ancestors of gammaproteobacteria long ago and has simply been maintained in the currently present organisms, even though their flagellation patterns and regulation diversified. Further insight into this topic is still necessary to better understand the role of this region, which has, so far, only been studied in *S. typhimurium* and *S. putrefaciens.*

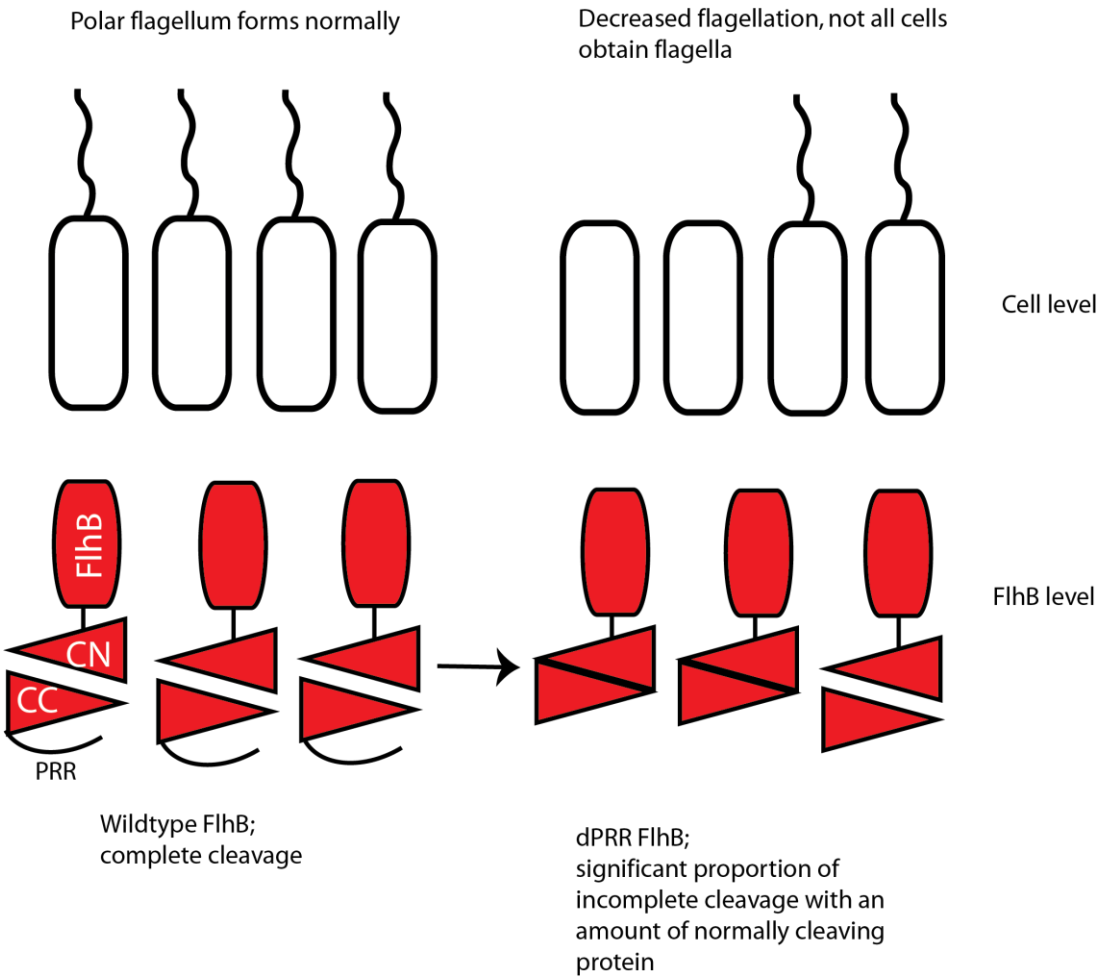

Figure 34: FlhB and the PRR motif. Effects of the PRR motif on FlhB cleavage (lower panel) and flagellation (upper panel). Upper panel depicts flagellated cells, where the presence of flagella depends on FlhB (shown in lower panel). The lower panel schematically depicts the FlhB protein, highlighting the wildtype case (bottom left panel) or a FlhB with a PRR deletion (bottom right panel), which leads to a partial cleavage inhibition and decrease in flagellation. CN and CC domains shown fused together indicate cleavage inhibition.

FlhB was also tested for interactions with other proteins that have been identified as interaction partners from other organisms (FliK, FlhA), as well as a new interaction partner (FliM) that had been identified in *S. putrefaciens* and not known from other organisms (Y2H experiment performed by Dieter Kressler, **Figure 30A**). Interestingly, FliK did not show binding to FlhB-C WT, FlhB-C dC20 or the PRR motif itself. FlhA and FliM/N did bind to FlhB, as clearly visible from **Figure 30**.

Additionally, FliM/N was observed as an interaction partner when added to GST-FlhA, but the interaction was shown to be clearly present and strong only when FlhB-C was also added into the incubation mixture. This would suggest that FlhB may represent a “bridge” between FliM/N and FlhA. The potential implications of this are

presented in the model (**Figure 35**) below: firstly, FliF, FlhA and FlhB localize to the pole (1). Then, the cytoplasmic domains of FlhB and FlhA interact with each other, as the flagellum, the secretion system or the C-ring are not assembled yet (2). FliG then interacts with FliF-C and C-ring assembly starts, and it is also likely that at some point close to this assembly stage, there is an interaction between FliM and FlhG which recruits FlhG to the pole.

This model, though, also proposes that FlhB-C interacts with FliM/N, which plays a role in the recruitment of FliM/N to the pole. Since FlhA-C and FlhB-C interact with each other, this would explain the pulldown results from **Figure 30**. It is unclear whether FlhG is interacting with FliM as the latter is bound to FlhB (and through FlhB to FlhA), or not. For this, the binding site of FlhB on FliM would need to be investigated to determine whether it is sterically possible that both interaction partners are bound at the same time. Finally, stage (3): The C-ring assembly is nearing completion, FliM now interacts with FliG and other FliM monomers to form the ring structure. As this occurs, FlhG is permanently released from FliM, and is now free to interact with FlrA, which overall leads to the inhibiton of further transcription of flagellar building blocks. The key question at this point is what FlhG is doing during the FlhB//FliM/N interaction (or, asking otherwise: at which point does this interaction actually occur)?

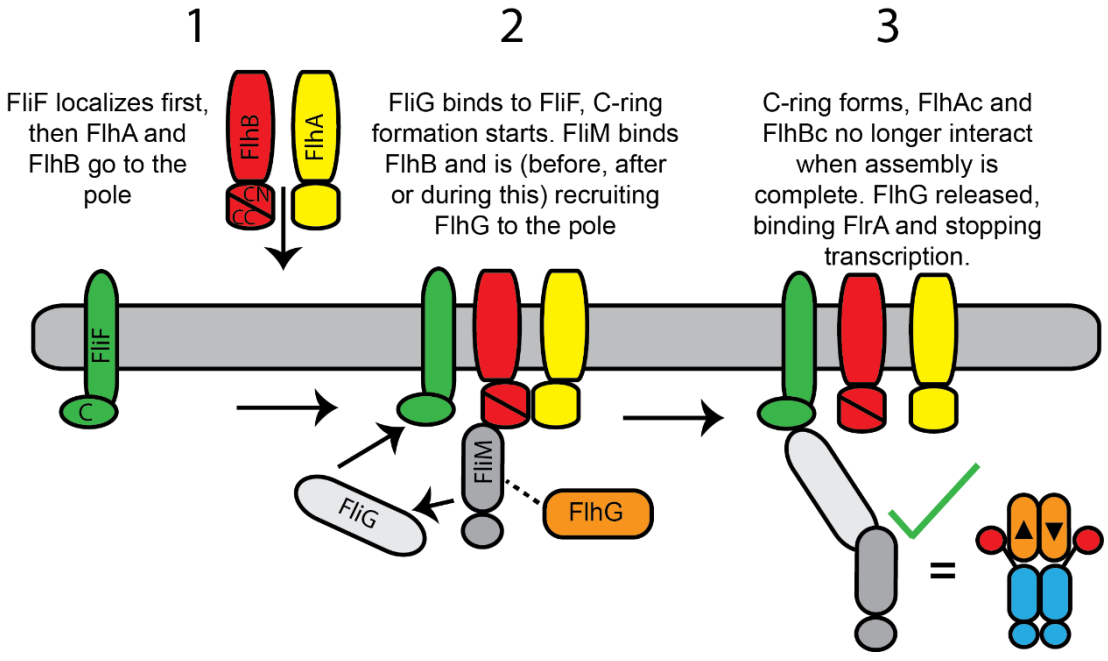

Figure 35: Model of the interaction between FlhA, FlhB and FliM/N, as well as potentially FlhG. The model depicts the interactions between key flagellar and regulatory proteins in several stages. FlhB shown in red, FlhA shown in yellow, FliF shown in green, FliM and FliG shown in grey, FlhG shown in orange. FlrA shown in blue, with the HTH domain indicated as red circles. The long horizontal, narrow grey shape connecting the different stages represents the membrane.

4.2.2.Future perspectives and outlook

4.2.2.1. FlhB in the context of C-ring assembly

As discussed in the previous chapter, in comparison to other interaction partners, FliM is relatively unknown as a binding partner of FlhB, and the interaction has not been studied in detail (also not in other organisms). As discussed previously, other interaction partners that have been confirmed to interact with FliM are FlhG, CheY, FliN and FlhG. It is also not likely that the FliM/FlhB interaction is a long-term and stable one, and the FliM may only transiently interact with FlhB, as the former is associating with the cell pole in *S. putrefaciens.* It is also highly unlikely that FliM and FlhB interact in the context of an assembled C-ring, since FliM/N are located directly below the FliG oligomers making up the top of the C-ring, which in turn interacts with the cytoplasmic domain of FliF.

Thus, the FlhB/FliM interaction could potentially take place at a similar time-point (and location) as the FliM/FlhG interaction, as C-ring building blocks are still being produced, and FlhG is being recruited to the pole by FliM. This is a potentially valid scenario, since it is known that FlhG itself also interacts with membrane lipids, as has been discussed earlier in the discussion and introduction of this work. It still needs to be investigated what effects FlhG has on the interaction of FlhB and FliM. Is such an interaction then disrupted, or is a complex of FliM/N, FlhB and FlhG possible?

Since the FliM/N complex can already be stably purified and used in pulldowns, the next key milestone would be a successful purification of a tri-membered complex containing FlhB, FliM and FliN. This complex could then be analysed using HDX-MS, to identify the binding interfaces on the individual complex components. Depending on the role of FlhG in this, further purification could be attempted to delineate cross-interactions in the context of FlhG, FliM, FliN and FlhB all being present. Additionally,

since FlhB is likely a bridging partner bringing FlhA and FliM/N together transiently, the possibility of a complex containing FlhA, FliM/N and FlhB should also be considered and investigated.

4.2.2.2. FlhB in the context of flagellar substrate secretion control

So far, only preliminary work has been performed to investigate the interaction between FlhB and FliK in *S. putrefaciens*. This preliminary work shown in this thesis (see **Figure 30E**) has not managed to show so far *in vitro* that different GST-FlhB-C constructs (GST-PRR, GST-FlhB-C WT and GST-FlhB-C dC20) can interact with FliK. It is possible that the interaction is disrupted by a GST tag on FlhB-C, and the experiments would also need to be performed by a Strep or GST affinity tag on FliK itself, to test for FlhB binding.

It should also be noted here that, as well as a number of other flagellar proteins in this organism, also FliK exists as the polar (1) and lateral (2) variety. All preliminary (and unpublished work, V. Blagotinsek) previously referred to in this thesis is related to the polar FliK (FliK1). The FliK/FlhB interaction is therefore not interesting only for the structural details of the interaction itself, but also because of the potential differences between the lateral and polar flagellar systems, in the context of secretion control. Unpublished work was performed by D. Mrusek that investigated some of these differences.

As a brief summary, an unpublished manuscript was previously prepared by Mrusek and colleagues (FliM and FliN enable flagellar specificity in *S. putrefaciens*), which focused on crosstalk interactions between the polar and lateral C-ring components. Mrusek et. al discovered that FliG1 is capable of binding both polar and lateral FliM/N, the same remains true even if FliF-C (polar or lateral) is present. From structural analysis, there are several key residues in the FliG/FliM interface that are conserved and identical in lateral/polar FliG and FliM. Only the polar FliG can interact with FlhF, and another important distinction occurs with FliF/FliG interactions; while the polar FliF-C binds only polar FliG, the lateral FliF-C can bind both lateral and polar FliG. These previous findings could be further expanded on by considering additional proteins such as FliK, as discussed below.

The *S. putrefaciens* lateral FliK (FliK2) contains a conserved disordered region, likely located between two spherical domains (the disordered region aligns well with *Salmonella* FliK, see PSIPRED secondary structure prediction data, **Appendix 7.5.2.5.**). This disordered region does not seem to be present in the *S. putrefaciens* polar FliK (FliK1). For these different FliK proteins, sequence identity values are in the low 20% range with one another (**Appendix 7.5.2.1.,** for pairwise alignments of SpFliK1, SpFliK2, *S. typhimurium* FliK see **Appendix 7.5.2.2-7.5.2.4**). This low similarity between the polar and lateral FliK in *Shewanella,* as well as the predicted lack of a long-disordered region in the polar FliK (and the polar FliK being roughly 100 residues longer than the lateral FliK), could hint at undiscovered differences between the proteins and their regulation. This would still need to be explored further, in the context of differences (and potential crosstalk interactions) between the polar and lateral flagellar system as a whole.

To continue with previous research (mentioned earlier in this chapter, unpublished, D. Mrusek), which was focused primarily on the crosstalk between polar and lateral FliG, FliM and FliF, crosstalk involving both lateral and polar FliK/FlhB would need to be investigated. This would involve investigation of the binding interfaces between both FlhB/FliK pairs and attempting to swap the polar/lateral proteins one at a time, to determine whether functional flagella can still be formed, and in which cases this is true (e.g., can a polar flagellum still function if both FliK1 and FlhB1 are replaced with FliK2 and FlhB2, or if only one of them is replaced with the lateral (2) counterpart). This can also be investigated *in vitro*, using GST pulldowns to determine the possibility of cross-interactions between the two secretion control systems.

In vivo fluorescence microscopy experiments could also be performed with swapped polar and lateral FliKs, to determine to what extent hook length is affected in the polar and lateral flagellar system. In this context, the residues equivalent to the *S. typhimurium* Val302/Ile304 [78]*,* suggested as crucial FlhB-interacting residues, could be mutated in *S. putrefaciens* to charged or non-hydrophobic residues, to determine the phenotypic effects (with fluorescence microscopy studies). Additionally, *in vitro* interaction studies, such as GST-pulldowns, could be attempted with these mutants. This would clarify whether these conserved residues also play a crucial role in the

Shewanella putrefaciens control of assembly of the flagellar hook, and secretion of different classes of flagellar substrates.

5. Methods and materials

5.1. Materials and consumables

Chemicals and medium/agar components were obtained from Carl Roth, Thermo Fisher Scientific, Sigma Aldrich and AppliChem and used as supplied.

Laboratory consumables such as falcon tubes, Eppendorf tubes, pipette tips, single-use streaking loops were all provided by Sarstedt AG.

Columns for affinity and size-exclusion purifications (including resins), as well as bead slurry for small scale expression tests and pulldown experiments were purchased from GE Healthcare. All FPLC machines belong to the AKTA line of purification systems from GE Healthcare (AKTA Prime, AKTA Purifier, AKTA Pure).

Nucleotides were provided in powdered form (Jena Bioscience), and stock solutions of 100 mM were prepared before use for experiments.

SDS-Page gel chambers, gel casting and running equipment were purchased from BioRad. SDS-gels were self-cast, employing 4% stacking layer and 15% separation layer as standard.

Cloning enzymes, DNAse, RNase and other enzymes were purchased from New England Biolabs and Thermo Fisher Scientific.

Crystallization core solution were purchased from Qiagen (JCSG core solutions I-IV and core ProComplex).

5.2.Solutions and buffers

Buffer A	20 mM HEPES pH 8.0 250 mM NaCl 20 mM KCl 20 mM MgCl2 40 mM imidazole
Buffer B	20 mM HEPES pH 8.0 250 mM NaCl 20 mM KCl 20 mM MgCl2 500 mM imidazole
SEC buffer	20 mM HEPES pH 7.5 200 mM NaCl 20 mM KCl 20 mM MgCl2
GSH elution buffer	50 mM Tris-HCl pH 8.0 20 mM L-glutathione
GST-pulldown buffer	20 mM HEPES pH 7.5 200 mM NaCl 20 mM KCl 20 mM MgCl2 0.6 uM Tween20

5.3. Methods

Additional details on methods not covered here that were performed in collaboration with other scientists/laboratories are provided in the two published research articles with V. Blagotinsek as shared first author, see references [175,180].

5.3.1. Transformation, protein expression and harvesting

Transformation was carried out using a 60 second heat-shock at 42 C. BL21 DE3 cells were used for protein overexpression. After heat-shock, cells were left for 5 minutes on ice and then grown for 30 minutes at 37 C, while shaking at 225 rpm. They were then streaked out on plates with the appropriate antibiotic resistance (Ampicillin or Kanamycin) and grown overnight at 37 C. Protein expression was carried out at 30 C and 180 rpm overnight in standard LB medium (Carl Roth), induction was performed by adding 1% w/v lactose monohydrate.

Cells were collected and centrifuged at 4500 rpm for 10 minutes, then resuspended in buffer (A or SEC, depending on whether a Ni-NTA or GST purification would follow). Cells were lysed using a microfluidizer (Microfluidics corporation) and passed through the device twice. Afterwards, the resulting suspension was centrifuged for 20

minutes at 20,000 rpm, and the pellet was discarded. The supernatant was loaded onto an affinity purification column.

5.3.2. Protein purification

Depending on the tag used, the proteins were purified using Ni-NTA or GST affinity resins. For the former, HisTrap columns were used, and for the latter, GSTrap columns, both from GE Healthcare. During the affinity purification stage, the post-cell lysis centrifugation supernatant was loaded onto the corresponding affinity column, then washed with 10 CV of wash buffer (Buffer A for Ni-NTA purifications, SEC buffer for GST purifications). Elution was then performed with 3 CV of high imidazole-containing Buffer B (Ni-NTA purifications) or GSH elution buffer (GST purifications). The load, flowthrough (lysate that passed through the column and contains unbound proteins), wash and elution fractions were checked on an SDS-PAGE gel before proceeding with the purification. The elution sample was concentrated using spin concentrators with an appropriate kDa cutoff point (10, 30 or 50 kDa), and injected onto a size-exclusion chromatography column, containing Sepharose Superdex S200 resin beads. The chromatogram showing the absorbance values at 280 nm was inspected, and the relevant fractions were pooled and concentrated, after checking them on an SDS-PAGE gel. The protein was aliquoted, flash-frozen in liquid nitrogen and stored at -80 C.

5.3.3. Sequence alignments and analysis

Pairwise sequence alignments were always performed by Emboss Needle (https://www.ebi.ac.uk/Tools/psa/emboss_needle/), while alignments for several sequences were carried out using the Muscle server [186]. Visualization and analysis of the multiple sequence alignments was carried out using Jalview [187,188] and UCSF Chimera [189,190] The multiple sequence alignments were coloured according to the degree of conservation of residues within the compared sequences, identifying conserved amino acids.

5.3.4. Structural homology modelling and conservation analysis with Consurf

Modelling was performed using the SwissModel server [176,177], to produce homology models of FlhB, FlhG, FlrA and FliM.

The structural homology models generated were then used as input for the Consurf server, to generate a 3D protein structure where conservation scores for individual residues were mapped onto the input model [191–193]. The sequence was compared to 150 most similar sequences, the cut-off points for sequence identity being 35% and 95%. The generated 3D model with colour-coded conservation scores was visualized and analysed in Pymol (www.pymol.org).

5.3.5. GST-pulldown assays

The assays were performed using spin columns from the company MobiTec. After assembly (inserting the filter into the spin column), 500 uL of GST-pulldown buffer was added into each column, and then 30 ul of resuspended bead slurry was pipetted in (GST-Sepharose beads). This suspension was centrifuged for 1 minute at 4000 rpm to wash the beads, which were then again resuspended in 500 uL of the GST-pulldown buffer. The beads were then exposed to 1 nmol of a GST-tagged protein and incubated together on a rotation machine for 15 minutes, and centrifuged under the same conditions as above. The interaction partner protein was then added (10 nmol), and another incubation period on the rotation machine (now for 30 minutes) was carried out. The sample was centrifuged again, then washed three times with 500 uL of the GST-pulldown buffer. The elution was carried out with 40 uL of the GSH elution buffer. The samples were then run on an SDS-PAGE gel and stained.

5.3.6. Protein crystallization and structure determination

After the previous purification steps (see **5.3.2.**), the size-exclusion peak corresponding to FlhB-C was concentrated to 0.5 mM concentration. It was then crystallized with the 96-needle Gryphon robot (Art Robbins). For crystallization, 2-well crystallization plates were used (Swiss MRC, sitting drop method plates), employing JCSG core solutions I-IV and ProComplex (Qiagen) solutions. Crystals could be located in the following conditions: (JCSG Core III B2, 0.2M Lithium sulfate, 0.1M Tris pH 8.5, 1.26 M ammonium sulfate; JCSG Core IV D5, 0.1 HEPES pH 7.5, 1.5M Lithium sulfate; Core ProComplex H6, 0.1M MES pH 6.5, 1.6M Magnesium sulfate). The crystals were first detected three weeks after the crystallization attempt. They were harvested and frozen four weeks after crystallization in liquid nitrogen until measurement (only Core IV D5 and Core III B2 crystals could be harvested, due to their large enough size). The X-ray diffraction was performed at the DESY facility in

Hamburg, Germany. Structure determination was carried out with molecular replacement, using the *S. typhimurium* FlhB-C (3B0Z)[37] as the search model.

Data were processed with XDS and scaled with XSCALE [194]. The structure was determined by molecular replacement with PHASER [195], manually built in COOT [196], and refined with PHENIX [197]. Final validation of the structures was carried out with the validation server of the Protein Data Bank (PDB) at https://validate-rcsb-1.wwpdb.org. Figures were prepared with Pymol (www.pymol.org).

5.3.7. Protein-protein interaction studies

To investigate the interaction interface between the PRR and the rest of FlhB-C in *S. putrefaciens*, the software LigPlot+ version 2.2 was used. The software was obtained from the website https://www.ebi.ac.uk/thornton-srv/software/LigPlus/applicence.html under a free academic licence. The FlhB-C structure was provided to the software as a single PDB file, with regions 312-356 (helices 3 and 4) and 357-376 (PRR) were as interacting regions of interest. The software then provided an image summarizing the direct interactions between specific residues, as well as listing the residues involved in hydrophobic contacts [182,183] . The image was exported in the PostScript format and then rearranged into three panels to fit into a vertical format.

5.3.8. ATPase assays and HPLC analysis

In order to investigate the ATPase activity of FlhG across different ATP concentrations, equimolar amounts of FlhG and FlrA-HTH were used (10 µM). The reactions were carried out in SEC buffer, with the addition of the following different ATP concentrations: 0.05 mM, 0.1 mM, 0.25 mM, 0.5 mM, 0.75 mM, 1.0 mM, 2.5 mM, 5.0 mM. Samples were incubated in a heat block at 37 °C for a total of 60 min (without FlrA-HTH) and a total of 15 min (with FlrA-HTH). Individual samples for measurement were taken every 12 minutes for FlhG alone (so 12, 24, 36, 48, 60 min), and every 3 minutes where FlrA-HTH was added (so 3, 6, 9, 12, 15 min). Immediately after retrieval of samples from the heat block, they were quenched by chloroform (volume ratio 2:1 chloroform:FlhG solution), thoroughly mixed for 15s, heat-

inactivated at 95 °C for 15s and frozen in liquid nitrogen. The samples were then thawed and centrifuged at 4 °C to separate the aqueous and organic phases. The aqueous phase was used for further HPLC-based analysis. This was carried out on an Agilent 1260 Series machine (from Agilent Technologies), using a C18 column (EC 250/4.6 Nucleodur HTec 3 µM; Macherey-Nagel). The samples were eluted from the column at 0.8 ml/min flow rate with the buffer containing the following additives: 50 mM KH_2PO_4, 50 mM K_2HPO_4, 10 mM tetrabutylammonium bromide and 15 % (v/v) acetonitrile. The hydrolyzed nucleotides were detected at 260 nm wavelength, based on ADP and ATP standards. GraphPad Prism (v6.04) was used for data analysis (GraphPad Software). The velocity of ATPase activity was determined by linear regression, based on the ADP amounts quantified at increasing incubation times. K_m and V_{max} were calculated from the fit of the v/S characteristic according to the equation $v = V_{max}[S]/(K_m + [S])$ where [S] is the concentration of substrate ATP.

For endpoint measurements (**Figure 14**), proteins of interest were incubated for 30 minutes (at a concentration of 10 uM, unless stated otherwise) with 1 mM ATP. They were then quenched and processed as described in the above paragraph for the kinetics samples.

5.3.9. HDX-MS (hydrogen/deuterium exchange mass spectrometry)

Samples for HDX-MS involving FlhG and FliM/N were prepared by a robotic autosampler (LEAP technologies), and manually for HDX-MS involving FlhG and FlrA. For the latter, the relevant proteins were incubated with one another for 1 min at 25 °C prior to HDX in the presence of 1 mM ATP. H/D exchange was started by 10-fold dilution in D_2O-containing SEC buffer (for the experiment involving FlhG and FlrA, 1 mM ATP concentration was maintained). Non-deuterated samples were prepared in normal SEC buffer instead. Samples were incubated at 25 °C for 30, 120 and 600s (for FlrA interaction) and 10, 30, 95, 1000 and 10000s (for FliM/N interaction). After incubation, the reaction was stopped by addition of an equal volume of ice-cold quench buffer (400 mM KH_2PO_4/H_3PO_4, pH 2.2) and directly injected into an ACQUITY UPLC M-class system with HDX technology (Waters). Digestion of the FlhG was then carried out with immobilized porcine pepsin at 12 °C at + 0.1 % (v/v) formic acid. The peptides were collected on a column filled with POROS 20 R2 material (Thermo Scientific) at 0.5 °C. After elution and ionization of the samples, mass spectra were

recorded on a G2-Si HDMS (Waters) mass spectrometer equipped with an electrospray ionization source in High-Definition MS (HDMS) or Enhanced High-Definition MS (HDMSE) positive ion mode for deuterated and undeuterated samples, respectively. Between samples, the pepsin column was washed three times with 80 µL of 4 % (v/v) acetonitrile and 0.5 M guanidine hydrochloride, blank runs were performed. Peptides were identified and deuterium uptake determined employing the PLGS and DynamX 3.0 softwares (both Waters) as described in previous work of Dr. W. Steinchen [198,199].

5.3.10. Mant-ADP fluorescence experiments

The Mant-ADP (2´/3´-O-(N-Methyl-anthraniloyl)-ADP)) reagent was used to investigate binding of ADP to FlhG alone and in the context of an FlhG/FliMN complex. This binding was quantified by using a fluorescence-based assay run with the FP-6300 spectrofluorometer (Jasco). 1 µM Mant-ADP in SEC buffer was excited at 360 nm, and emission was monitored at 450 nm. The interaction partner was added every 30s at 0.5 µM intervals. The effect of dilution on fluorescence was accounted for by titrating Mant-ADP with SEC buffer alone. The data obtained was analyzed with Spectra Manager for Windows 1.05.03 (Jasco) and GraphPad Prism (v6.04).

5.3.11. SDS-PAGE

SDS-PAGE (sodium dodecyl sulphate polyacrylamide gel electrophoresis) was used to separate protein samples and subsequently visualize them with Coomassie stain after protein purifications and GST affinity pulldowns experiments. BioRad casting equipment, gel chamber and running chamber were used for SDS-PAGE. Self-cast gels were used with 4% stacking gel and 15% separating gel. Protein samples were loaded onto the gel after mixing with 1:5 SDS loading dye. The SDS-PAGE method was performed at 270V, for 30-45 minutes depending on the expected protein size and task. Running buffer containing 25 mM TRIS, 200 mM glycine and 0.1% SDS (w/v) was used. After SDS-PAGE, the gels were stained by boiling them in a Coomassie brilliant blue solution, and leaving on a shaker for 10 minutes. Afterwards, the gels were destained by incubation in a destaining solution containing 60% distilled H_20, 30% acetic acid and 10% ethanol, on a shaker. The solution was replaced with fresh destaining solution upon blue colouring during destaining.

6. References

1. Harshey, R. M. Bacterial Motility on a Surface: Many Ways to a Common Goal. *Annu. Rev. Microbiol.* **57**, 249–273 (2003).

2. Kearns, D. B. A field guide to bacterial swarming motility. *Nature Reviews Microbiology* **8**, 634–644 (2010).

3. Verstraeten, N. *et al.* Living on a surface: swarming and biofilm formation. *Trends in Microbiology* **16**, 496–506 (2008).

4. Overhage, J., Bains, M., Brazas, M. D. & Hancock, R. E. W. Swarming of Pseudomonas aeruginosa is a complex adaptation leading to increased production of virulence factors and antibiotic resistance. *J. Bacteriol.* **190**, 2671–2679 (2008).

5. Overhage, J., Lewenza, S., Marr, A. K. & Hancock, R. E. W. Identification of genes involved in swarming motility using a Pseudomonas aeruginosa PAO1 mini-Tn5-lux mutant library. *J. Bacteriol.* **189**, 2164–2169 (2007).

6. Jones, B. V., Young, R., Mahenthiralingam, E. & Stickler, D. J. Ultrastructure of Proteus mirabilis swarmer cell rafts and role of swarming in catheter-associated urinary tract infection. *Infect. Immun.* **72**, 3941–3950 (2004).

7. Armbruster, C. E., Hodges, S. A. & Mobley, H. L. T. Initiation of swarming motility by Proteus mirabilis occurs in response to specific cues present in urine and requires excess L-glutamine. *J. Bacteriol.* **195**, 1305–1319 (2013).

8. Merino, S., Shaw, J. G. & TomÃ¡s, J. M. Bacterial lateral flagella: an inducible flagella system. *FEMS Microbiol. Lett.* **263**, 127–135 (2006).

9. Ferreira, J. L. *et al.* γ-proteobacteria eject their polar flagella under nutrient depletion, retaining flagellar motor relic structures. *PLOS Biol.* **17**, e3000165 (2019).

10. Mattick, J. S. Type IV Pili and Twitching Motility. *Annu. Rev. Microbiol.* **56**, 289–314 (2002).

11. Craig, L. & Li, J. Type IV pili: paradoxes in form and function. *Current Opinion in Structural Biology* **18**, 267–277 (2008).

12. Johnson, T. L., Abendroth, J., Hol, W. G. J. & Sandkvist, M. Type II secretion: from structure to function. *FEMS Microbiol. Lett.* **255**, 175–186 (2006).

13. Merz, A. J., So, M. & Sheetz, M. P. Pilus retraction powers bacterial twitching motility. *Nature* **407**, 98–102 (2000).

14. Clausen, M., Koomey, M. & Maier, B. Dynamics of type IV Pili Is controlled by switching between multiple states. *Biophys. J.* **96**, 1169–1177 (2009).

15. Wang, F. *et al.* Cryoelectron Microscopy Reconstructions of the Pseudomonas aeruginosa and Neisseria gonorrhoeae Type IV Pili at Sub-nanometer Resolution. *Structure* **25**, 1423-1435.e4 (2017).

16. Craig, L., Forest, K. T. & Maier, B. Type IV pili: dynamics, biophysics and functional consequences. *Nature Reviews Microbiology* **17**, 429–440 (2019).

17. Skerker, J. M. & Berg, H. C. Direct observation of extension and retraction of type IV pili. *Proc. Natl. Acad. Sci. U. S. A.* **98**, 6901–6904 (2001).

18. Maier, B., Potter, L., So, M., Seifert, H. S. & Sheetz, M. P. Single pilus motor forces exceed 100 pN. *Proc. Natl. Acad. Sci. U. S. A.* **99**, 16012–16017 (2002).

19. Recht, J. & Kolter, R. Glycopeptidolipid acetylation affects sliding motility and biofilm formation in Mycobacterium smegmatis. *J. Bacteriol.* **183**, 5718–5724 (2001).

20. Murray, T. S. & Kazmierczak, B. I. Pseudomonas aeruginosa exhibits sliding motility in the absence of type IV pili and flagella. *J. Bacteriol.* **190**, 2700–2708 (2008).

21. Matsuyama, T., Fujita, M. & Yano, I. *Wetting agent produced by Serratia marcescens (Surface activity; aminolipid; serratamolide; biosurfactant)*. *FEMS Microbiology Letters* **28**, (1985).

22. Brown, I. I. & Häse, C. C. Flagellum-independent surface migration of Vibrio cholerae and Escherichia coli. *J. Bacteriol.* **183**, 3784–3790 (2001).

23. Kinsinger, R. F., Shirk, M. C. & Fall, R. Rapid surface motility in Bacillus subtilis is dependent on extracellular surfactin and potassium ion. *J. Bacteriol.* **185**, 5627–5631 (2003).

24. Park, S. Y., Pontes, M. H. & Groisman, E. A. Flagella-independent surface motility in Salmonella enterica serovar Typhimurium. *Proc. Natl. Acad. Sci. U. S. A.* **112**, 1850–1855 (2015).

25. Minamino, T. & Imada, K. The bacterial flagellar motor and its structural diversity. *Trends in Microbiology* **23**, 267–274 (2015).

26. Erhardt, M., Namba, K. & Hughes, K. T. Bacterial nanomachines: the flagellum and type III injectisome. *Cold Spring Harbor perspectives in biology* **2**, (2010).

27. Altegoer, F. & Bange, G. Undiscovered regions on the molecular landscape of flagellar assembly. *Curr. Opin. Microbiol.* **28**, 98–105 (2015).

28. Chevance, F. F. V. & Hughes, K. T. Coordinating assembly of a bacterial macromolecular machine. *Nature Reviews Microbiology* **6**, 455–465 (2008).

29. Schuhmacher, J. S., Thormann, K. M. & Bange, G. How bacteria maintain location and number of flagella? *FEMS Microbiol. Rev.* **39**, 812–822 (2015).

30. Blocker, A., Komoriya, K. & Aizawa, S. I. Type III secretion systems and bacterial flagella: Insights into their function from structural similarities. *Proceedings of the National Academy of Sciences of the United States of America* **100**, 3027–3030 (2003).

31. Wagner, S. *et al.* Bacterial type III secretion systems: a complex device for the delivery of bacterial effector proteins into eukaryotic host cells. *FEMS Microbiol. Lett.* **365**, (2018).

32. Kuhlen, L. *et al.* Structure of the Core of the Type Three Secretion System Export Apparatus. *bioRxiv* 249128 (2018). doi:10.1101/249128

33. Kuhlen, L. *et al.* The substrate specificity switch FlhB assembles onto the export gate to regulate type three secretion. *Nat. Commun.* **11**, 1–10 (2020).

34. Bange, G. *et al.* FlhA provides the adaptor for coordinated delivery of late flagella building blocks to the type III secretion system. *Proc. Natl. Acad. Sci. U. S. A.* **107**, 11295–11300 (2010).

35. Lountos, G. T., Austin, B. P., Nallamsetty, S. & Waugh, D. S. Atomic resolution structure of the cytoplasmic domain of Yersinia pestis YscU, a regulatory switch involved in type III secretion. *Protein Sci.* (2009). doi:10.1002/pro.56

36. Deane, J. E. *et al.* Crystal structure of Spa40, the specificity switch for the Shigella flexneri type III secretion system. *Mol. Microbiol.* **69**, 267–76 (2008).

37. Meshcheryakov, V., Kitao, A., Matsunami, H. & Samatey, F. Inhibition of a type III secretion system by the deletion of a short loop in one of its membrane proteins. *Acta Crystallogr. D. Biol. Crystallogr.* **69**, 812–820 (2013).

38. Kihara, M., Minamino, T., Yamaguchi, S. & Macnab, R. M. Intergenic suppression between the flagellar MS ring protein FliF of Salmonella and FlhA, a membrane component of its export apparatus. *J. Bacteriol.* **183**, 1655–1662 (2001).

39. Minamino, T. *et al.* Role of the C-terminal cytoplasmic domain of FlhA in bacterial flagellar type III protein export. *J. Bacteriol.* **192**, 1929–1936 (2010).

40. McMurry, J. L., Van Arnam, J. S., Kihara, M. & Macnab, R. M. Analysis of the cytoplasmic domains of Salmonella FlhA and interactions with components of the flagellar export machinery. *J. Bacteriol.* **186**, 7586–7592 (2004).

41. Johnson, S., Kuhlen, L., Deme, J. C., Abrusci, P. & Lea, S. M. The structure of an injectisome export gate demonstrates conservation of architecture in the core export gate between flagellar and virulence type III secretion systems. *MBio* **10**, (2019).

42. Minamino, T., Inoue, Y., Kinoshita, M. & Namba, K. FLIK-driven conformational rearrangements of FlhA and FlhB are required for export switching of the flagellar protein export apparatus. *J. Bacteriol.* **202**, (2020).

43. Minamino, T., Morimoto, Y. V., Kinoshita, M., Aldridge, P. D. & Namba, K. The bacterial flagellar protein export apparatus processively transports flagellar proteins even with extremely infrequent ATP hydrolysis. *Sci. Rep.* **4**, (2014).

44. Minamino, T. & Macnab, R. M. Interactions among components of the Salmonella flagellar export apparatus and its substrates. *Mol. Microbiol.* **35**, 1052–1064 (2000).

45. Bai, F. *et al.* Assembly dynamics and the roles of FliI ATPase of the bacterial flagellar export apparatus. *Sci. Rep.* **4**, (2014).

46. Zhu, K., González-Pedrajo, B. & Macnab, R. M. Interactions among membrane and soluble components of the flagellar export apparatus of Salmonella. *Biochemistry* **41**, 9516–9524 (2002).

47. Ferris, H. U. *et al.* FlhB regulates ordered export of flagellar components via autocleavage mechanism. *J. Biol. Chem.* **280**, 41236–42 (2005).

48. Minamino, T. & Macnab, R. M. Domain structure of Salmonella FlhB, a flagellar export component responsible for substrate specificity switching. *J. Bacteriol.* **182**, 4906–4914 (2000).

49. Fraser, G. M. *et al.* Substrate specificity of type III flagellar protein export in Salmonella is controlled by subdomain interactions in FlhB. *Mol. Microbiol.* **48**, 1043–1057 (2003).

50. Meshcheryakov, V. A., Barker, C. S., Kostyukova, A. S. & Samatey, F. A. Function of FlhB, a Membrane Protein Implicated in the Bacterial Flagellar Type III Secretion System. *PLoS One* **8**, e68384 (2013).

51. Williams, A. W. *et al.* Mutations in fliK and flhB Affecting Flagellar Hook and Filament Assembly in Salmonella typhimurium. *J. Bacteriol.* **178**, 2960–2970 (1996).

52. Minamino, T., Iino, T. & Kutsukakel, K. Molecular Characterization of the Salmonella typhimurium flhB Operon and Its Protein Products. *J. BACrERIOLOGY* **176**, 7630–7637 (1994).

53. Morris, D. P. *et al.* Kinetic Characterization of *Salmonella* FliK−FlhB Interactions Demonstrates Complexity of the Type III Secretion Substrate-Specificity Switch. *Biochemistry* **49**, 6386–6393 (2010).

54. Inoue, Y., Kinoshita, M., Namba, K. & Minamino, T. Mutational analysis of the C-terminal cytoplasmic domain of FlhB, a transmembrane component of the flagellar type III protein export apparatus in Salmonella. *Genes to Cells* **24**, 408–421 (2019).

55. Kutsukake, K., Minamino, T. & Yokoseki, T. *Isolation and Characterization of FliK-Independent Flagellation Mutants from Salmonella typhimurium*. *JOURNAL OF BACTERIOLOGY* **176**, (1994).

56. Hughes, K. T., Gillen, K. L., Semon, M. J. & Karlinsey, J. E. Sensing structural intermediates in bacterial flagellar assembly by export of a negative regulator. *Science (80-.).* **262**, 1277–1280 (1993).

57. Calvo, R. A. & Kearns, D. B. FlgM Is secreted by the flagellar export apparatus in Bacillus subtilis. *J. Bacteriol.* **197**, 81–91 (2015).

58. Grünenfelder, B., Gehrig, S. & Jena, U. Role of the cytoplasmic C terminus of the FliF motor protein in flagellar assembly and rotation. *J. Bacteriol.* **185**, 1624–1633 (2003).

59. Kihara, M., Miller, G. U. & Macnab, R. M. Deletion analysis of the flagellar switch protein FliG of Salmonella. *J. Bacteriol.* **182**, 3022–3028 (2000).

60. Francis, N. R., Irikura, V. M., Yamaguchi, S., DeRosier, D. J. & Macnab, R. M. Localization of the Salmonella typhimurium flagellar switch protein FliG to the cytoplasmic M-ring face of the basal body. *Proc. Natl. Acad. Sci. U. S. A.* **89**, 6304–6308 (1992).

61. Terashima, H. *et al.* Assembly mechanism of a supramolecular MS-ring complex to initiate bacterial flagellar biogenesis in Vibrio species. . *J. Bacteriol.* (2020). doi:10.1128/jb.00236-20

62. Thormann, K. M. & Paulick, A. Tuning the flagellar motor. *Microbiology* **156**, 1275–1283 (2010).

63. Braun, T. F., Al-Mawsawi, L. Q., Kojima, S. & Blair, D. F. Arrangement of Core Membrane Segments in the MotA/MotB Proton-Channel Complex of Escherichia coli. *Biochemistry* **43**, 35–45 (2004).

64. Hosking, E. R. & Manson, M. D. Clusters of Charged Residues at the C Terminus of MotA and N Terminus of MotB Are Important for Function of the Escherichia coli Flagellar Motor. *J. Bacteriol.* **190**, 5517–5521 (2008).

65. B Baker, M. A. *et al.* Domain-swap polymerization drives the self-assembly of the bacterial flagellar motor. *Nat. Publ. Gr.* **23**, (2016).

66. Xue, C. *et al.* Crystal structure of the FliF-FliG complex from Helicobacter pylori yields insight into the assembly of the motor MS-C ring in the bacterial flagellum. *J. Biol. Chem.* **293**, 2066–2078 (2018).

67. Lam, K.-H. *et al.* Structural basis of FliG-FliM interaction in *Helicobacter pylori*. *Mol.*

Microbiol. **88**, 798–812 (2013).

68. Lee, L. K., Ginsburg, M. A., Crovace, C., Donohoe, M. & Stock, D. Structure of the torque ring of the flagellar motor and the molecular basis for rotational switching. *Nature* **466**, 996–1000 (2010).

69. Lam, K.-H. *et al.* Article Multiple Conformations of the FliG C-Terminal Domain Provide Insight into Flagellar Motor Switching. *Struct. Des.* **20**, 315–325 (2012).

70. Minamino, T., Imada, K. & Namba, K. Molecular motors of the bacterial flagella. *Current Opinion in Structural Biology* **18**, 693–701 (2008).

71. Sircar, R., Greenswag, A. R., Bilwes, A. M., Gonzalez-Bonet, G. & Crane, B. R. Structure and Activity of the Flagellar Rotor Protein FliY. *J. Biol. Chem.* **288**, 13493–13502 (2013).

72. Szurmant, H., Bunn, M. W., Cannistraro, V. J. & Ordal, G. W. *Bacillus subtilis* Hydrolyzes CheY-P at the Location of Its Action, the Flagellar Switch. *J. Biol. Chem.* **278**, 48611–48616 (2003).

73. Bubendorfer, S. *et al.* Specificity of motor components in the dual flagellar system of Shewanella putrefaciens CN-32. *Mol. Microbiol.* **83**, 335–350 (2012).

74. Schuhmacher, J. S. *et al.* MinD-like ATPase FlhG effects location and number of bacterial flagella during C-ring assembly. *Proc. Natl. Acad. Sci. U. S. A.* **112**, 3092–7 (2015).

75. Minamino, T., Gonzalez-Pedrajo, B., Yamaguchi, K., Aizawa, S.-I. & Macnab, R. M. FliK, the protein responsible for flagellar hook length control in Salmonella, is exported during hook assembly. *Mol. Microbiol.* **34**, 295–304 (1999).

76. Mizuno, S., Amida, H., Kobayashi, N., Aizawa, S.-I. & Tate, S. The NMR Structure of FliK, the Trigger for the Switch of Substrate Specificity in the Flagellar Type III Secretion Apparatus. *J. Mol. Biol.* **409**, 558–573 (2011).

77. Kinoshita, M. *et al.* The flexible linker of the secreted FliK ruler is required for export switching of the flagellar protein export apparatus. *Sci. Rep.* **10**, (2020).

78. Kinoshita, M., Aizawa, S., Inoue, Y., Namba, K. & Minamino, T. The role of intrinsically disordered C-terminal region of FliK in substrate specificity switching of the bacterial flagellar type III export apparatus. *Mol. Microbiol.* **105**, 572–588 (2017).

79. Kodera, N., Uchida, K., Ando, T. & Aizawa, S. I. Two-ball structure of the flagellar hook-length control protein flik as revealed by high-speed atomic force microscopy. *J. Mol. Biol.* **427**, 406–414 (2015).

80. Correa, N. E., Peng, F. & Klose, K. E. Roles of the regulatory proteins FlhF and FlhG in the Vibrio cholerae flagellar transcription hierarchy. *J. Bacteriol.* **187**, 6324–32 (2005).

81. Gulbronson, C. J. *et al.* FlhG employs diverse intrinsic domains and influences FlhF GTPase activity to numerically regulate polar flagellar biogenesis in Campylobacter jejuni. *Mol. Microbiol.* **99**, 291–306 (2016).

82. Bange, G. *et al.* The crystal structure of the third signal-recognition particle GTPase FlhF reveals a homodimer with bound GTP. (2007).

83. Van Amsterdam, K. & Van Der Ende, A. Helicobacter pylori HP1034 (ylxH) is required for motility. *Helicobacter* **9**, 387–395 (2004).

84. Dasgupta, N., Arora, S. K. & Ramphal, R. fleN, a gene that regulates flagellar number in Pseudomonas aeruginosa. *J. Bacteriol.* **182**, 357–64 (2000).

85. Dasgupta, N. & Ramphal, R. Interaction of the antiactivator FleN with the transcriptional activator FleQ regulates flagellar number in pseudomonas aeruginosa. *J. Bacteriol.* **183**, 6636–6644 (2001).

86. Bange, G. *et al.* Structural basis for the molecular evolution of SRP-GTPase activation by protein. *Nat. Struct. Mol. Biol.* **18**, 1376–1380 (2011).

87. Kusumoto, A. *et al.* Collaboration of FlhF and FlhG to regulate polar-flagella number and localization in Vibrio alginolyticus. *Microbiology* **154**, 1390–9 (2008).

88. Banerjee, P., Chanchal & Jain, D. Sensor i Regulated ATPase Activity of FleQ Is Essential for Motility to Biofilm Transition in Pseudomonas aeruginosa. *ACS Chem. Biol.* **14**, 1515–1527 (2019).

89. Jyot, J., Dasgupta, N. & Ramphal, R. FleQ, the major flagellar gene regulator in Pseudomonas aeruginosa, binds to enhancer sites located either upstream or atypically downstream of the RpoN binding site. *J. Bacteriol.* **184**, 5251–60 (2002).

90. Ono, H., Takashima, A., Hirata, H., Homma, M. & Kojima, S. The MinD homolog FlhG regulates the synthesis of the single polar flagellum of *V ibrio alginolyticus*. *Mol. Microbiol.* **98**, 130–141 (2015).

91. Zhou, H. & Lutkenhaus, J. Membrane binding by MinD involves insertion of hydrophobic residues within the C-terminal amphipathic helix into the bilayer. *J. Bacteriol.* **185**, 4326–4335 (2003).

92. Szeto, T. H., Rowland, S. L., Habrukowich, C. L. & King, G. F. The MinD membrane targeting sequence is a transplantable lipid-binding helix. *J. Biol. Chem.* **278**, 40050–40056 (2003).

93. Chanchal, Banerjee, P. & Jain, D. ATP-Induced Structural Remodeling in the Antiactivator FleN Enables Formation of the Functional Dimeric Form. *Structure* **25**, 243–252 (2017).

94. Harshita, Chanchal & Jain, D. Cloning, expression, purification, crystallization and initial crystallographic analysis of FleN from Pseudomonas aeruginosa. *Acta Crystallogr. Sect. Struct. Biol. Commun.* **72**, 135–138 (2016).

95. Green, J. C. D. *et al.* Recruitment of the Earliest Component of the Bacterial Flagellum to the Old Cell Division Pole by a Membrane-Associated Signal Recognition Particle Family GTP-Binding Protein. *J. Mol. Biol.* **391**, 679–690 (2009).

96. Kojima, S., Terashima, H. & Homma, M. Regulation of the single polar flagellar biogenesis. *Biomolecules* **10**, 533 (2020).

97. Baraquet, C. & Harwood, C. S. FleQ DNA binding consensus sequence revealed by studies of FleQ-dependent regulation of biofilm gene expression in Pseudomonas aeruginosa. *J. Bacteriol.* **198**, 178–186 (2016).

98. Peña-Sánchez, J. *et al.* Identification of the binding site of the σ 54 hetero-oligomeric FleQ/FleT activator in the flagellar promoters of Rhodobacter sphaeroides. *Microbiology* **155**, 1669–1679 (2009).

99. Morett, E. & Segovia, L. The σ54 bacterial enhancer-binding protein family: Mechanism of action and phylogenetic relationship of their functional domains.

Journal of Bacteriology **175**, 6067–6074 (1993).

100. Arora, S. K., Ritchings, B. W., Almira, E. C., Lory, S. & Ramphal, R. A transcriptional activator, FleQ, regulates mucin adhesion and flagellar gene expression in Pseudomonas aeruginosa in a cascade manner. *J. Bacteriol.* **179**, 5574–5581 (1997).

101. Baraquet, C., Murakami, K., Parsek, M. R. & Harwood, C. S. The FleQ protein from Pseudomonas aeruginosa functions as both a repressor and an activator to control gene expression from the Pel operon promoter in response to c-di-GMP. *Nucleic Acids Res.* **40**, 7207–7218 (2012).

102. Hickman, J. W. & Harwood, C. S. Identification of FleQ from Pseudomonas aeruginosa as a c-di-GMP-responsive transcription factor. *Mol. Microbiol.* **69**, 376–389 (2008).

103. Matsuyama, B. Y. *et al.* Mechanistic insights into c-di-GMP-dependent control of the biofilm regulator FleQ from Pseudomonas aeruginosa. *Proc. Natl. Acad. Sci. U. S. A.* **113**, E209–E218 (2016).

104. Su, T. *et al.* The REC domain mediated dimerization is critical for FleQ from Pseudomonas aeruginosa to function as a c-di-GMP receptor and flagella gene regulator. *J. Struct. Biol.* **192**, 1–13 (2015).

105. Claudine, B. & Harwood, C. S. Cyclic diguanosine monophosphate represses bacterial flagella synthesis by interacting with the Walker a motif of the enhancer-binding protein FleQ. *Proc. Natl. Acad. Sci. U. S. A.* **110**, 18478–18483 (2013).

106. Jain, R. & Kazmierczak, B. I. A conservative amino acid mutation in the master regulator FleQ renders Pseudomonas aeruginosa aflagellate. *PLoS One* **9**, e97439 (2014).

107. Wadhams, G. H. & Armitage, J. P. Making sense of it all: Bacterial chemotaxis. *Nature Reviews Molecular Cell Biology* **5**, 1024–1037 (2004).

108. Sourjik, V. & Wingreen, N. S. Responding to chemical gradients: Bacterial chemotaxis. *Current Opinion in Cell Biology* **24**, 262–268 (2012).

109. Waite, A. J., Frankel, N. W. & Emonet, T. Behavioral Variability and Phenotypic Diversity in Bacterial Chemotaxis. *Annu. Rev. Biophys.* **47**, 595–616 (2018).

110. Cremer, J. *et al.* Chemotaxis as a navigation strategy to boost range expansion. *Nature* **575**, 658–663 (2019).

111. Pailan, S. & Saha, P. Chemotaxis and degradation of organophosphate compound by a novel moderately thermo-halo tolerant Pseudomonas sp. strain BUR11: Evidence for possible existence of two pathways for degradation. *PeerJ* **2015**, (2015).

112. Ahmad, F., Zhu, D. & Sun, J. Bacterial chemotaxis: a way forward to aromatic compounds biodegradation. *Environmental Sciences Europe* **32**, 1–18 (2020).

113. Pandey, G. & Jain, R. K. Bacterial chemotaxis toward environmental pollutants: Role in bioremediation. *Applied and Environmental Microbiology* **68**, 5789–5795 (2002).

114. Krell, T. *et al.* Bioavailability of pollutants and chemotaxis. *Current Opinion in Biotechnology* **24**, 451–456 (2013).

115. Vardar, G., Barbieri, P. & Wood, T. K. Chemotaxis of Pseudomonas stutzeri OX1 and Burkholderia cepacia G4 toward chlorinated ethenes. *Appl. Microbiol. Biotechnol.* **66**, 696–701 (2005).

116. Parales, R. E., Ditty, J. L. & Harwood, C. S. Toluene-degrading bacteria are chemotactic towards the environmental pollutants benzene, toluene, and trichloroethylene. *Appl. Environ. Microbiol.* **66**, 4098–4104 (2000).

117. Wuichet, K. & Zhulin, I. B. Origins and diversification of a complex signal transduction system in prokaryotes. *Sci. Signal.* **3**, ra50 (2010).

118. Ortega, Á., Zhulin, I. B. & Krell, T. Sensory Repertoire of Bacterial Chemoreceptors. *Microbiol. Mol. Biol. Rev.* **81**, (2017).

119. Bi, S., Pollard, A. M., Yang, Y., Jin, F. & Sourjik, V. Engineering Hybrid Chemotaxis Receptors in Bacteria. *ACS Synth. Biol.* **5**, 989–1001 (2016).

120. Sarkar, M. K., Paul, K. & Blair, D. Chemotaxis signaling protein CheY binds to the rotor protein FliN to control the direction of flagellar rotation in Escherichia coli. *Proc. Natl. Acad. Sci. U. S. A.* **107**, 9370–9375 (2010).

121. Khan, S., Pierce, D. & Vale, R. D. Interactions of the chemotaxis signal protein CheY with bacterial flagellar motors visualized by evanescent wave microscopy. *Curr. Biol.* **10**, 927–930 (2000).

122. Bi, S., Jin, F. & Sourjik, V. Inverted signaling by bacterial chemotaxis receptors. *Nat. Commun.* **9**, (2018).

123. Bi, S. & Sourjik, V. Stimulus sensing and signal processing in bacterial chemotaxis. *Current Opinion in Microbiology* **45**, 22–29 (2018).

124. Altegoer, F., Schuhmacher, J., Pausch, P. & Bange, G. From molecular evolution to biobricks and synthetic modules: A lesson by the bacterial flagellum. *Biotechnology and Genetic Engineering Reviews* **30**, 49–64 (2014).

125. Nakamura, S. & Minamino, T. Flagella-driven motility of bacteria. *Biomolecules* **9**, 279 (2019).

126. Schmitt, C. K. *et al.* Absence of all components of the flagellar export and synthesis machinery differentially alters virulence of Salmonella enterica serovar typhimurium in models of typhoid fever, survival in macrophages, tissue culture invasiveness, and calf enterocolitis. *Infect. Immun.* **69**, 5619–5625 (2001).

127. Stecher, B. *et al.* Flagella and chemotaxis are required for efficient induction of Salmonella enterica serovar typhimurium colitis in streptomycin-pretreated mice. *Infect. Immun.* **72**, 4138–4150 (2004).

128. Partridge, J. D. & Harshey, R. M. More than motility: Salmonella flagella contribute to overriding friction and facilitating colony hydration during swarming. *J. Bacteriol.* **195**, 919–929 (2013).

129. Ping, L. The asymmetric flagellar distribution and motility of Escherichia coli. *J. Mol. Biol.* **397**, 906–916 (2010).

130. Darnton, N. C., Turner, L., Rojevsky, S. & Berg, H. C. On torque and tumbling in swimming Escherichia coli. *J. Bacteriol.* **189**, 1756–1764 (2007).

131. Mears, P. J., Koirala, S., Rao, C. V., Golding, I. & Chemla, Y. R. Escherichia coli swimming is robust against variations in flagellar number. *Elife* **2014**, 1916 (2014).

132. Yamaichi, Y. *et al.* A multidomain hub anchors the chromosome segregation and chemotactic machinery to the bacterial pole. *Genes Dev.* **26**, 2348–2360 (2012).

133. Takekawa, N., Kwon, S., Nishioka, N., Kojima, S. & Homma, M. HubP, a polar landmark protein, regulates flagellar number by assisting in the proper polar localization of FlhG in Vibrio alginolyticus. *J. Bacteriol.* **198**, 3091–3098 (2016).

134. Rossmann, F. M. *et al.* The GGDEF domain of the phosphodiesterase PdeB in Shewanella putrefaciens mediates recruitment by the polar landmark protein HubP. *J. Bacteriol.* **201**, (2019).

135. Rossmann, F. *et al.* The role of FlhF and HubP as polar landmark proteins in *S hewanella putrefaciens* CN-32. *Mol. Microbiol.* **98**, 727–742 (2015).

136. Pandza, S. *et al.* The G-protein FlhF has a role in polar flagellar placement and general stress response induction in Pseudomonas putida. *Mol. Microbiol.* **36**, 414–423 (2000).

137. Guttenplan, S. B., Shaw, S. & Kearns, D. B. The cell biology of peritrichous flagella in Bacillus subtilis. *Mol. Microbiol.* **87**, 211–229 (2013).

138. Mukherjee, S. & Kearns, D. B. The structure and regulation of flagella in bacillus subtilis. *Annu. Rev. Genet.* **48**, 319–340 (2014).

139. Mukherjee, S. *et al.* Adaptor-mediated Lon proteolysis restricts Bacillus subtilis hyperflagellation. *Proc. Natl. Acad. Sci. U. S. A.* **112**, 250–255 (2015).

140. Mazzantini, D. *et al.* FlhF is required for swarming motility and full pathogenicity of Bacillus cereus. *Front. Microbiol.* **7**, (2016).

141. Mazzantini, D. *et al.* GTP-Dependent FlhF Homodimer Supports Secretion of a Hemolysin in Bacillus cereus. *Front. Microbiol.* **11**, (2020).

142. Salvetti, S. *et al.* FlhF, a signal recognition particle-like GTPase, is involved in the regulation of flagellar arrangement, motility behaviour and protein secretion in Bacillus cereus. *Microbiology* **153**, 2541–2552 (2007).

143. Pilizota, T. *et al.* A molecular brake, not a clutch, stops the Rhodobacter sphaeroides flagellar motor. *Proc. Natl. Acad. Sci. U. S. A.* **106**, 11582–11587 (2009).

144. Armitage, J. P. & Macnab, R. M. Unidirectional, intermittent rotation of the flagellum of Rhodobacter sphaeroides. *J. Bacteriol.* **169**, 514–518 (1987).

145. Balaban, M. & Hendrixson, D. R. Polar Flagellar Biosynthesis and a Regulator of Flagellar Number Influence Spatial Parameters of Cell Division in Campylobacter jejuni. *PLoS Pathog.* **7**, e1002420 (2011).

146. Ren, F. *et al.* Insights into the impact of flhF inactivation on Campylobacter jejuni colonization of chick and mice gut. *BMC Microbiol.* **18**, (2018).

147. Ren, F. *et al.* Could FlhF be a key element that controls Campylobacter jejuni flagella biosynthesis in the initial assembly stage? *Microbiol. Res.* **207**, 240–248 (2018).

148. Ardissone, S. & Viollier, P. H. Interplay between flagellation and cell cycle control in Caulobacter. *Current Opinion in Microbiology* **28**, 83–92 (2015).

149. Lam, H., Schofield, W. B. & Jacobs-Wagner, C. A landmark protein essential for establishing and perpetuating the polarity of a bacterial cell. *Cell* **124**, 1011–1023 (2006).

150. Davis, N. J. *et al.* De- and repolarization mechanism of flagellar morphogenesis during a bacterial cell cycle. *Genes Dev.* **27**, 2049–2062 (2013).

151. Huitema, E., Pritchard, S., Matteson, D., Radhakrishnan, S. K. & Viollier, P. H. Bacterial birth scar proteins mark future flagellum assembly site. *Cell* **124**, 1025–1037 (2006).

152. Xu, H., He, J., Liu, J. & Motaleb, M. A. BB0326 is responsible for the formation of periplasmic flagellar collar and assembly of the stator complex in *Borrelia burgdorferi*. *Mol. Microbiol.* **113**, 418–429 (2020).

153. Kumar, B., Miller, K., Charon, N. W. & Legleiter, J. Periplasmic flagella in Borrelia burgdoferi function to maintain cellular integrity upon external stress. *PLoS One* **12**, (2017).

154. Zhang, K. *et al.* FlhF regulates the number and configuration of periplasmic flagella in Borrelia burgdorferi. *Mol. Microbiol.* **113**, 1122–1139 (2020).

155. Semple, K. M., Doran, J. L. & Westlake, D. W. S. DNA relatedness of oil-field isolates of *Shewanella putrefaciens*. *Can. J. Microbiol.* **35**, 925–931 (1989).

156. Khashe, S. & Michael Janda, J. Biochemical and pathogenic properties of Shewanella alga and Shewanella putrefaciens. *J. Clin. Microbiol.* **36**, 783–787 (1998).

157. Hau, H. H. & Gralnick, J. A. Ecology and Biotechnology of the Genus *Shewanella*. *Annu. Rev. Microbiol.* **61**, 237–258 (2007).

158. Bozal, N., Montes, M. J., Tudela, E., Jiménez, F. & Guinea, J. Shewanella frigidimarina and Shewanella livingstonensis sp. nov. isolated from Antarctic coastal areas. *Int. J. Syst. Evol. Microbiol.* **52**, 195–205 (2002).

159. Bowman, J. P. *et al.* Shewanella gelidimarina sp. nov. and Shewanella frigidimarina sp. nov., novel antarctic species with the ability to produce eicosapentaenoic acid (20:5ω3) and grow anaerobically by dissimilatory fe(III) reduction. *Int. J. Syst. Bacteriol.* **47**, 1040–1047 (1997).

160. Chen, Y. *et al.* Skin and Soft-Tissue Manifestations of *Shewanella putrefaciens* Infection. *Clin. Infect. Dis.* **25**, 225–229 (1997).

161. Pagani, L. *et al.* Soft tissue infection and bacteremia caused by Shewanella putrefaciens. *J. Clin. Microbiol.* **41**, 2240–2241 (2003).

162. Butt, A. A., Figueroa, J. & Martin, D. H. Ocular Infection Caused by Three Unusual Marine Organisms. *Clin. Infect. Dis.* **24**, 740–740 (1997).

163. Stenström, I. -M & Molin, G. Classification of the spoilage flora offish, with special reference to Shewanella putrefaciens. *J. Appl. Bacteriol.* **68**, 601–618 (1990).

164. Bagge, D., Hjelm, M., Johansen, C., Huber, I. & Gram, L. Shewanella putrefaciens Adhesion and Biofilm Formation on Food Processing Surfaces. *Appl. Environ. Microbiol.* **67**, 2319–2325 (2001).

165. Fredrickson, J. K. *et al.* Biogenic iron mineralization accompanying the dissimilatory reduction of hydrous ferric oxide by a groundwater bacterium. *Geochim. Cosmochim. Acta* **62**, 3239–3257 (1998).

166. DiChristina, T. J. & DeLong, E. F. Design and application of rRNA-targeted oligonucleotide probes for the dissimilatory iron- and manganese-reducing bacterium Shewanella putrefaciens. *Appl. Environ. Microbiol.* **59**, 4152–4160 (1993).

167. Wildung, R. E. *et al.* Effect of electron donor and solution chemistry on products of dissimilatory reduction of technetium by Shewanella putrefaciens. *Appl. Environ.*

Microbiol. **66**, 2451–2460 (2000).

168. Payne, A. N. & DiChristina, T. J. A rapid mutant screening technique for detection of technetium [Tc(VII)] reduction-deficient mutants of *Shewanella oneidensis* MR-1. *FEMS Microbiol. Lett.* **259**, 282–287 (2006).

169. Bubendorfer, S., Koltai, M., Rossmann, F., Sourjik, V. & Thormann, K. M. Secondary bacterial flagellar system improves bacterial spreading by increasing the directional persistence of swimming. *Proc. Natl. Acad. Sci. U. S. A.* **111**, 11485–90 (2014).

170. McCarter, L. L. Dual Flagellar Systems Enable Motility under Different Circumstances. *J. Mol. Microbiol. Biotechnol.* **7**, 18–29 (2004).

171. Kühn, M. J. *et al.* Spatial arrangement of several flagellins within bacterial flagella improves motility in different environments. *Nat. Commun.* **9**, 1–12 (2018).

172. Kühn, M. J., Schmidt, F. K., Eckhardt, B. & Thormann, K. M. Bacteria exploit a polymorphic instability of the flagellar filament to escape from traps. *Proc. Natl. Acad. Sci. U. S. A.* **114**, 6340–6345 (2017).

173. Hintsche, M. *et al.* A polar bundle of flagella can drive bacterial swimming by pushing, pulling, or coiling around the cell body. *Sci. Rep.* **7**, 1–10 (2017).

174. Steinchen, W., Linne, U. & Bange, G. HDX-MS in den Lebenswissenschaften. *BIOspektrum* **23**, 772–775 (2017).

175. Blagotinsek, V. *et al.* An ATP-dependent partner switch links flagellar C-ring assembly with gene expression. *Proc. Natl. Acad. Sci. U. S. A.* **117**, 20826–20835 (2020).

176. Bienert, S. *et al.* The SWISS-MODEL Repository-new features and functionality. *Nucleic Acids Res.* **45**, D313–D319 (2017).

177. Waterhouse, A. *et al.* SWISS-MODEL: Homology modelling of protein structures and complexes. *Nucleic Acids Res.* **46**, W296–W303 (2018).

178. Fernández, I. *et al.* Three-Dimensional Structure of Full-Length NtrX, an Unusual Member of the NtrC Family of Response Regulators. *J. Mol. Biol.* **429**, 1192–1212 (2017).

179. Su, T. *et al.* The REC domain mediated dimerization is critical for FleQ from Pseudomonas aeruginosa to function as a c-di-GMP receptor and flagella gene regulator. *J. Struct. Biol.* **192**, 1–13 (2015).

180. Hook, J. C. *et al.* A Proline-Rich Element in the Type III Secretion Protein FlhB Contributes to Flagellar Biogenesis in the Beta- and Gamma-Proteobacteria. *Front. Microbiol.* **11**, 2908 (2020).

181. Evans, L. D. B., Poulter, S., Terentjev, E. M., Hughes, C. & Fraser, G. M. A chain mechanism for flagellum growth. *Nature* **504**, 287–290 (2013).

182. Laskowski, R. A. & Swindells, M. B. LigPlot+: Multiple ligand-protein interaction diagrams for drug discovery. *J. Chem. Inf. Model.* **51**, 2778–2786 (2011).

183. Wallace, A. C., Laskowski, R. A. & Thornton, J. M. Ligplot: A program to generate schematic diagrams of protein-ligand interactions. *Protein Eng. Des. Sel.* **8**, 127–134 (1995).

184. Albert-Weissenberger, C., Cazalet, C. & Buchrieser, C. Legionella pneumophila - A human pathogen that co-evolved with fresh water protozoa. *Cellular and Molecular*

Life Sciences **64**, 432–448 (2007).

185. Molina-Henares, M. A., Ramos-González, M. I., Daddaoua, A., Fernández-Escamilla, A. M. & Espinosa-Urgel, M. FleQ of Pseudomonas putida KT2440 is a multimeric cyclic diguanylate binding protein that differentially regulates expression of biofilm matrix components. *Res. Microbiol.* **168**, 36–45 (2017).

186. Edgar, R. C. MUSCLE: Multiple sequence alignment with high accuracy and high throughput. *Nucleic Acids Res.* **32**, 1792–1797 (2004).

187. Troshin, P. V, Procter, J. B., Barton, G. J. & Bateman, A. Sequence analysis Java bioinformatics analysis web services for multiple sequence alignment-JABAWS:MSA. *Bioinforma. Appl. NOTE* **27**, 2001–2002 (2011).

188. Waterhouse, A. M., Procter, J. B., Martin, D. M. A., Clamp, M. & Barton, G. J. Sequence analysis Jalview Version 2-a multiple sequence alignment editor and analysis workbench. *Bioinforma. Appl. NOTE* **25**, 1189–1191 (2009).

189. Pettersen, E. F. *et al.* UCSF Chimera?A visualization system for exploratory research and analysis. *J. Comput. Chem.* **25**, 1605–1612 (2004).

190. Meng, E. C., Pettersen, E. F., Couch, G. S., Huang, C. C. & Ferrin, T. E. Tools for integrated sequence-structure analysis with UCSF Chimera. *BMC Bioinformatics* **7**, 339 (2006).

191. Ashkenazy, H. *et al.* ConSurf 2016: an improved methodology to estimate and visualize evolutionary conservation in macromolecules. *Nucleic Acids Res.* **44**, W344–W350 (2016).

192. Ashkenazy, H., Erez, E., Martz, E., Pupko, T. & Ben-Tal, N. ConSurf 2010: calculating evolutionary conservation in sequence and structure of proteins and nucleic acids. *Nucleic Acids Res.* **38**, W529–W533 (2010).

193. Glaser, F. *et al.* ConSurf: Identification of functional regions in proteins by surface-mapping of phylogenetic information. *Bioinformatics* **19**, 163–164 (2003).

194. Kabsch, W. *et al. XDS*. *Acta Crystallogr. Sect. D Biol. Crystallogr.* **66**, 125–132 (2010).

195. Mccoy, A. J. *et al.* Phaser crystallographic software. *J. Appl. Cryst* **40**, 658–674 (2007).

196. Emsley, P. & Cowtan, K. Coot: Model-building tools for molecular graphics. *Acta Crystallogr. Sect. D Biol. Crystallogr.* **60**, 2126–2132 (2004).

197. Adams, P. D. *et al.* PHENIX: A comprehensive Python-based system for macromolecular structure solution. *Acta Crystallogr. Sect. D Biol. Crystallogr.* **66**, 213–221 (2010).

198. Schäper, S. *et al.* AraC-like transcriptional activator CuxR binds c-di-GMP by a PilZ-like mechanism to regulate extracellular polysaccharide production. *Proc. Natl. Acad. Sci. U. S. A.* **114**, E4822–E4831 (2017).

199. Steinchen, W. *et al.* Catalytic mechanism and allosteric regulation of an oligomeric (p)ppGpp synthetase by an alarmone. *Proc. Natl. Acad. Sci. U. S. A.* **112**, 13348–53 (2015).

7. Appendix/supplementary data

7.1. Genome identification IDs of genes/proteins used

All genes/proteins below from *Shewanella putrefaciens strain CN-32.*

Gene/protein name	SputCN32 genome identifier
FlhB1	SputCN_2563
FlhG	SputCN_2560
FliM1	SputCN_2569
FliN1	SputCN_2568
FlrA1	SputCN_2580
FliK1	SputCN_2571
FlhB2	SputCN_3484
FliK2	SputCN_3451
FlhF	SputCN_2561
FlhA1	SputCN_2562

7.2. List of constructs used

Name	Tags	Vector/resistance
FlhB-C dN221 WT	His	pET 24d/Kan
FlhB-C dN221 N269A	His	pET 24d/Kan
GST-FlrA-HTH	GST, His	pGAT3/Amp
GST-FlrA-FleQ	GST, His	pGAT3/Amp
GST-FlrA-AAA-HTH	GST, His	pGAT3/Amp
GST-FlrA-HTH-L400E	GST, His	pGAT3/Amp
GST-FlrA-HTH-d389-409	GST, His	pGAT3/Amp
FlrA WT	His	pET 24d/Kan
FlrA D233A	His	pET 24d/Kan
FlhG WT	His	pET 16b/Amp
FlhG D58A	His	pET 24d/Kan
FliM	His	pET 24d/Kan
FliN	/	pET 16b/Amp
GST-FliM-N	GST, His	pGAT3/Amp
GST-FlhB-C dN221 WT	GST, His	pGAT3/Amp
GST-FlhB-C dN221 N269A	GST, His	pGAT3/Amp
GST-FlhA-C	GST, His	pGAT3/Amp
GST-FlhB-C dC20	GST, His	pGAT3/Amp
GST-PRR	GST, His	pGAT3/Amp
GST-FlrA-HTH-dN16	GST, His	pGAT3/Amp
GST-FlrA-HTH-dN36	GST, His	pGAT3/Amp
FliK WT	His	pET 24d/Kan

Strains for fluorescence microscopy experiments were prepared, used by and are stored by AG Thormann, Gießen. Different constructs for protein purification were provided by D. Mrusek, A. Dornes and A. Lepak.

7.3. FlhG and FlrA purification optimization gels

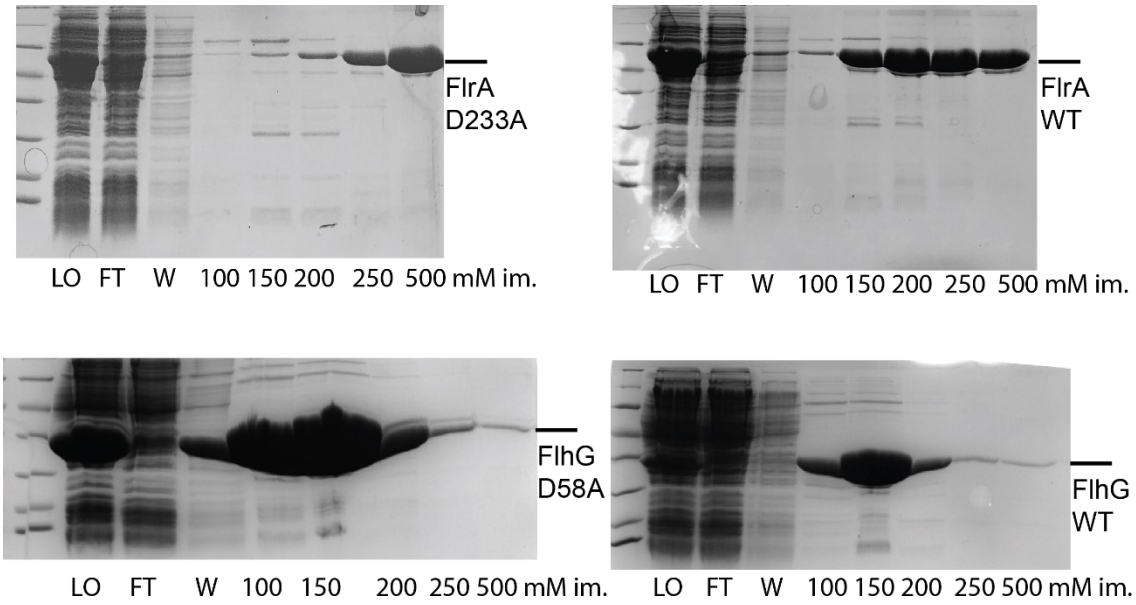

Appendix 7.3 SDS-PAGE gel images of affinity (His-tag) purifications of different FlrA and FlhG constructs (mentioned in Results **3.1.3.**) . Fractions and concentrations of imidazole used in the elution step indicated under the image (also see Methods **5.3.1., 5.3.2.**). LO – "load" fraction, sample from clear supernatant after cell lysis and centrifugation before applying it to the affinity column. FT – "flow-through", sample gathered after "load" fraction has fully passed through the affinity column. W – "wash", sample from a 10 column volume washing of the column with buffer before elution.

7.4. Refinement statistics for FlhB-C

Data collection and refinement statistics

	*Sp*FlhB-C
Data collection	
Space group	R 3 2
Cell dimensions	
a, *b*, *c* (Å)	152.436 152.436 126.886
α, β, γ (°)	90, 90, 120
Resolution (Å)	46.44 - 2.1 (2.175 - 2.1)
R_{merge}	0.1412 (1.233)
$I / \sigma I$	13.46 (1.64)
Completeness (%)	99.96 (99.94)
Redundancy	19.9 (18.3)
Refinement	
Resolution (Å)	46.44 - 2.1
No. reflections	33095 (3286)
R_{work} / R_{free}	0.21/0.24
No. atoms	4134
Protein	3932
Ligand/ion	-
Water	202
B-factors	48.30
Protein	48.31
Ligand/ion	-
Water	47.97
Ramachandran favored (%)	97.88
Ramachandran allowed (%)	2.12
Ramachandran outlier (%)	0.00
R.m.s. deviations	
Bond lengths (Å)	0.011
Bond angles (°)	1.16

*Values in parentheses are for highest-resolution shell.

These refinement statistics were also published in [180].

7.5. Sequence alignments (EMBOSS Needle) and related analysis

Alignments performed with Emboss Needle (see Methods **5.3.3.**). The images shown in all the following subsections are screen captures of the output of the EMBOSS Needle server. Alignments were always performed in a pairwise manner (e.g. two FASTA sequences at once). SalTy refers to *Salmonella typhimurium. Pa – Pseudomonas aeruginosa, Sp – Shewanella putrefaciens.*

7.5.1. SpFlhB (polar) and SalTyFlhB alignment and conservation of critical residues

```
# Length: 391
# Identity:     154/391 (39.4%)
# Similarity:   242/391 (61.9%)
# Gaps:          23/391 ( 5.9%)
# Score: 732.0
#
#
#=======================================

SalTy               1 MAEESDDDKTEAPTPHRLEKAREEGQIPRSRELTSLLILLVGVCIIWFGG     50
                      |||||..:::|.||..|||:|||:||:.||:||.:..:||......:..|
ShewPol             1 MAEESSGERSEEPTGRRLEQAREKGQVARSKELGTAAVLLSAATGFYMLG     50

SalTy              51 ESLARQLAGMLSAGLHFDHRMVNDPN-------LILGQIILLIKAAMMAL     93
                      ..:|..|:.:.......|...:.|.|       ::.|:|       ...:
ShewPol            51 PGIATALSHVFERVFTMDRAQIYDTNQMFNVWGVVAGEI-------AWPM     93

SalTy              94 LPLIAGVVLVALISPVMLGGLIFSGKSLQPKFSKLNPLPGIKRMFSAQTG    143
                      |.::..:|:||.|..|.|||:.||.:::.||.||::||.|.||||..|..
ShewPol            94 LKIMLLIVVVAFIGNVSLGGMNFSTQAMMPKASKMSPLAGFKRMFGVQAL    143

SalTy             144 AELLKAVLKSTLVGCVTGFYLWHHWPQMMRLMAESPIVAMGNALDLVGLC    193
                      .||.|.:.|.::|.....|.|.:::..::.|.::.....:.:||||:...
ShewPol           144 VELTKGIAKFSVVAFSAYFLLSYYFNDILLLSSDHLPGNVHHALDLLIWM    193

SalTy             194 ALLVVLGVIPMVGFDVFFQIFSHLKKLRMSRQDIRDEFKESEGDPHVKGK    243
                      .:|:...|:.:|..||.|||::|.|:|:|::|:::||:|::||.|.|||:
ShewPol           194 FILLCSSVLLIVVIDVPFQIWNHNKQLKMTKQEVKDEYKDTEGKPEVKGR    243

SalTy             244 IRQMQRAAAQRRMMEDVPKADVIVTNPTHYSVALQYDENKMSAPKVVAKG    293
                      :|||||..||||||.:||.|||||.||.||:||::||..:.:||.|:|||
ShewPol           244 VRQMQRELAQRRMMAEVPNADVIVVNPEHYAVAVKYDVKRSAAPFVIAKG    293

SalTy             294 AGLIALRIREIGAEHRVPTLEAPPLARALYRHAEIGQQIPGQLYAAVAEV    343
                      ...:|.:|||:..|:.:..:.|||||||:|...::.||||..|:.|||:|
ShewPol           294 VDDVAFKIREVAREYNIAIVSAPPLARAIYHTTKLDQQIPEGLFTAVAQV    343

SalTy             344 LAWVWQLKRWRLAGGQRP-PQPENLPVPEALDFMNEKNTDG    383
                      ||:|:||:::::...|::| |.|.|.|:|:.|.:
ShewPol           344 LAYVFQLRQYQKGRGRKPIPIPLNQPIPDDLKY--------    376
```

Alignment of SpFlhB (polar) and *S. typhimurium* FlhB sequences (above, Emboss Needle), conservation of critical residues (below).

Salmonella residue (Evans et. al 2013)	Shewanella (polar) residue
A286	A286
P287	P287
A341	A341
L344	L344

Salmonella residue (Inoue et. al 2019)	Shewanella residue
L318	L318
A319	A319
R320	R320
L322	I322
L350	L350
P311	A311
V340	V340

7.5.2. SpFliK(1/2) and SalTyFliK alignment data

Protein Pair	Identity	Similarity	Gaps
SpFliK1/SalTyFliK	24%	36.8%	26.7%
SpFliK2/SalTyFliK	24.3%%	36.4%	23.8%
SpFliK1/SpFliK2	22.1%	38.5%	29.0%

Protein length (residues): SpFliK1:491, SpFliK2:393, SalTyFliK:405

Appendix 7.5.2.1. (above) Summary of sequence identity, similarity and gaps between different combinations of SpFliK1/2 and SalTyFliK. (Obtained through Emboss Needle)

```
ShewanellaFli      1 MQQMTNILLPK--AANNNASAGKASTPETRS-EDFSAALASVNSVSSSTQ     47
                       .|.||:  ..:.:.:||..|...|.| |||.|.||
SalmonellaTyp      1 -----MITLPQLITTDTDMTAGLTSGKTTGSAEDFLALLA----------     35

ShewanellaFli     48 KPSTSQERAIELTKSASSNDISQDEEDDVSLIFAQISMANEMKKTAAEGD     97
                             .|...|.:|.::       |:|::|:    ..|.|.
SalmonellaTyp     36 --------------GALGADGAQGKD-------ARITLAD----LQAAGG     60

ShewanellaFli     98 KLPLLQEMDLDIGTSAVEAEGCFSSELDKLAELLVDPSPA-DESGVALIA    146
                     ||.  :|:....|.         ..:..|||:||...:.| ||:
SalmonellaTyp     61 KLS--KELLTQHGE---------PGQAVKLADLLAQKANATDET------     93

ShewanellaFli    147 EADATNLPDINLALPLSTPAMLDGAIA-----SQNNGELPEQSVLVEEST    191
                        .|:|......|...||::...|:|     :|::.:.|   .|.:|
SalmonellaTyp     94 ---LTDLTQAQHLLSTLTPSLKTSALAALSKTAQHDEKTP---ALSDE--    135

ShewanellaFli    192 VELVSQEAAKQQKQGIVDAQPIMGENDSIRSFS------ADKSSIAQQNA    235
                      :|.|..|......|...|.|:.||..:....:      .|..|..|:..
SalmonellaTyp    136 -DLASLSALFAMLPGQPVATPVAGETPAENHIALPSLLRGDMPSAPQEET    184

ShewanellaFli    236 FTTGLKDTNSIDGTKKESFV-----SATTAALNTLGTAEDVATPKNIELD    280
                     .|....:...  |..:.|..     .||..||..|..|. .||...:|:|
SalmonellaTyp    185 HTLSFSEHEK--GKTEASLARASDDRATGPALTPLVVAA-AATSAKVEVD    231

ShewanellaFli    281 GSERLATNVQLKDAKLAVTLESSSPTSFNLDDEVASEFKPVSVTTSPTQP    330
                             .....||..::.||   |....|   :|:.|.::|.
SalmonellaTyp    232 ------------SPPAPVTHGAAMPT---LSSATA---QPLPVASAPV--    261

ShewanellaFli    331 QVNRQDIPQIQLSLRQGVETPNQMQEMIQRFSPVMKQQLITMVSNGIQHA    380
                                 :..|....|..|.||    ||::.....|.|.|
SalmonellaTyp    262 -----------------LSAPLGSHEWQQTFS----QQVMLFTRQGQQSA    290

ShewanellaFli    381 EIRLDPPELGHMTVKIQVHGDQTQVQFHVTQSQTRDMVEQAIPRLRELLQ    430
                     ::||.|.|||.:.:.:::..:|.|:|.....|..|..:|.|:|.||..|.
SalmonellaTyp    291 QLRLHPEELGQVHISLKLDDNQAQLQMVSPHSHVRAALEAALPMLRTQLA    340

ShewanellaFli    431 EQGMQLADSHVSQGEQEQGRDGGFGESNGSGSTNLDEFSAEELDLGLNQT    480
                     |.|:||..|.:| .|...|:.....:...|.:.:.|.|.||: |:.|...
SalmonellaTyp    341 ESGIQLGQSSIS-SESFAGQQQSSSQQQSSRAQHTDAFGAED-DIALAAP    388

ShewanellaFli    481 TSL------HSGIDYYA    491
                     .||      :..:|.:|
SalmonellaTyp    389 ASLQAAARGNGAVDIFA    405
```

Appendix 7.5.2.2. Above: SpFliK1/SalTyFliK alignment (Emboss Needle)

```
SalTyFliK          1 MITLPQLIT-----TDTDMTAGLTSGKTTGSAEDF--LALLAGALGADGA     43
                     .:..|::     |:.::|..:||......||.|  |||..........
SpFliK2            1 --MISDLLSTRHMGTNPNVTTKVTSAVDQDKAESFTLLALPVEPSAESMP     48

SalTyFliK         44 QGKDARITLADLQAAGGKLSKELLTQH------GEPGQAVKLADLLAQ--     85
                     |.:...||....|.:|   ....|.||      ..|...|......|.
SpFliK2           49 QERSLDITTEQSQESG---YNPFLNQHINNLVESAPFTGVNAVTQGAMFN     95

SalTyFliK         86 ---KANATDETLTDLTQAQHLLSTLT------PSLKTSALAALSKTAQHD    126
                        :.|:|...|.|:..|.  |::||      |.:..:.....|||....
SpFliK2           96 SEAEINSTSIRLDDVAFAP--LNSLTTPTVVAPLVPVTLPIEASKTESVG    143

SalTyFliK        127 EKTPALSDEDLAS-LSALFAMLPGQPVATPVAGETPAENHIALPSLLRGD    175
                     :.:.:|....:|| ..|||:......:|...:...||.....:     ..
SpFliK2          144 QTSASLVGLSVASQRGALFSSGMASSMALVGSASQPASMSTEI-----SP    188

SalTyFliK        176 MPSAPQEETHTLSFS-----EHEKGKT---EASLA-----RASDDRATGP    212
                     :.||..::..|..||     :|.|..|   :..||     .|.|..|.|
SpFliK2          189 ISSALAKDAMTTPFSDSSRFDHLKADTSMFQRVLAELRGHEAKDINAIG-    237

SalTyFliK        213 ALTPLVVAAAATSAKVEVDSPPAPVTHGAAMPTLSSATAQPLPVASAPVL    262
                       |..:|:..|.||   ....|..:|     ||.|.|       ..|..:
SpFliK2          238 --TQPIVSTQAASA---TQWGPVSLT-----PTASLA-------QQAQEI    270

SalTyFliK        263 SAPLGSHEWQQTFSQQVMLFTRQGQQSAQLRLHPEELGQVHISLKLDDNQ    312
                     ..||..|         :.....|..:.|:|||.|.|||::.::::|:.::
SpFliK2          271 LTPLREH---------LRFQVDQHIKKAELRLDPPELGKIDLNIRLEGDR    311

SalTyFliK        313 AQLQMVSPHSHVRAALEAALPMLRTQLA-ESGIQLGQSSISSESFAGQQQ    361
                     .|:.|.:.:..:|.||...|..||..|| :.|   ||..:.    .||..
SpFliK2          312 LQVHMHAVNPAIRDALLNGLERLRMDLAMDHG---GQIDVD----VGQGG    354

SalTyFliK        362 SSSQQQSSRAQHTDAFGAEDDIALAAPASLQAAARGNGA---------VD    402
                     |..|||              :.||.|.:.....|..|||         :|
SpFliK2          355 SQQQQQ--------------ETALFASSIAPETAMENGADVMTREKSQLD    390

SalTyFliK        403 IFA    405
                     :.|
SpFliK2          391 LLA    393
```

Appendix 7.5.2.3. Above: SpFliK2/SalTyFliK alignment (Emboss Needle)

```
SpFliK1           1 MQQMTNILLPKAANNNASAGKASTPETRSEDFSAALASVNSVSS--STQK     48
                                                          .:|.  ||:.
SpFliK2           1 ----------------------------------------MISDLLSTRH     10

SpFliK1          49 PSTSQERAIELTKSASSNDISQDEEDDVSLIFAQISMANEMKKTAAEGDK     98
                    ..|:.....::|.:     :.||:.:..:|:...:..:.|         .
SpFliK2          11 MGTNPNVTTKVTSA-----VDQDKAESFTLLALPVEPSAE---------S     46

SpFliK1          99 LPLLQEMDLDIGTSAVEAEGCFSSELDKLAELLVDPSP-----ADESGVA    143
                    :|  ||..|||.|...:..| ::..|::....||:.:|     |...|..
SpFliK2          47 MP--QERSLDITTEQSQESG-YNPFLNQHINNLVESAPFTGVNAVTQGAM     93

SpFliK1         144 LIAEAD----ATNLPDINLALP---LSTPAMLDGAIASQNNGELPEQSVL    186
                    ..:||:    :..|.|:..| |   |:||.:    :|......||.::..
SpFliK2          94 FNSEAEINSTSIRLDDVAFA-PLNSLTTPTV----VAPLVPVTLPIEASK    138

SpFliK1         187 VE---ESTVELVSQEAAKQQ----KQGIVDAQPIMGENDSIRSFSADKSS    229
                    .|   :::..||....|.|:    ..|:..:..::|......|.|.:.|.
SpFliK2         139 TESVGQTSASLVGLSVASQRGALFSSGMASSMALVGSASQPASMSTEISP    188

SpFliK1         230 IAQ---QNAFTTGLKDTNSIDGTKKESFVSATTAALNTLGTAEDVATPKN    276
                    |:.   ::|.||...|::..|..|.::.:.....|
SpFliK2         189 ISSALAKDAMTTPFSDSSRFDHLKADTSMFQRVLA---------------    223

SpFliK1         277 IELDGSERLATNVQLKDAKLAVTLESSSPTSFNLDDEVASEFKPVSVTTS    326
                     ||.|.|  |.::.....:..|:.:::|          |:::.|||:|
SpFliK2         224 -ELRGHE--AKDINAIGTQPIVSTQAAS----------ATQWGPVSLT--    258

SpFliK1         327 PTQPQVNRQDIPQIQLSLRQGVETPNQMQEMIQRFSPVMKQQLITMVSNG    376
                    ||             .||.|      |.||::   :| :::.|...|...
SpFliK2         259 PT-------------ASLAQ------QAQEIL---TP-LREHLRFQVDQH    285

SpFliK1         377 IQHAEIRLDPPELGHMTVKIQVHGDQTQVQFHVTQSQTRDMVEQAIPRLR    426
                    |:.||:||||||||.:.:.|::.||:.||..|......||.:...:.|||
SpFliK2         286 IKKAELRLDPPELGKIDLNIRLEGDRLQVHMHAVNPAIRDALLNGLERLR    335

SpFliK1         427 -ELLQEQGMQLADSHVSQ-GEQEQGRDGGFGESNGSGSTNLDEFSAEELD    474
                     :|..:.|.|: |..|.| |.|:|.::.....|:.:..|.::.
SpFliK2         336 MDLAMDHGGQI-DVDVGQGGSQQQQQETALFASSIAPETAMEN-------    377

SpFliK1         475 LGLNQTTSLHSGIDYYA    491
                     |.:..|...|.:|..|
SpFliK2         378 -GADVMTREKSQLDLLA    393
```

Appendix 7.5.2.4. Above: SpFliK1/SpFliK2 alignment (Emboss Needle)

Appendix 7.5.2.5. Below (upper panel): PSIPRED secondary structure prediction: SpFliK2 (containing disordered linker region). Below (middle panel): PSIPRED secondary structure prediction of SalTyFliK (containing disordered linker region). Below (lower panel): PSIPRED secondary structure prediction of SpFliK1 (corresponding to the same region as shown for the relevant proteins in upper and middle panel; SpFliK1 does not have such a long stretch without secondary structural elements).

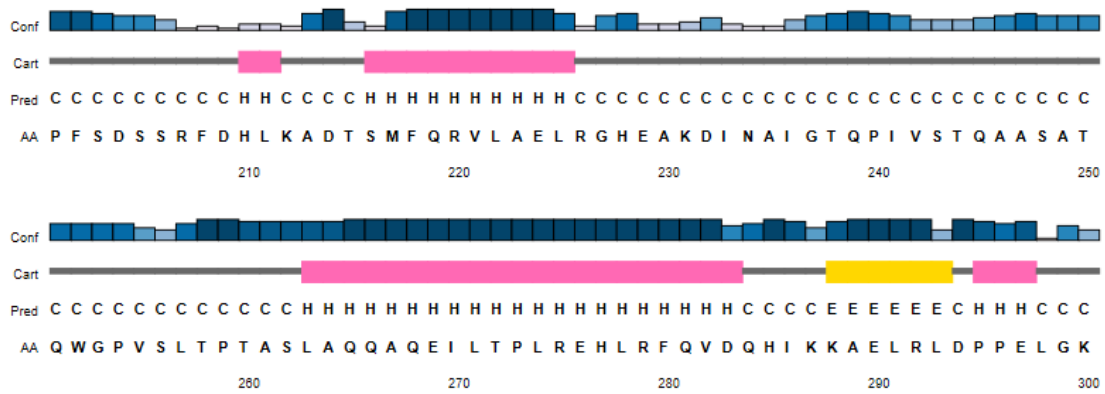

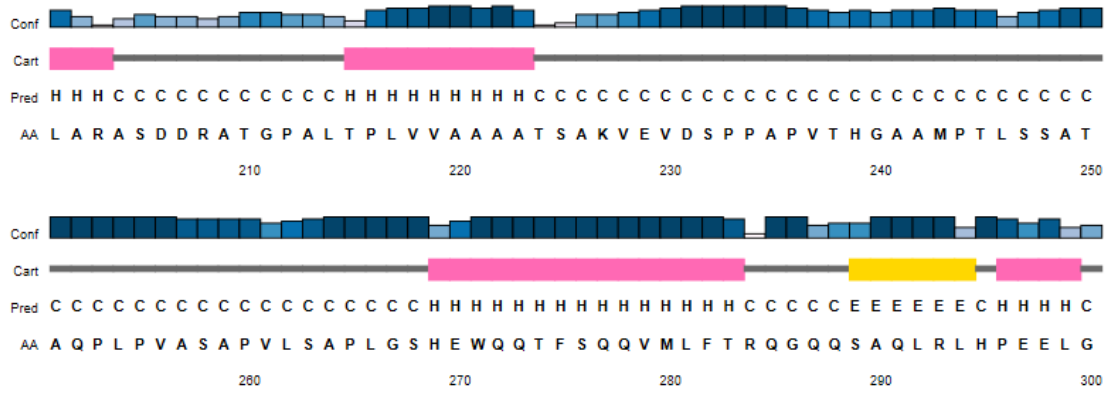

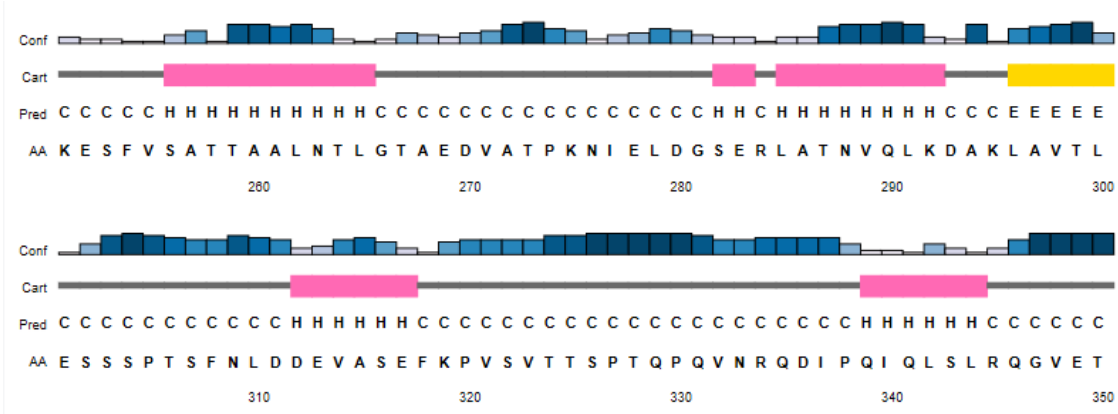

7.5.3: Identification of the Pfam Bac_export_2 domain

Image kindly provided by Dr. Jane Pane Farre and published in [180]; Dr. Pane Farre performed the phylogenetics investigation; image shows the presence of this domain in different species.

7.5.4 Alignment of *Sp*FlhG/*Pa*FleN and *Sp*FlrA /*Pa*FleQ

Appendix 7.5.4.1. (below): EMBOSS Needle alignment of SpFlhG and PaFleN, showing sequence identity-related values and the side-by-side alignment with numbering shown.

```
# Length: 295
# Identity:     174/295 (59.0%)
# Similarity:   227/295 (76.9%)
# Gaps:          17/295 ( 5.8%)
# Score: 895.5
#
#
#=======================================

PseudomonasFl      1 --------MKQMGSMH--PVQVIAVTGGKGGVGKTNVSVNLALALADLGR     40
                           ::.|...:  .|:|||||||||||||:||:|.|:|||:.|:
ShewanellaFlh      1 MTLDQASGLRMMNQPYNEKVKVIAVTGGKGGVGKTSVSINTAVALAEKGK     50

PseudomonasFl     41 RVMLLDADLGLANVDVLLGLTPKRTLADVIEGRCELRDVLLLGPGGVRIV     90
                     ||::|||||||||||:||:..:|.|:.|:.|..||.|:::.||.|:.||
ShewanellaFlh     51 RVLVLDADLGLANVDVMLGIRAERNLSHVLSGDAELDDIIVRGPKGIGIV    100

PseudomonasFl     91 PAASGTQSMVHLSPMQHAGLIQAFSDISDNLDVLVVDTAAGIGDSVVSFV    140
                     ||.||||.||.|||.||||||:|||::....|:|||||||.|.|:||.
ShewanellaFlh    101 PATSGTQGMVELSPAQHAGLIRAFSEMRTQFDILVVDTAAGISDMVLSFS    150

PseudomonasFl    141 RAAQEVLLVVCDEPTSITDAYALIKLLNRDHGMTRFRVLANMAHSPQEGR    190
                     ||:|:||:||||||||||||||:|:|:||:.||:::|||..|.:||.
ShewanellaFlh    151 RASQDVLVVVCDEPTSITDAYALIKILSREHGVFRFKIVANMVRSLREGM    200

PseudomonasFl    191 NLFAKLTKVTDRFLDVALQYVGVIPYDESVRKAVQKQRAVYEAFPRSKAS    240
                     .|||||:||||||||||:.|..||:||::||:|:||:.|.||:|:|.|:
ShewanellaFlh    201 ELFAKLSKVTDRFLDVALELVATIPFDENLRKSVRKQKLVVEAYPKSPAA    250

PseudomonasFl    241 LAFKAVAQKVDSWPLPANPRGHLEFFVERLVQHP-----ATGSAV    280
                     :|::.:|.|:.|||:|..|.||||||||||||.|     .|..
ShewanellaFlh    251 IAYQGLANKIMSWPVPQQPGGHLEFFVERLVQRPDFQEEKTSE--    293


#---------------------------------------
#---------------------------------------
```

Appendix 7.5.4.2. (below): EMBOSS Needle alignment of SpFlrA and PaFleQ, showing sequence identity-related values and the side-by-side alignment with numbering shown.

```
# Length: 506
# Identity:     263/506 (52.0%)
# Similarity:   329/506 (65.0%)
# Gaps:          45/506 ( 8.9%)
# Score: 1188.0
#
#
#=======================================

SpFlrA            1 MMQTDQRILLVGTPSERLSRLCCIFEFLGEQIDVIAPEKLNSYLQDTR--     48
                    |..:.::||:....:|...|..|..||||       ::|....:|.|
PaFleQ            1 -MWRETKLLLIDDNLDRSRDLAVILNFLGE-------DQLTCNSEDWREV     42

SpFlrA           49 -------YRALVLFTDTMPS--DAIKLLATQFAWQ---PILLFGE--IGD     84
                           ..||.:...::.|  .|::||....:|.   ||||.||  ..|
PaFleQ           43 AAGLSNSREALCVLLGSVESKGGAVELLKQLASWDEYLPILLIGEPAPAD     92

SpFlrA           85 FQVS---NVLGQIEEPLSYPQLTELLHFCQVYGQV-KRPQVPTSANQTKL    130
                    :...   .||..:|.|.||.:|.:.||..|||.:: .:.:....:.:..|
PaFleQ           93 WPEELRRRVLASLEMPPSYNKLLDSLHRAQVYREMYDQARERGRSREPNL    142

SpFlrA          131 FRSLVGRSDGIAHVRHLINQVATSDATVLVLGQSGTGKEVVARNIHYLSE    180
                    ||||||.|..|..||.::.|||.:||:||:||:||||||||||:||.|:
PaFleQ          143 FRSLVGTSRAIQQVRQMMQQVADTDASVLILGESGTGKEVVARNLHYHSK    192

SpFlrA          181 RRDGPFIPVNCGAIPPELLESELFGHEKGSFTGAICSRKGRFELAEGGTL    230
                    ||:|||:||||||||.|||||||||||||:|||||.||.||||||.||||
PaFleQ          193 RREGPFVPVNCGAIPAELLESELFGHEKGAFTGAITSRAGRFELANGGTL    242

SpFlrA          231 FLDEIGDMPLQMQVKLLRVLQERVFERVGGTKTINVDVRVVAATHRDLES    280
                    ||||||||||.||||||||||||.|||||..||.|||||::||||::||.
PaFleQ          243 FLDEIGDMPLPMQVKLLRVLQERTFERVGSNKTQNVDVRIIAATHKNLEK    292

SpFlrA          281 MISGNEFREDLYYRLNVFPIEMPALSERKDDVPLLLQELVSRVYNEGRGK    330
                    ||....|||||||||||||..|.||.:|:.|||.||:||:.:|.||.
PaFleQ          293 MIEDGTFREDLYYRLNVFPIEMAPLRERVEDIALLLNELISRMEHEKRGS    342

SpFlrA          331 VRFTQRAIESLKEHAWSGNVRELSNLVERLTILYPGGLVDVNDLPVKYRH    380
                    :||...||.||..|.|.||||||:||||||.|::|.|::.|.:||.|:||
PaFleQ          343 IRFNSAAIMSLCRHDWPGNVRELANLVERLAIMHPYGVIGVGELPKKFRH    392

SpFlrA          381 ID--VPEYCVEMSEEQQERDALASIFSSEEPVEIPETRFPNELPPEGVNL    428
                    :|  ..:....:.||.:||.|:.:        .:|....|..||.||::|
PaFleQ          393 VDDEDEQLASSLREELEERAAINA--------GLPGMDAPAMLPAEGLDL    434


SpFlrA          429 KDLLAELEIDMIRQALELQDNVVARAAEMLGIRRTTLVEKMRKYGMTKE-    477
                    ||.||.||..:|:|||:....|||||||.|.|||||||||||||::.
PaFleQ          435 KDYLANLEQGLIQQALDDAGGVVARAAERLRIRRTTLVEKMRKYGMSRRD    484

SpFlrA          478 ------    477

PaFleQ          485 DDLSDD    490


#---------------------------------------
#---------------------------------------
```

7.6. Supplementary fluorescence microscopy data

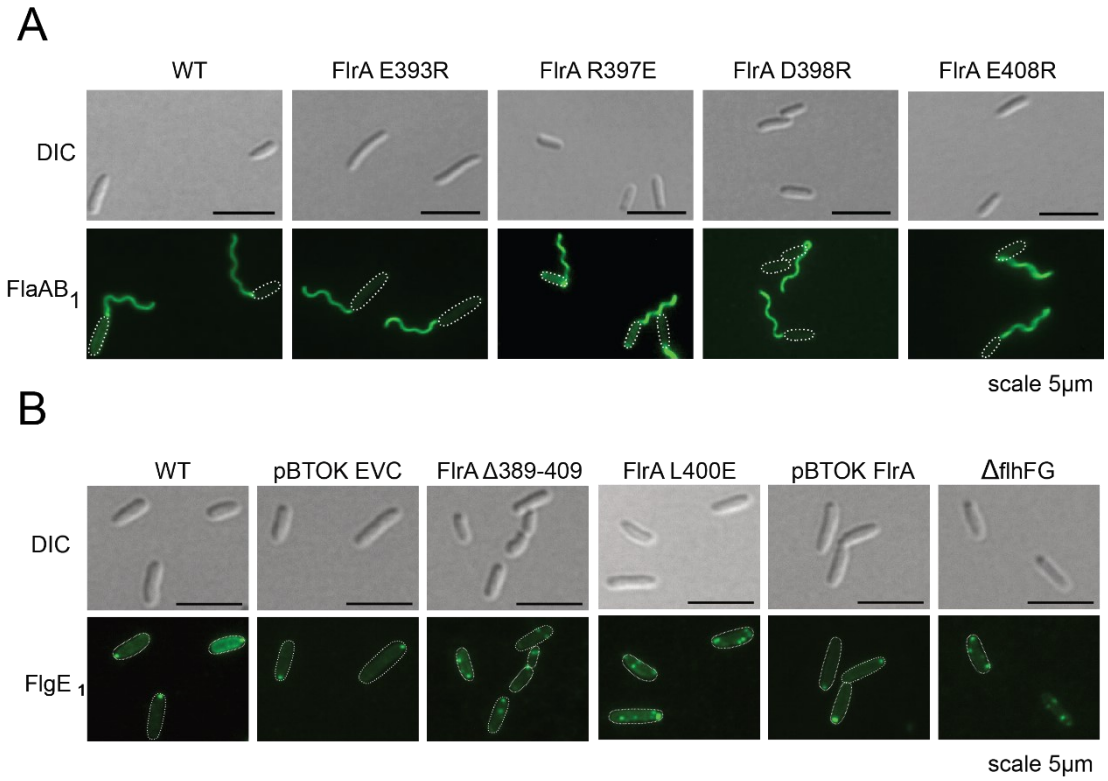

Appendix 7.6. Hook and filament stains of different FlrA mutants. A – Fluorescence microscopy and DIC images of filaments in *S. putrefaciens* with WT and WT-like phenotypes, see **Results 3.1.7. B –** Fluorescence microscopy and DIC images of hooks corresponding to filament stains from **Figure 19a**. Data obtained in collaboration with Meike Schwan, AG Thormann, JLU Gießen, who kindly provided the images; data was additionally published in [175], Supplementary information.

8. Academic curriculum

-Platzhalterseite, Lebenslauf entfernt-

-Platzhalterseite, Lebenslauf entfernt-